DETECTION AND CHARACTERISATION OF SECONDARY RELAXATIONS IN SOLIDS USING THERMALLY STIMULATED CURRENT SPECTROSCOPY

By

ANTHONY JOHN CHERRY [BSc. (Hons)]

A thesis submitted in partial fulfilment of the requirements of the University of Greenwich for the degree of Doctor of Philosophy

May, 2013

School of Science
University of Greenwich, Medway Campus
Chatham Maritime
Kent ME4 4TB, UK

DECLARATION

"I certify that this work has not been accepted in substance for any degree, and is not concurrently being submitted for any degree other than that of Doctor of Philosophy being studied at the University of Greenwich. I also declare that this work is the result of my own investigations except where otherwise identified by references and that I have not plagiarised the work of others".

Anthony J. Cherry (Candidate)

……

PhD Thesis Supervisors

Dr. M.D. Antonijevic

Prof. B.Z. Chowdhry

May, 2013

ACKNOWLEDGEMENTS

I wish to express my sincere thanks to Dr Milan Antonijevic and Prof. Babur Z. Chowdhry for their invaluable guidance and encouragement offered to me as my supervisors; and for the initial opportunity to undertake my PhD. They have always made themselves, their time and their theoretical and technical knowledge freely available; for the foregoing I am profoundly grateful.

Without the School of Science (funding, resources and technical staff) this thesis would not have come to fruition and I owe them my thanks.

My colleague Samuel and I have undertaken this endeavour together and it is with him I have shared the highs and lows of life as a PhD student. I would like to express my appreciation for his support as a professional and as a friend. I wish him the best of luck in his chosen career path.

I am eternally grateful for the support of my family and friends throughout my period as a PhD student; and through the years of education leading up to it. In particular, my parents - Julia and Peter - have enduringly encouraged me to pursue my aspirations. They have played a part in all the successes in my life and I will forever be thankful for their love and support. Similarly, my Nan (Jean) has equally encouraged and supported me throughout my life and I thank her for always being there for me.

Last -but by no means least- I would like to thank Kira for her kindness, generosity, patience and loving support. Kira, you have - undoubtedly - made my life, over the past few years, very happy; for that I love you and will be forever grateful.

ABSTRACT

DETECTION AND CHARACTERISATION OF SECONDARY RELAXATIONS IN SOLIDS USING THERMALLY STIMULATED CURRENT SPECTROSCOPY

Thermally stimulated current (TSC) spectroscopy has been used, in these reported investigations, as an innovative experimental technique for the detection and characterisation of secondary relaxation phenomena in the crystalline state for a number of low-molecular weight organic materials (LOMs), namely α-alanine, β-alanine, a co-crystal system (salicylic acid and benzamide) and the drug paracetamol (form I). The aim of the research was to significantly improve the contemporary understanding of secondary relaxation phenomena in crystalline LOMs; an area of science that is of significant inter-disciplinary interest throughout academia and industry.

In all the materials examined, secondary relaxations were detected and characterised by TSC; in order to achieve the foregoing different experimental methodologies (e.g. thermal windowing) and data processing techniques (e.g. relaxation map analysis) were employed. Of significant prevalence throughout is the phenomenon of compensation behaviour; in both the thermodynamic (i.e. enthalpy and entropy compensation) and in the kinetic (i.e. pre-exponent and activation energy (of the Arrhenius equation)) sense. Derived compensation points were linked to real physical processes; identifying a relationship between secondary relaxations and primary transitions. It is proposed, herein, that secondary relaxations have a pre-requisite relationship with primary transitions. Secondary relaxations are preparatory motions, essential for primary transitions to occur.

In addition, throughout this thesis, additional information on topics such as co-crystal synthesis, chirality, degradation, the nature of secondary/primary relaxations, the nature of primary transitions and physical properties of LOMs, are examined in relation to the LOMs under investigation. TSC has proven to be an effective, and perhaps unique, instrumental technique for the detection and characterisation of secondary relaxations in LOMs.

A.J. Cherry [B.Sc. (Hons)]

CONTENTS

LIST OF FIGURES

LIST OF TABLES

LIST OF ABBREVIATIONS

ABBREVIATION	MEANING
A	amperes
A_e	effective area (of electrodes)
Ala	alanine
API	active pharmaceutical ingredient
ATR	attenuated total reflectance
BA	benzamide
CC	co-crystal
D-	dextrorotatory
DEA	dielectric analysis
DETA	dielectric thermal analysis
DMA	dynamic mechanical analysis
DOC	degree of crystallinity
DSC	differential scanning calorimetry
dTG	derivative thermo-gravimetric
DVS	dynamic vapour sorption
EGA	evolved gas analysis
E_p	applied electrical field
FT	Fourier-transform
HCH	heat-cool-heat
HSM	hot stage microscopy
I	current intensity
IR	infra-red
J	rate of decrease in polarisation
L-	laevorotatory
LMW	low-molecular weight
LN_2	liquid nitrogen
MWS	Maxwell-Wagner-Sillars
P	polarisation
PA	paracetamol
PM	physical mixture
PTFE	polytetrafluoroethylene
q	heating rate
q_c	cooling rate
RMA	relaxation map analysis
RT	room temperature
SA	salicylic acid
SDC	spontaneous depolarisation current
T	temperature
t	time
T_0	lowest experimental temperature
t_0	time at T_0
T_a	annealing temperature
TA	thermal analysis

t_a	time at T_a
T_f	final experimental temperature
t_f	time at T_f
T_g	glass transition temperature
TG	thermo-gravimetric (curve)
TGA	thermal gravimetric analysis
T_K	Kauzmann temperature
T_m / T_{max}	maximum temperature
T_p	temperature of polarisation
t_p	time at T_p
TSC	thermally stimulated current
TSDC	thermally stimulated depolarisation current
TSPC	thermally stimulated polarisation current
T_w	thermal window temperature
TW	thermal windowing
t_w	time of T_w
V	voltage
XRD	x-ray diffractometry
XRPD	x-ray powder diffractometry
τ	relaxation time

CONFERENCE PRESENTATIONS/PUBLICATIONS

Title: **Thermal studies of L-, D- and β-alanine**
Date: 30/03/2010
Type: Abstract/Poster
Co-authors: Steve A Leharne, Babur Z Chowdhry, Milan D Antonijevic
Details: National conference – Thermal analysis and calorimetry *Aldermaston, Reading, UK.*

Title: **Application of thermal methods to the study of structural- and stereo-isomeric amino acids in the solid state**
Date: 07/09/2010
Type: Abstract/Poster
Co-authors: Steve A Leharne, Babur Z Chowdhry, Milan D Antonijevic
Details: National conference - UK Pharmaceutical Sciences Conference. *Nottingham, UK.*

Title: **Thermal stability assessment of alanine stereo-isomers using Thermally Stimulated Current (TSC) spectroscopy**
Date: 14/11/2010
Type: Abstract/Poster
Co-authors: Steve A Leharne, Babur Z Chowdhry, Milan D Antonijevic
Details: International conference - American Association of Pharmaceutical Sciences World Congress**.** *New Orleans, USA.*

Title: **Thermal Analysis of a new co-crystal system**
Date: 24/11/2010
Type: Abstract/Poster
Co-authors: Steve A Leharne, Babur Z Chowdhry, Milan D Antonijevic
Details: National symposium – Thermal methods group**.** *Manchester, UK.*

Title: **Characterisation of a pharmaceutical co-crystal by thermal analysis**
Date: 19/04/2011
Type: Abstract/Poster
Co-authors: Steve A Leharne, Babur Z Chowdhry, Milan D Antonijevic
Details: National conference – Thermal analysis and calorimetry. *Belfast, UK.*

Title: **Thermogravimetric, calorimetric and Thermally Stimulated Current (TSC) spectroscopy studies of alanine**
Date: 19/04/2011
Type: Abstract/Poster
Co-authors: Steve A Leharne, Babur Z Chowdhry, Milan D Antonijevic
Details: National conference – Thermal analysis and calorimetry. *Belfast, UK.*

Title: **The use of Thermally Stimulated Current (TSC) spectroscopy in the study of low-molecular weight materials**
Date: 19/04/2011
Type: Abstract/Oral presentation
Co-authors: Steve A Leharne, Babur Z Chowdhry, Milan D Antonijevic
Details: National conference – Thermal analysis and calorimetry. *Belfast, UK.*

Title: **Thermogravimetric, calorimetric and Thermally Stimulated Current (TSC) spectroscopy studies of D-α, L-α and β-alanine in the solid state**
Date: 31/08/2011
Type: Abstract/Poster
Co-authors: Steve A Leharne, Babur Z Chowdhry, Milan D Antonijevic
Details: National conference – Thermal analysis and calorimetry *Nottingham, UK.*

Title: **Characterisation of a pharmaceutically relevant co-crystal by thermal analysis**
Date: 31/08/2011
Type: Abstract/Poster
Co-authors: Steve A Leharne, Babur Z Chowdhry, Milan D Antonijevic
Details: National conference – Thermal analysis and calorimetry *Nottingham, UK.*

Title: **Thermal analysis of polymorphic biphenyl motifs**
Date: 14/10/2011
Type: Abstract/Poster
Co-authors: Steve A Leharne, Babur Z Chowdhry, Milan D Antonijevic
Details: International conference - American Association of Pharmaceutical Sciences World Congress**.** *Washington DC, USA.*

Title: **Thermally Stimulated Current (TSC) spectroscopy studies of a pharmaceutically relevant co-crystal**
Date: 14/10/2011
Type: Abstract/Poster
Co-authors: Steve A Leharne, Babur Z Chowdhry, Milan D Antonijevic
Details: International conference - American Association of Pharmaceutical Sciences World Congress**.** *Washington DC, USA.*

Title: **Thermally Stimulated Current (TSC) spectroscopy studies of co-crystals**
Date: 12/08/2012
Type: Abstract/Poster
Co-authors: Steve A Leharne, Babur Z Chowdhry, Milan D Antonijevic
Details: International conference – Thermal Analysis and Calorimetry**.** *Osaka, Japan.*

Title: **Thermally Stimulated Current (TSC) spectroscopy studies of alanine**
Date: 20/08/2012
Type: Abstract/Poster
Co-authors: Steve A Leharne, Babur Z Chowdhry, Milan D Antonijevic
Details: International symposium – North American Thermal Analysis**.** *Florida, USA.*

Title:	**The use of TSC spectroscopy in the characterisation of pharmaceutical materials.**
Date:	09/04/2013
Type:	Abstract/Oral presentation
Co-authors:	Steve A Leharne, Babur Z Chowdhry, Milan D Antonijevic
Details:	National conference – Thermal analysis and calorimetry**.** *Chatham, UK.*

…….

PUBLICATIONS

Publication type:	Journal Manuscript
Title:	Solid-state molecular mobility and relaxations in β-alanine: thermally stimulated current spectroscopy studies
Year:	2013
Journal/Conference:	Submitted to: RSC Advances (July, 2013)
Publication type:	Journal Manuscript
Title:	Characterisation of a co-crystal system by thermally stimulated current (TSC) spectroscopy.
Year:	2013
Journal/Conference:	To be submitted to: CrystEngComm (August, 2013)
Publication type:	Journal Manuscript
Title:	Molecular mobility and secondary relaxations in paracetamol.
Year:	2013
Journal/Conference:	To be submitted to: Pharm. Res. (September, 2013)
Publication type:	Journal Manuscript
Title:	Secondary relaxations in α-alanine: thermally stimulated current (TSC) spectroscopy studies
Year:	2013
Journal/Conference:	To be submitted to: Phys.Chem.Chem.Phys. (October, 2013)

CHAPTER 1: INTRODUCTION

1.1 GENERAL INTRODUCTION

The field of low-molecular weight organic materials (LOMs) is a significant inter-disciplinary area of contemporary research and development throughout industry and academia. This type of research mainly focuses on the characterisation of materials, evaluation of their properties and experimentation into how these properties can be improved/tailored to specific applications. A major area of research and development in this field exists within the pharmaceutical industry.

Despite significant investment ($60 billion/year) by the pharmaceutical industry the number of new products that are reaching market is declining (Kessel 2011). One of the reasons for this trend is the high attrition of successful drug candidates; often caused by inappropriate selection or the non-technical discontinuation of drug candidates (Cuatrecasas 2006). Novel or new technologies are being increasingly employed to gain more useful/pertinent detailed information about the physicochemical properties of LOMs; thereby optimising the selection of appropriate candidates and ensuring informed decisions when considering discontinuing developmental compounds (Sigurd 2010; Darroch and Miles 2011).

Thermally stimulated current (TSC) spectroscopy is a dielectric/thermal analysis technique which has been used for, approximately, the last 40 years since the fundamental development of the technique in 1964 by Bucci and Fieschi (Vanderscheuren and Gasiot 1979). However, this technique remains confined to the realms of highly specialised applications such as discrete areas of polymer science, semi-conductor research and dielectric analysis. TSC spectroscopy rarely features in publications outside of these fields of research.

A study of the specialist TSC spectroscopy literature indicates that several authors have recently (in the last decade or so) noticed the potential benefits such an instrumental technique can bring to the field of LOMs research and have begun to use TSC spectroscopy in the fields of biochemical, pharmaceutical, healthcare and biotechnological research (Ikeda et al. 2005; Diogo et al. 2007; Antonijevic et al. 2008; Moura Ramos et al. 2008; Pinto et al. 2010; Barker and Antonijevic 2011; Neagu et al. 2011; Antonijevic 2012).

The majority of such recent TSC LOMs research has focused on glass-forming materials, attempting to apply existing TSC knowledge and theories (derived from its common

application in polymer science) to characterize the primary glass transition and any secondary sub-glass relaxations (Pinto et al. 2010; Collins 2011; Neagu et al. 2011; Panagopoulou et al. 2011). Examples of molecular mobility studies by TSC of materials in the crystalline state are sparse (Moura Ramos et al. 2005; Shmeis and Krill 2005; Chamarthy and Pinal 2008).

Of particular interest in the field of TSC LOMs research are secondary relaxation phenomena. Secondary (sometimes called 'sub-glass' or 'β') relaxations occur at temperatures below the primary (or 'α') transition (usually a glass transition). They are often difficult or impossible to detect by 'conventional' thermal techniques (Vyazovkin and Dranca 2006). However, secondary relaxations represent temperature regions of molecular mobility; intrinsically linked to both short and long term stability (Jimenez-Ruiz et al. 2009; Bhattacharya and Suryanarayanan 2009). Their detection, characterization and subsequent understanding of their fundamental scientific basis as well as relationship to other thermal events are, therefore, of paramount importance.

A more comprehensive theoretical understanding of secondary relaxation phenomena is attractive not only within the context of commercial applications, but equally from a purely scientific/academic standpoint. Hence, one of the aims of the research reported herein is to develop experimental methodologies, or gain new knowledge, that can be useful from an industrial perspective. Of equal, or perhaps greater, importance is to use TSC spectroscopy to improve our understanding of the solid-state properties of molecules/higher order systems from a purely knowledge based scientific perspective.

1.2 IMPORTANT DEFINITIONS

The following section outlines some non-conventional definitions, specific to this thesis, in order to avoid ambiguity.

LOM = Low molecular weight organic material

Refers to organic solids whose constituent molecules do not contain repeating units and whose molecular weight is less than 1000 g mol^{-1}. Excludes polymers but is inclusive of dimers/trimers.

HTR = High-temperature region

A temperature region beginning at the temperature at which the primary transition or relaxation begins, encompassing all temperatures above. It is therefore material (or sample) dependent.

LTR = Low-temperature region

A temperature region ending at the temperature at which the primary transition or relaxation begins, encompassing all temperatures below; it is therefore material (or sample) dependent.

1.3 THERMALLY STIMULATED CURRENT SPECTROSCOPY

TSC spectroscopy is used to measure dipolar currents in response to changes in temperature and/or the application of an external, static electrical field. TSC spectroscopy essentially probes molecular motion within a system by monitoring changes in, and manipulating, dipole moments (Shmeis and Krill 2005). The technique is considered a bridge between thermal and dielectric analysis for two main reasons: firstly, due to the ability to simultaneously vary temperature (thermal analysis) and external electrical field (dielectric analysis), and secondly, because a typical TSC experimental output uses temperature as the 'X-axis' (common in thermal analysis) and current as the 'Y-axis' (common in dielectric analysis).

Current is the primary output from a TSC experiment and is, specifically, a dipolar current generated by perturbations in dipole moment, usually via rotation of whole, parts or groups of molecules. Current is detected via an external circuit in contact with the sample, connected to an extremely sensitive ammeter able to detect current as small as 10^{-18} A, but typically between 10^{-14} and 10^{-8} A.

The remainder of this section will introduce the associated theory of TSC spectroscopy relevant to the research reported in this doctoral thesis. Additional information for those who wish to gain a more in-depth understanding of the technique, or its alternative applications, should refer to the accompanying references in this section.

1.3.1 External electrical fields and polarisation

In most instances an external static electrical field is used to 'polarise' (i.e. displace or preferentially orientate towards a continuum) the dipoles within a sample prior to, or during, an experiment. This is achieved via the application of a voltage bias across the external circuit in contact with the sample. The polarisation of a solid dielectric via exposure to an external electric field exhibits no exclusivity towards dipolar polarisation alone, and as a result, a 'global' polarisation via a number of different mechanisms involving microscopic and macroscopic charge displacement occurs (Vanderschueren and Gasiot 1979).

Electronic polarisation: a microscopic, internal polarisation process resulting from the deformation of the electronic shell. Due to the small distances involved in electronic displacements inside an atom, this is the fastest polarisation process and occurs over a time period of *ca*. 10^{-15} seconds.

Atomic polarisation: microscopic, internal polarisation resulting from the deformation of atoms within molecules containing heteropolar bonds. It is a relatively fast process with a timescale of 10^{-14} to 10^{-12} seconds.

Dipolar polarisation: an internal polarisation process, which can occur in materials containing permanent molecular or ionic dipoles. The time required ranges from 10^{-10} seconds to a time so long it cannot be observed under experimental conditions. The time period is dependent on the frictional resistance of the medium (Vanderschueren and Gasiot 1979).

Intrinsic space-charge polarisation: a macroscopic, internal polarisation mechanism which can occur in materials containing intrinsic free charges (ions, electrons, or both). This type of polarisation is due to macroscopic charge transfer towards the electrodes. The time-scale varies from milliseconds too years, depending on the bulk properties of the material.

Interfacial polarisation: sometimes referred to as Maxwell-Wagner-Sillars (MWS) polarisation is characteristic of systems with a heterogeneous structure. This type of internal polarisation results from the formation of charged layers at interfaces, due to unequal conduction currents within the various solid phases of the sample (Vanderschueren and Gasiot 1979). Interfacial polarisation is often observed in partially crystalline systems and has a time scale of milliseconds to years. Interfacial polarisation phenomena can also occur in

samples which contain an interface between two different phases, i.e. polymorphic samples or partially amorphous/crystalline samples.

All of the above are internal polarisation mechanisms and arise from the rotation, translation, motion and/or migration of charges originating from, and remaining within, the dielectric. They therefore lead to surface charges of opposite polarity to those of the polarising electrodes and are termed heterocharges. In addition to these internal polarisation mechanisms it is also possible to produce a space charge of extrinsic origin.

Extrinsic space-charge polarisation: a space charge polarisation of extrinsic origin may be created in dielectrics exposed to high static electrical fields when excess electronic or ionic charge carriers are generated; either by injection mechanisms from the polarising electrodes (Schottky emission), or from Townsend breakdowns in the surrounding atmosphere as a result of imperfect contact between the dielectric sample and the polarising electrode (Vanderschueren and Gasiot 1979). Excess charge formed in this manner has the same polarity as the counterpart electrode and is thus termed a homocharge.

The aforementioned polarisation mechanisms are all able to produce a current and can therefore potentially interfere with the collection and analysis of the intended dipolar current. Electronic and atomic polarisations occur extremely fast (see time-frames above) and are therefore never represented in a TSC output. Space-charge and interfacial polarisation can occur on a similar time-scale to dipolar polarisation. However, in most instances their contribution to the TSC output can be eliminated experimentally, or identified as anomalous during data processing. Therefore, the final experimental output from a polarisation TSC experiment is, generally, exclusively representative of dipolar contributions. Dipolar relaxations are spatially uniform, can be easily distinguished from space charge formation, and can be treated theoretically with the minimal number of simplifying assumptions (Vanderschueren and Gasiot 1979).

1.3.2 Depolarisation and the TSDC methodology

Thermally stimulated depolarisation current (TSDC) spectroscopy is one of several TSC techniques/methodologies, and probably the most commonly used. The TSDC method is used to measure the response of a sample to prior polarisation. Most of the associated theory relating to TSC is tailored towards TSDC methodology (Figure 1.1).

A static electrical field, E_p, is applied at the temperature of polarisation, T_p, (above the expected relaxation phenomena) for a length of time, t_p, longer than the relaxation time, $\tau(T_p)$, of the charge carriers. This results in the system being polarised until at equilibrium with the electrical field. Maintaining the electrical field under cooling to the lowest experimental temperature, T_o, which is sufficiently low as to increase the relaxation time of the dipoles to longer than the experimental time-frame results in the dipoles becoming practically 'frozen' in the polarised state achieved at T_p. Removal of E_p at T_o does not induce a depolarisation response from the "frozen-in -dipoles". However, maintaining T_o for a time period of t_o, allows enough time for faster depolarisation processes (such as electronic, atomic, space-charge and interfacial depolarisation) to take place before the data collection stage of the experiment begins. The final stage (where current is recorded) involves heating the sample, consequently decreasing the relaxation time, $\tau(T)$, until it falls within the experimental time-frame, and induces a movement of charge as the dipoles relax to their native state at the transition temperature(s).

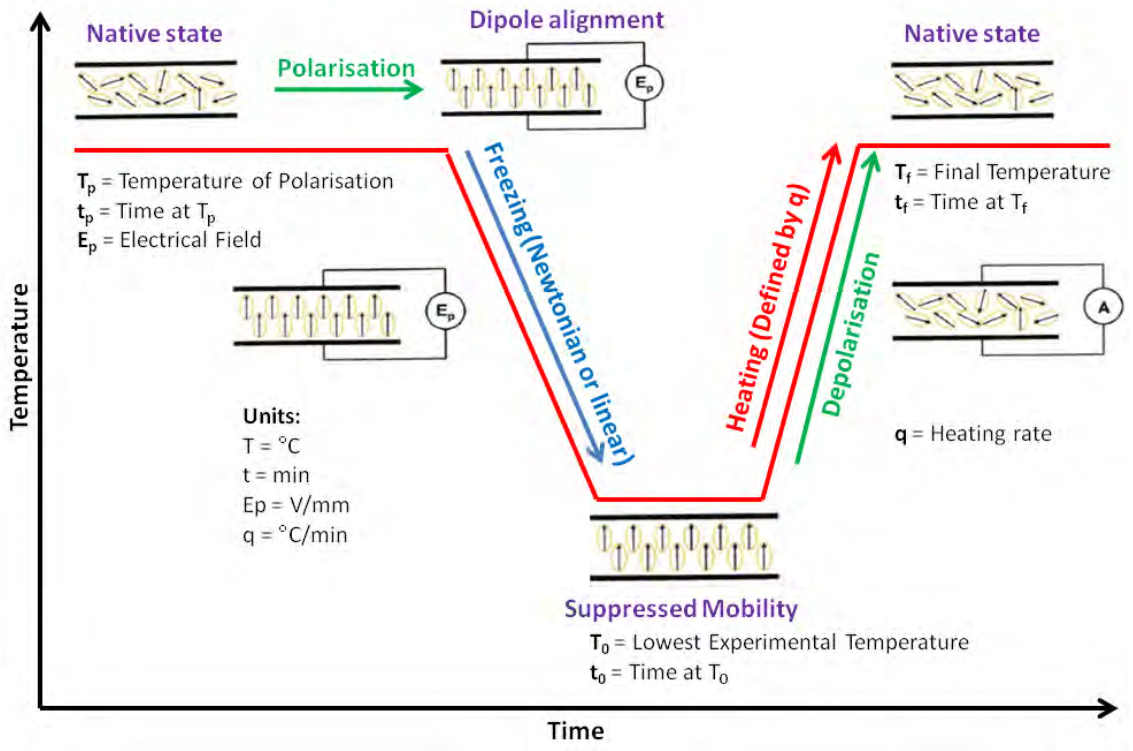

Figure 1.1 Schematic representation of the principle method of TSPC spectroscopy, and the movement of dipoles.

The experimental output from a TSDC experiment is depolarisation current as a function of temperature (Figure 1.2). Depolarisation current density ($J(T)$) is the rate of decrease of the polarisation, and as such can be expressed as:

$$J(T) = I(T) / A_e = \delta P(T) / \delta t \qquad \text{(Eq. 1.1)}$$

where $I(T)$ is the current intensity at a given temperature, T (or at time, t), using a constant heating rate, P(T) is the remaining polarisation at temperature T (or at time, t) and A_e is the effective area of the electrodes. Analysis of TSC data is based on the Debye relaxation concept where it is assumed that the decay of polarisation is a first-order rate process at each temperature of linear heating. For an elementary single relaxation process:

$$\delta P(T) / \delta t = -P(T) / \tau(T) \qquad \text{(Eq. 1.2)}$$

where $P(T)$ is the polarisation at temperature T and $\tau(T)$ is the temperature dependent relaxation time. Where the temperature is monotonically varied (i.e. during linear heating) the temperature dependent relaxation time can be expressed as:

$$\tau(T) = P(T) / I(T) \qquad \text{(Eq. 1.3)}$$

where τ, P and I are now expressed as a function of temperature, T; τ can now be extracted from the elementary spectrum (Figure 1.2).

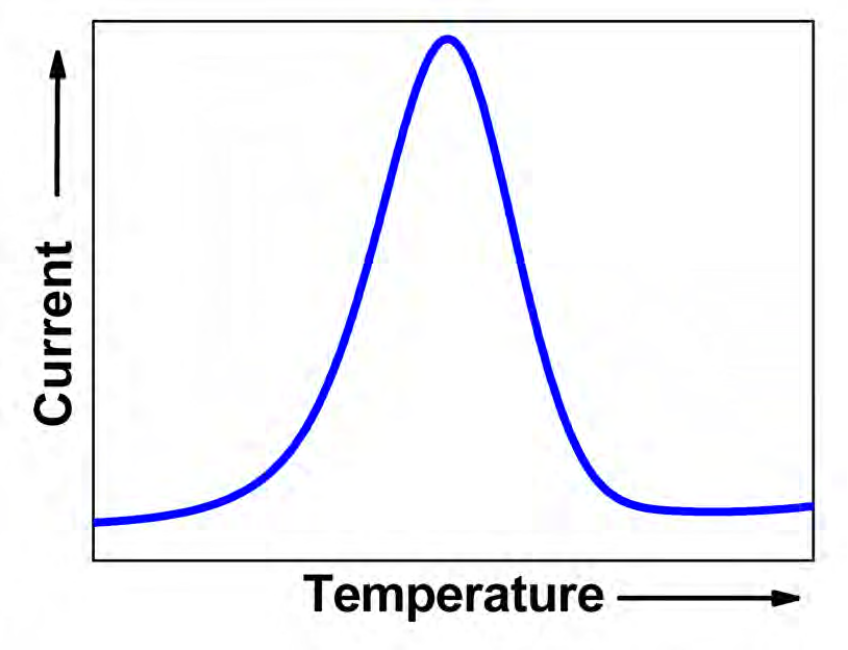

Figure 1.2 A typical TSCS experimental output.

1.4 THE SOLID-STATE

The solid state is a condensed phase, resulting from the cooling of a gas or a liquid (Patterson et al. 2007). A solid is a rigid material which does not flow when subjected to moderate forces and maintains its shape indefinitely. Molecules or atoms within a solid have a fixed spatial arrangement and are essentially 'locked' into position; void of any large amplitude motion (Roesslle r et al. 2009). However, molecules or atoms in the solid are not static; they vibrate (and sometimes rotate) around their equilibrium positions.

The many ways in which atoms or molecules can be orientated, packed together and layered, gives rise to many sub-phases of solids. Solids are classified as crystalline or amorphous in the broadest sense, and are then sub-divided into many categories (Figure 1.3).

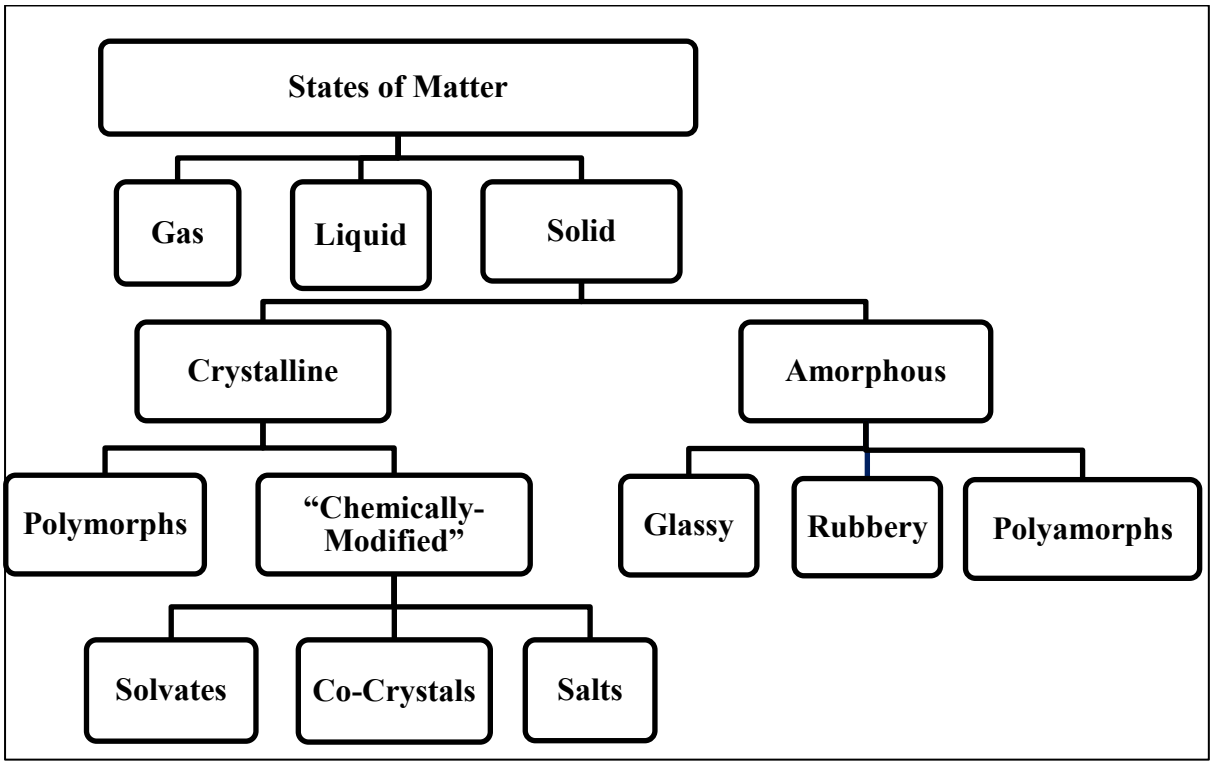

Figure 1.3 States of matter (particular emphasis is placed on the solid-state).

1.4.1 Crystalline Solids

When applied to solids, the adjective crystalline implies an ideal crystal in which the structural units, termed unit cells, are repeated regularly and indefinitely in all three dimensions in space (Vippagunta et al. 2001). The unit cell contains all the molecules and/or atoms necessary to generate the entire crystal structure, it has a definite orientation and shape

(defined by the translational vectors a, b and c) and hence, has a definitive volume, V (Brittain 1999; Byrn et al. 1999). A crystal is essentially a repetition of a large number of unit cells. Crystalline solids are, therefore, said to possess long-range order. Thermodynamically, crystalline solids are considered to be highly stable (with respect to amorphous solids) due to their highly-ordered and, therefore, low potential energy arrangement.

1.4.1.1 Polycrystalline solids

Crystalline polymorphs have the same chemical composition but different crystal structures; hence they possess different physico-chemical properties. The divergent crystal structures of polymorphs arise when the substance crystallises in a contrasting packing arrangement or conformation (Vippagunta et al. 2001). It has been suggested that one-third of organic substances exhibit crystalline polymorphism under ambient conditions (Giron 1995).

It is well documented that different polymorphic forms exhibit different physico-chemical properties (Grant and Byrn 2004) and variances in potential energy levels. Thermodynamics would therefore dictate that only one polymorphic form should be present, under a given set of conditions, at any one time; as eventually the polymorph of higher potential energy will ultimately convert to the polymorph of lower potential energy.

From a kinetic perspective, however, this is not always the case and two polymorphs can be found at the same time, under the same conditions (Vippagunta et al. 2001). The Arrhenius law states that the rate of conversion from one polymorph form to the other is determined by the magnitude of the activation energy for a particular transition. Activation energy is the energy barrier which needs to be overcome for a transition to occur; the higher the activation energy, and the lower the storage temperature, the slower the conversion of one polymorphic form to another. The rate of conversion can be so slow that it takes months or years for a transition to occur, much longer than a typical experimental time-frame. This non-equilibrium phase that persists for an extended period of time is termed a metastable state (Singhal and Curatolo 2004).

According to differences in thermodynamic properties, polymorphs can be classified as either monotropic or enantiotropic in nature. Put quite simply this depends on whether or not two forms can transform reversibly into one another (Morissette et al., 2004). In an enantiotropic system, a reversible transition between polymorphs is possible at a definitive transition temperature below the melting point. A monotropic system is one in which no reversible

transition is observed between polymorphic forms. Several sets of rules such as those outlined by Burger and Ramberger or Giron can be used to qualitatively distinguish between monotropic and enantiotropic states (Burger and Ramberger, 1979; Giron, 1995).

1.4.1.2 "Chemically-modified" crystalline species

The term chemically modified is used to distinguish the remaining classes of crystalline materials from polymorphs. Polymorphs contain only one chemical species, whereas solvates, hydrates, salts, co-crystals, etc., contain at least two different chemical species.

Crystalline solvates

Solvates are crystalline adducts containing solvent molecules (liquids). The most common solvent in use throughout the chemical industry is water, and as a result the term hydrate has evolved to describe 'water solvates'. It has been estimated that approximately one-third of active pharmaceutical ingredients (APIs) are capable of forming crystalline hydrates (Stahl et al. 1980). Due to its relatively small size and multi-directional hydrogen bonding capabilities, water is ideal in linking drug molecules into stable crystalline structures (Khankari and Grant 1995).

Crystalline hydrates can be classified into the three following categories based on their structure.

Class I – Isolated site hydrates; where water molecules are separated from direct contact with each other.

Class II – Channel hydrates; in which water molecules reside next to other water molecules of adjoining unit cells along an axis of the lattice, forming channels through the crystal.

Class III – Ion associated hydrates; where water molecules are co-ordinated with metal ions, generally alkali metals, such as sodium or calcium.

The addition of a liquid (in its native state under standard conditions) into the crystal lattice of a solid can significantly influence its physico-chemical properties. As such, solvate screening techniques have been developed to exploit this phenomenon with the intention of hopefully discovering a solvate with beneficial physicochemical properties compared to the pure crystalline material.

Co-Crystals (CCs)

CCs are similar to solvates in the sense that a modification of the crystal lattice occurs via inclusion of a different chemical species. However, the main difference between a solvate and a CC is the physical state of the components at room temperature (RT). Compared with a solvate for example, in which one of the components is a liquid at RT, all components of a CC are solid at RT (Vishweshwar et al. 2006). Neutrality of these components is also a feature of a CC; with no exchange of protons, CCs are stabilised via a variety of intermolecular interactions such as hydrogen bonding, aromatic π-stacking and van der Waals forces. These seemingly trivial differences have a profound effect on the ultimate physicochemical properties of the CC material.

Despite the potential benefits associated with CC formation no currently marketed drug product intentionally utilises CCs (Schartman 2009) (the antidepressant 'escitalopram', developed by Lundbeck, was formulated as an oxalate salt, but was later recognised to be a CC (Schartman 2009)). One reason for this may be related to uncertainty surrounding the physical and chemical stability of CCs. Pharmaceutical companies are unlikely to market a metastable CC due to the risk of product recall should the CC undergo a change in chemical composition or physical arrangement during its shelf life.

1.4.2 Amorphous Solids

Amorphous solids are fundamentally different from crystalline solids, in that structurally, they possess no long-range order. The arrangement of molecules in an amorphous solid is often thought of as being random. However, this is not always entirely true, as some amorphous solids possess a degree of order at the molecular level (short-range order). From a thermodynamic perspective amorphous materials have higher entropy and free energy compared to the corresponding crystals (Yu 2001) and thus, their physiochemical properties vary from those of their crystalline counterparts.

Amorphous materials are generated in many different ways; most commonly via vapour condensation, super-cooling from melt, precipitation from solution or compaction of crystals. Super-cooling of the melt is the most common method of obtaining an amorphous solid and involves heating the material to above its melting point, and cooling it at a rate sufficiently fast as to prevent crystallisation. Preventing crystallisation is the key to the formation of an amorphous solid (Wunderlich 1999; Yu 2001; Yong Cui 2007).

As mentioned above, amorphous solids possess higher energy and entropy than their crystalline counterparts. It is therefore, thermodynamically unfavourable for a material to form, or remain, in an amorphous state. The presence of a seed crystal or an impurity during the cooling of a liquid to a solid will act as a nucleation site for crystal growth. This will ultimately result in the formation of a crystalline solid during cooling of the melt. However, lacking such a nucleation site for crystallisation, the liquid phase can be maintained down to a temperature where large amplitude motions become extremely slow, and the resulting material possesses solid-like behaviour. The result is a super-cooled liquid with an extremely high viscosity; or in other words, an amorphous solid (Yu 2001).

1.4.2.1 Glass forming amorphous solids

Many solids when heated above their melting temperature (Tm) and then rapidly cooled, do not crystallise but form super-cooled liquids. It is also possible, providing crystallisation is prevented, that the super-cooled liquid itself may pass through a heat capacity change, known as a glass transition, to form a brittle transparent solid, commonly known as a glass (Kerc and Srcic 1995). Kerc and Srcic (1995) defined a glass as an amorphous solid with the structure of a liquid and the energy level of a solution. What they were referring to was the liquid-like structure of glassy materials, combined with a very high viscosity, which causes solid-like behaviour to be observed.

To fully understand glassy states and the glass transition it is important to state some definitions.

Glass: a glassy material is an amorphous solid which exhibits a transition from the glassy to the rubbery state. This transition is called the glass transition; and the temperature at which it occurs is referred to as the glass transition temperature.

Rubbery state: the intermediate phase between the liquid and glassy states; characterised by a low elastic modulus and the ability to undergo large elastic deformation.

Glass transition temperature (T_g): the temperature of transition between glass and rubbery state.

1.4.2.2 T_g - Glass Transition Temperature

A liquid cooled to below its Tm (super-cooled) can still exhibit equilibrium behaviour providing crystallisation is prevented. As a super-cooled liquid is cooled further, a substantial

increase in viscosity is observed, hindering the large amplitude motions of molecules. Increased super-cooling increases the time-scale of large amplitude molecular motions so that they coincide with the experimental time-scale resulting in a loss of equilibrium, and a transition into the glassy state. The viscosity of the glassy state is so high, pseudo-solid behaviour is observed, and the timescale of large amplitude molecular motions so slow, the glassy material appears to be 'frozen'. The glass transition represents a change from equilibrium to non-equilibrium conditions on cooling, and the reverse process on heating (Crowley and Zografi 2001).

Figure 1.4 shows the changes in free volume (V)/enthalpy (H)/entropy (S) that occur during cooling of a melt at temperatures below a first-order melting transition at T_m. During cooling there is a continuous change in enthalpy with temperature, due to established equilibrium conditions. At T_g, a departure from equilibrium conditions results in a discontinuous change in enthalpy. Kauzmann's temperature, T_k, is representative of the isoentropic point between a super-cooled liquid and a crystal (Crowley and Zografi 2001).

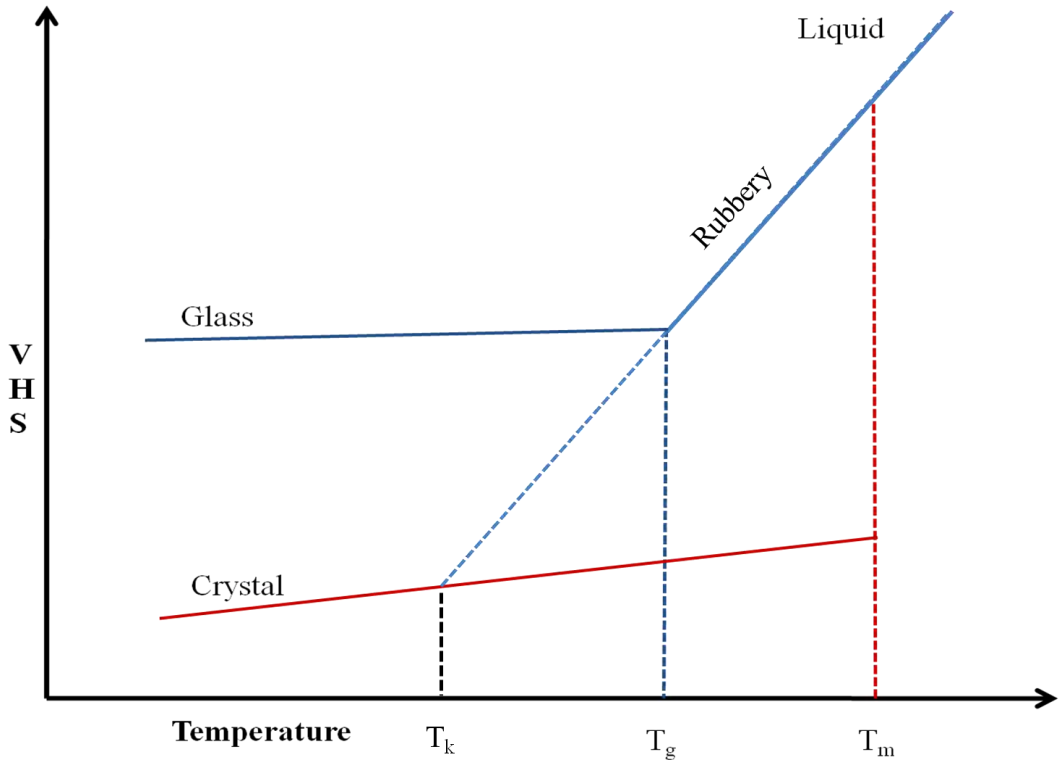

Figure 1.4 Schematic depiction of the relationship between free volume (V), enthalpy (H) and entropy (S) as a function of temperature for the liquid, super-cooled liquid, glass and crystalline phases (reproduced from Chawla and Bansal 2009).

The tendency of a material to form a glass has been shown to be related to the asymmetry of the molecule in question. In general, the more asymmetric a molecule, the greater the likelihood it will form a glass upon rapid cooling. It has not been shown that glass formation is reliant on any particular physicochemical property (Yu 2001). However, it is widely accepted that (most) liquids, if subjected to a sufficiently fast cooling rate, will form a glass. In the majority of cases however crystallisation occurs, and a crystalline solid results.

In comparison to a crystalline system, amorphous systems are not at equilibrium and thus possess higher internal energy. This, therefore, dictates that the activation energy required to promote molecular motions in an amorphous system is smaller than in a crystal. It is expected that the amorphous state is more physically unstable than the crystalline, but more chemically reactive. Upon heating, for example, amorphous glasses possess more complex kinetic and enthalpic relaxation processes than crystalline systems. Heating of a glass through the T_g into the rubbery state and then through the Tm to the liquid state, results in the need for rigorous analysis when using thermal methods.

1.4.2.3 Polyamorphous Solids

The theory of polyamorphicity is controversial and originates from the fact that although amorphous materials lack long-range order, they do exhibit short-range order. Where there is order, there is the possibility of different types of order and as such the possibility of different amorphous phases is plausible. Examples of materials which exhibit two or more glass transitions are not uncommon, particularly in the field of polymer science. The explanation for such experimental observations is the existence of regions of polyamorphicity within the same sample. Unlike crystalline polymorphs, it is difficult to isolate and differentiate a polyamorph via a measurable physical property such as T_g (T_m in the case of crystalline polymorphs); making it difficult to fundamentally 'prove' the existence of polyamorphicity.

1.5 SECONDARY RELAXATIONS

Secondary relaxations are thermal events that occur before primary transitions; in terms of their position on the temperature scale, and/or the frequency at which they occur, i.e. secondary relaxations occur at lower temperatures, or lower frequencies, than primary transitions (Vyazovkin and Dranca 2006).

The theoretical descriptions, and most experimental observations, of secondary relaxations are based on the amorphous state (particularly in polymeric systems). The glass transition is considered the primary transition and any lower temperature thermal events are considered secondary relaxations; sometimes termed β-relaxation processes. Primary transitions are characterised by global, cooperative motions; whereas, secondary relaxations are considered non- (or low-) -cooperative, localised motions (Jimenez-Ruiz et al. 2009; Bhattacharya and Suryanarayanan 2009). A dichotomy also exists between the Arrhenius dependence of the relaxation times associated with the glass transition and secondary relaxations. The relaxation times of the glass transition (commonly thought to be around 100 s) do not exhibit an Arrhenius type dependence, and are therefore instead commonly described using the Vogel-Tammann-Fulcher equation (Crowley and Zografi 2001). The relaxation times of secondary relaxations, on the other hand, are currently thought to adhere to an Arrhenius type dependence (Bhattacharya and Suryanarayanan 2009).

The nature of secondary relaxations at the molecular level is unclear. It is commonly believed that secondary relaxations result from intra-molecular motions, i.e. side-chains, hydrocarbon 'back-bones', or functional groups (Smith and Bedrov 2007). However, it has also been suggested that the rotation of entire molecules can also manifest themselves in the form of secondary relaxations. Perhaps the most notable explanation of secondary relaxation phenomena was proposed by Johari and Goldstein in 1970 in the reporting of their studies involving simple rigid molecules.

As mentioned, the majority of research in the field of secondary relaxation phenomena focuses on the amorphous state of polymers. The second most popular field by research output are secondary relaxations in LOMs. The least reported, and perhaps the newest emerging field of secondary relaxation research is that of crystalline LOMs; the focus of the research reported herein (based on anecdotal evidence, no such data has been published).

Unlike their amorphous counterparts, secondary relaxations in the crystalline state are rarely reported, and therefore poorly understood. In the last decade, or so, several authors have utilised TSC techniques for the study of LOMs and have thus began to study crystalline LOMs; reporting their findings via original research manuscripts (Moura Ramos et al. 2005; Shmeis and Krill 2005; Diogo et al. 2007; Chamarthy and Pinal 2008).

Lack of the 'traditional' primary transition, i.e. the glass transition, in the crystalline state warrants the need for a different type of primary process to be selected as the primary

transition/relaxation. Currently there are no 'rules' or generally accepted practices for determining the primary transition in crystalline materials. In light of this, some authors prefer not to classify non-cooperative slow molecular mobility in the crystalline state as a secondary relaxation; although by virtue of its position on the temperature/frequency axis (relative to an assumed primary transition) they should possibly be considered as such.

Throughout this thesis, the primary transition in crystalline materials will be considered the lowest temperature phase transition (e.g. melting, sublimation, solid-solid transition), or, the lowest temperature chemical process (e.g. degradation) if a phase transition does not occur, or is preceded by a chemical process. Any lower temperature events (most likely, those detected by TSC spectroscopy) will be considered secondary relaxations.

1.6 SOLID STATE ANALYSES

Solid-state analysis techniques can be generally divided into two fields: structural-spectroscopic and thermal-analytical. Structural spectroscopy concerns itself with deriving the exact structure (or sometimes lack of) of solids; i.e. their arrangement in space/bonding properties. Thermal analysis utilises the influence of changes in temperature to detect and characterise changes in structure and/or (less frequently) the chemical reactivity/stability of solids. It is therefore easy to reconcile how these two groups of techniques complement each other, but equally why they are considered separate fields.

1.6.1 Structural techniques

The information in Table 1.1 provides an overview of a range of commonly used structural techniques in the physical characterisation of LOMs. Such techniques are generally described as probing the solid at the molecular level (properties of individual molecules), particulate level (properties of individual solid particles) or the bulk level (properties of an assembly of particles). A combination of techniques is therefore required to comprehensively understand the solid properties of a given material; as such 90% of the published studies use at least two solid-state techniques. The median number of techniques used is four; with at least one molecular level and one particulate level technique included (Chieng et al. 2011).

Table 1.1 Overview of some commonly used solid-state structural analytical techniques.

TECHNIQUE	THEORETICAL PRINCIPLE	DATA/INFORMATION ACQUIRED	POSITIVE FEATURES	NEGATIVE FEATURES
Powder x-ray diffraction (PXRD)	A single beam X-ray is directed at the sample where atoms absorb some energy and coherently scatter it at the same λ as the incident radiation. Diffraction of the x-rays is described by the Bragg equation: $n\lambda = 2d\sin\theta$ where λ is the wavelength, d is the distance between diffracting planes and θ is diffraction angle. The measurement output is the distance between diffracting planes in relation to 2θ.	• Unique diffraction pattern for crystalline samples • Lack of diffraction pattern for amorphous samples • Quantitative amorphicity/crystallinity • SCXRD allows for the determination of crystal structure, i.e. atomic arrangement in space	• Non-destructive • "fingerprint" technique •Qualitative and quantitative • Can be combined with a variable temperature accessory • SCXRD provides an in-depth understanding of the crystalline state	• Large sample size required • "preferred orientation" a common issue • Only sensitive to the crystalline phase - high limit of detection for the amorphous phase • SCXRD requires a large high purity crystal which can be difficult to obtain
Single crystal x-ray diffraction (SCXRD)				
Mid-infrared spectroscopy (MIR)	Molecular vibrational spectroscopy technique which measures the IR radiation absorbed by molecular bond vibrations. Absorbed frequencies correspond to vibrational modes within the molecule. IR data is acquired by the generation of an interferogram, converted to an absorption/transmittance spectrum via Fourier transformation.	• Different molecular environments possess unique vibrational modes • H-bonding • Peak shifting/broadening identifies amorphous/polycrystalline forms	• Small sample size • Rapid throughput technique • ATR accessory allows rapid analysis if solid samples • Can be combined with a variable temperature accessory	• Highly moisture sensitive • Requires consistent atmospheric conditions • Poor sensitivity and selectivity • Some sampling methods are time consuming
Terahertz pulse spectroscopy (TPS)	Generated pulsed terahertz radiation is directed onto the sample. Lattice vibrations in the crystalline sample cause a change in the electric field of the incident radiation, as a result of absorption and dispersion. The ratio between the incident and transmitted field strengths are then calculated and converted into absorption spectra.	• Intra-molecular and lattice vibrations • Unique peaks/bands for crystalline forms • No spectral features for amorphous phases	• Small sample size • Rapid throughput technique • Can be combined with a variable temperature accessory	• Only sensitive to the crystalline phase - high limit of detection for the amorphous phase • Highly moisture sensitive
Raman spectroscopy	Inelastic scattering of monochromatic light is used to observe rotational, vibrational and other low-frequency modes.	• Wavenumber spectrum • Intramolecular and lattice modes • Peak shifting/broadening identifies amorphous/polycrystalline forms	• Non-destructive sampling • Little or no sample preparation • Can be combined with a variable temperature accessory	• Sample fluorescence causes significant issues • Intense light can cause photo-degradation of certain sample types

Solid-state nuclear magnetic resonance spectroscopy (SS-NMR)	Measures the spin properties of atomic nuclei in the presence of a strong magnetic field. Radio frequency radiation is applied to raise nuclei to a higher potential energy resonance state where energy is re-emitted at a specific resonance frequency specific to the chemical environment of the nuclei.	• Molecular information derived from nuclei environments • Conformational information • Structural elucidation • Can provide information about secondary relaxation processes complementary to some thermal techniques	• Large number of available nuclei (typically ^{1}H or ^{13}C) • Non-destructive sampling • Qualitative and quantitative • Can detect and characterise secondary relaxations	• Expensive • Slow data acquisition • Expert knowledge required
Time-of-flight secondary ion mass spectrometry (TOF-SIMS)	Pulsed particle beam is focused onto the sample and the impact removes chemical species from the surfaces of the material surfaces. Generated species at the impact sites are positive and negative ions (primary ions) and those generated farther from site of impact are parent or molecular ions (secondary ions). These species are accelerated into a flight path to the detector. The time taken from the impact to the detector is recorded.	• Provides chemical image of specific components over a two-dimensional area of the sample	• Provides information about the chemical distribution on a solid surface • Qualitative and quantitative information	• Cannot differentiate between solid forms • Irradiation may cause sample degradation
Scanning electron microscopy (SEM)	High energy electron beam is focused onto the sample. Electron-sample interaction results in the dissipation of this energy, generating secondary ions. These secondary ions are detected and information generates SEM image of the sample.	• Topographical properties • High resolution images	• Small sample size • Higher resolution of solid morphology than microscope	• Sample preparation and stage condition set up (vacuum settings) is required • Large and expensive
Atomic force microscopy (AFM)	Measures the forces acting between a fine tip and a samples surface. During experiments a tip attached to the free end of a cantilever is brought very close to the surface of the sample (distance between the probe and sample surfaces is usually in the order of angstroms). Positive or negative bending of the cantilever is realised when the interaction of the fine tip of the cantilever with the sample results in repulsive or attractive forces. The bending of the cantilever is detected by a laser beam reflected from the backside of the cantilever.	• Topographical map of sample surfaces • Interaction forces and mechanical properties at the nanoscale	• Wide range of materials can be analysed • Provides a 3-dimensional image of the sample surface • Does not require any special pre-treatment as in SEM • Possible to achieve atomic level resolution of sample surfaces	• Relatively slower scan speed • Forces on sample can cause distortion, tip wear and sample damage

1.6.2 Thermal Analysis (TA)

TA is one of the principal groups of techniques for the physical and chemical characterisation of LOMs. TA provides information regarding the chemical properties (mainly purity and degradation) and the physical properties (those relating to 'physical structure') of materials (Craig 2007). 'Physical structure' is the study of the arrangement of molecules (usually known) and the events associated with changes in those physical arrangements (Craig 2007). This is generally achieved via the use of well-established (classical) solid-state thermal methods such as TGA, DSC, HSM, dynamic vapour sorption (DVS) and dynamic mechanical analysis (DMA) (Table 1.2)

Such classical TA techniques are predominantly (but not exclusively) used to study primary transitions in the high-temperature region (HTR). More novel, less established thermal techniques such as TSC spectroscopy are also used to study primary transitions in the HTR. TSC spectroscopy is particularly useful in the study of glass-forming amorphous materials. However, the main 'selling-point' of TSC spectroscopy is its ability to be used to study secondary relaxations in the low-temperature region (LTR) of both crystalline and amorphous materials.

Table 1.2 Overview of some commonly used TA techniques.

TECHNIQUE	THEORETICAL PRINCIPLE	DATA/INFORMATION ACQUIRED	POSITIVE FEATURES	NEGATIVE FEATURES
Thermal gravimetric analysis (TGA)	Used to measures the mass of a sample as it is subjected to a temperature programme in a controlled atmosphere. Temperature programmes can be simple linear profiles or complex high resolution/modulated methodologies.	• Mass loss as a function of time and/or temperature • Levels of hydration/solvation • Physical/chemical stability • Kinetics of mass loss processes	• Small sample size • Qualitative and quantitative • Some overlapping processes can be resolved • Contained sampling allows for analysis through phase transitions • Atmospheres can be changed during analysis • No previous knowledge of sample required • No specialist training necessary	• Destructive sampling • Limited to the detection of processes involving mass loss • Kinetic analysis is time consuming • Not sensitive to secondary relaxations
Differential scanning calorimetry (DSC)	Used to measures a difference in heat flow rate between a sample and reference pan as they are both subjected to the same temperature programme. Thermal events are registered as endo- or exo-thermic peaks in a thermogram.	• Heat flow and/or heat capacity as a function of temperature and/or time • Physical and chemical stability • Polycrystalline form determination • Kinetic analysis is possible	• Small sample size • Fast data acquisition • Qualitative and quantitative • Sensitive to all thermal events, including secondary relaxations • Contained sampling allows for analysis through phase transitions • No specialist training necessary	• Destructive sampling • Analysis atmosphere must remain constant • Measurement cell contamination is a common issue • Some previous knowledge of sample properties must be known • Difficult/impossible to separate overlapping thermal events • Sensitivity to glass transitions and secondary relaxations is limited
Modulated temperature - DSC (MT-DSC)	Similar to standard DSC but utilises sinusoidal heating methodologies to resolve time/temperature dependent events.	• Same as standard DSC • The global DSC thermogram is split into reversing and non-reversing curves • Time/temperature dependent events may appear in only one curve	• Small sample size • Can separate certain thermal events • Particularly useful in the study of amorphous materials	• Modulated methodology is time consuming • Extensive previous knowledge of sample is essential • Specialist training is required
Hot stage microscopy (HSM)	Optical analysis of a sample as it is subjected to a controlled temperature programme.	• Crystallinity • Birefringence • Morphology • Crystal habit	• Small sample size • Minimal sample preparation • Fast data acquisition • No specialist training necessary • No previous knowledge of sample required	• Destructive sampling • Difficult/impossible to separate overlapping thermal events • Not sensitive to secondary relaxations • Uncontrolled atmosphere (in most cases)

Dynamic mechanical analysis (DMA)	Used to measures the deformation response of a sample subjected to a controlled sinusoidal stress/strain programme at a single temperature or whilst subjected to a temperature programme.	• Mechanical properties • Viscoelasticity • Physical stability • Secondary relaxations	• Sometimes non-destructive sampling • Sensitive to low enthalpy transitions (i.e. glass or sub-glass) • Only technique to provide mechanical data	• Sample preparation more complex • Cannot be used to measure certain phase transitions • Uncontrolled atmosphere (in most cases)
Dielectric thermal analysis (DETA)	The dielectric response of a sample to a periodic electrical field at variable frequencies at a fixed temperature, or variable temperatures at a fixed frequency is ascertained.	• Dipolar current as a function of electrical field frequency and/or temperature • Dielectric properties • Viscoelasticity • Physical stability • Secondary relaxations •Molecular mobility	• Sometimes non-destructive sampling • Sensitive to low enthalpy transitions (i.e. glass or sub-glass) • Unique dielectric measurements • Sensitive to all thermal events, including secondary relaxations • Can undertake time/temperature independent measurements • Second greatest measurement resolution of techniques mentioned here	• Complex sample preparation • Limited to dielectric samples • Functionality of non-isothermal measurements is limited • Cannot experimentally resolve cooperative relaxation processes • Difficult/impossible to separate closely neighbouring/overlapping spectral peaks • Specialist training is required
Thermally stimulated current spectroscopy (TSCS)	Used to measures the dielectric response of a sample to a static (but adjustable) electrical field whilst it is subjected to a controlled temperature programme.	• Dipolar current as a function of time and/or temperature • Dielectric properties • Viscoelasticity • Physical stability • Secondary relaxations •Molecular mobility	• Sensitive to low enthalpy transitions • Sensitive to all thermal events, including a very high sensitivity to secondary relaxations • Greatest measurement resolution of all techniques mentioned • Comparatively lowest equivalent frequency of all thermal techniques • Simultaneous dielectric and thermal measurements • Can experimentally resolve cooperative relaxation processes • Can separate closely neighbouring and overlapping spectral peaks • Thermal windowing and relaxation map analysis allows for a very thorough analysis of sample properties	• Complex sample preparation • Limited to dielectric samples • Specialist training is required • Cannot be used to measure certain phase transitions • Extensive previous knowledge of sample is essential • Sample reproducibility is an issue • Dipolar currents must be distinguished from other spurious dielectric behaviour • Data acquisition and post analysis processing is/can be time consuming

1.6.3 Comparison of TSC spectroscopy and other instrumental techniques

1.6.3.1 TSCS and dielectric spectroscopy

DEA is an alternative form of dielectric spectroscopy and is the closest technique to TSC spectroscopy. The defining difference between the techniques is that in TSC spectroscopy static electrical fields are used as opposed to periodic electrical fields in DEA. Both techniques share common attributes in that they utilise electrical fields, measure current and can be used as a function of temperature. However, several limitations exist as to how each of these attributes can be utilised and in turn afford practical advantages and disadvantages for each technique (Table 1.3).

Table 1.3 Comparisons between DEA and TSC techniques.

	TSC	DEA
Temperature	• Can scan temperature ranges in a single experiment • Can build complex temperature programmes	• Generally has to be used in isothermal mode/step changes • In non-isothermal mode electrical field must remain constant
Electrical field	• Limited to static electrical fields which can only be varied in strength and time applied • Frequency cannot be changed so relies on non-isothermal methods to exploit time/temperature dependence of relaxations	• Periodic electrical fields allow for a greater number of experimental variables • Frequency can be altered to study an extended/specific frequency range avoiding dependence on time/temperature
Resolution	• Higher resolution	• Lower resolution
Equivalent frequency	• Lower equivalent frequency means greater separation of closely neighbouring peaks	• Higher equivalent frequency • Unable to separate closely neighbouring peaks or those with similar activation energies
Cooperative relaxation processes	• Can be separated and/or isolated	• Cannot be separated and/or isolated

[a]Perceived advantages in blue/disadvantages in red.

TSC and DEA are both considered ‘low (equivalent) frequency’ techniques in comparison to a calorimetric technique such as DSC. However, TSC has a lower equivalent frequency, a higher resolution and a lower noise level than DEA. It has been shown that a typical TSDC experiment is equivalent to a low frequency dielectric loss experiment, with an equivalent frequency of 10^{-5} Hz or lower (Saffell et al. 1991) (Figure 1.5). This often means that TSC spectroscopy is the favoured technique. In reality these two techniques rarely complement each other and one is nearly always used in preference to the other.

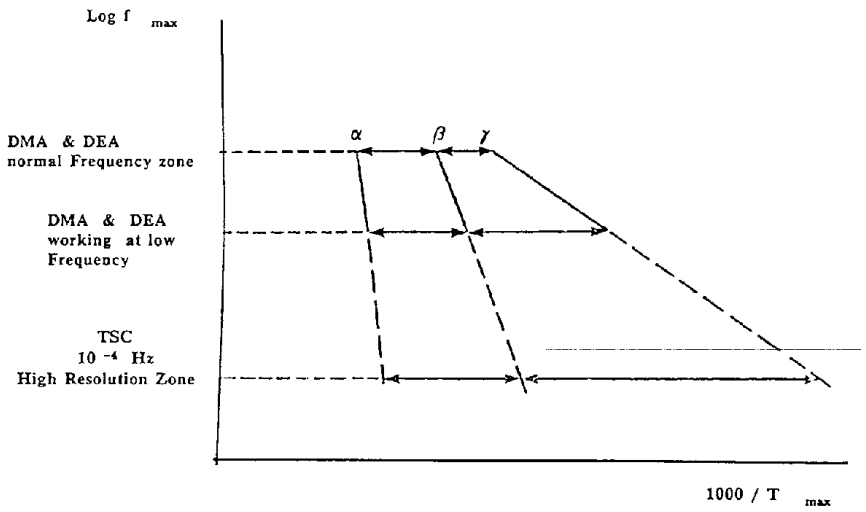

Figure 1.5 Comparison of the resolution obtained from DEA at normal and low frequencies and TSC experiments (reproduced from Saffell et al., 1991).

1.6.3.2 TSC and DSC

TSC and DSC are complementary techniques; they can both be used to detect similar transition phenomena and are used in preference to each other in detecting and characterising, other, instrument specific phenomenon (see Table 1.4).

A significant advantage of DSC is that it is a well-established and a highly developed technique; DSC hardware and software is far advanced in comparison to TSC spectroscopy. Due to a significantly larger DSC user base, considerably more supporting literature is available. Such advances in DSC technology have permitted it to become a 'user friendly' technique status; it can generally be operated effectively with no specialised training. TSC spectroscopy on the other hand requires specialist training and detailed knowledge to be used effectively.

DSC and TSC are commonly used to study the glass transition (T_g), but detect it in very different ways. DSC is reliant on a change in heat capacity as a material passes through the T_g. Heat capacity changes during the T_g are often very small in LOMs; especially in weak glass formers. T_g's can therefore be difficult (or impossible) to detect by DSC as the change in heat capacity can sometimes be close to, or smaller, than the instruments limit of detection.

This is never an issue in TSC spectroscopy, as the glass transition is measured by detecting visco-elastic changes as a material passes through the T_g range. No matter how small the heat capacity change, there is always a measurable change in the visco-elastic modulus. A further issue that may be encountered with DSC is the phenomena of enthalpic relaxation which can occur at temperatures or time periods soon after the T_g. Should this occur it is often impossible to characterise the T_g and modulated DSC must be employed to resolve the global DSC curve into its kinetic and heat capacity components. This process is time consuming, requires specialised instrumentation and a thorough understanding/competency level on the part of the user.

DSC and TSC are also commonly used to study secondary relaxations in crystalline and amorphous LOMs. Secondary relaxations, and their possible relationship to primary transitions, are of contemporary scientific interest. The equivalent frequencies of measurement of TSC and DSC afford an explanation as to their effectiveness in studying secondary relaxations; which typically involves 'subtle' changes in physical arrangement and are subsequently 'fast' in relation to a primary transition. A typical DSC and TSC experiment has an equivalent frequency of 0.01 to 0.1 Hz and 10^{-3} to 10^{-5} Hz, respectively (Saffell et al. 1991). The lower equivalent frequency of TSC spectroscopy means it is able to capture 'fast' relaxations more effectively than DSC (Saffell et al. 1991). Secondary relaxations also involve very small changes in heat capacity; therefore, similarly to the detection of the T_g, they may be difficult to detect by DSC. When studying the glass transition itself, or any sub-glass phenomena, TSC is generally the superior technique.

1.6.3.3 TSC spectroscopy and TGA

TGA cannot be directly compared to TSC, but the two techniques are complementary. Mass loss during a TSCS experiment is highly undesirable due to contamination of the instrument, its effects on data quality and loss of sample-electrode contact. For this reason, TGA is essential to ensure any physical or chemical processes which may involve a mass loss in the sample are fully characterised prior to introduction to the TSC instrument. The results obtained from TGA experiments, therefore often dictates the temperature limitations of TSC analysis.

Table 1.4 Comparisons between DSC and TSC[a].

	TSC	DSC
Technology	• Niche technique: hardware and software has undergone less development	• Very popular technique. Hardware and software is more advanced
User friendliness	• Specialist training and advanced knowledge is required for effective use	• No specialist training or knowledge is required for general use
Sample preparation	• Can be more time consuming but a single sample is used numerous times • Few, or no, consumables are used	• Generally faster per sample but more samples are generally required • A new disposable pan must be used for each sample. Pans are expensive
Cell design	• Utilises a flushing system; no gas flow during experiments meaning cell contamination is an issue • Large cell size means less efficient heating, less temperature control and slower heating/cooling	• Utilises a flow cell; cell contamination is less likely • Cells have been miniaturised allowing for tight temperature control and faster heating/cooling rates
Equivalent frequency	• Much lower equivalent frequency • Can capture fast relaxation processes (i.e. secondary relaxations)	• Higher equivalent frequency • Often unable to capture fast relaxation processes
Sensitivity to amorphous	• Highly sensitive to glass transitions; specifically viscoelastic changes throughout	• Less sensitive to glass transitions as relies on small change in heat capacity

[a]Perceived advantages in blue/disadvantages in red.

1.6.3.4 TSC spectroscopy and XRD

TSC spectroscopy is not a structural technique in the sense that a structure can be derived from the data obtained, or in referencing a spectrum to identify a material; TSC spectra are not unique enough to do so. However, TSC data can be used to directly compare some information with those obtained by structural spectroscopy; mainly in the quantitative sense.

XRD relies on the diffraction pattern of crystalline materials to identify them and their structure (Chieng et al. 2011). Although not sensitive to the amorphous phase, it is represented in an XRD diffractogram as a 'halo' above the baseline. The ratio of the halo to the intensity of the crystalline peaks can be used to quantify the amorphous and crystalline phase. XRD can therefore be used to assess the degree of crystallinity (DOC) of a sample.

There is concern, particularly in the pharmaceutical industry, in quantifying the DOC. Concern has arisen as it has been shown that even small amounts of amorphous material in a crystalline bulk phase can have profound effects on physicochemical properties (Chieng et al. 2011). This unease is amplified as many of the common structural techniques are relatively insensitive to small amounts of amorphous material (several percent) (Yu 2001). This is the case with XRD; although there are examples of low limits of detection the technique can generally not maintain such low limits with most samples.

As previously mentioned, TSC is sensitive to the detection of the amorphous phase and so could prove invaluable in this area. Additionally, the TSC data output is quantitative. Few quantitative TSC studies have been undertaken; but those that have, have reported a limit of detection as low as 2% for amorphous lactose (Galop and Collins 2001). With a greater investment of time in this area, TSC could potentially become the primary technique for measurements of low amorphous content in a bulk crystalline phase.

Another point of contention is the phenomena of microcrystalline materials. Such materials have been milled rigorously to produce a particle size so small they show few traces of crystallinity by XRD (Yu 2001). This often leads to the question: is the material microcrystalline or amorphous? TSC spectroscopy could potentially offer an answer to such a question by probing the material for the presence of a glass transition. The presence of a glass transition is not guaranteed as the material may be in the rubbery state; but if one is found the material can be considered amorphous.

Another area where structural techniques such as XRD can be ineffective is when studying the phenomena of polyamorphicity, i.e. the presence of more than one amorphous phase or region within the same sample. As mentioned, XRD is not sensitive to the amorphous phase besides a distorted baseline; therefore it cannot possibly distinguish amorphous phases. There have been examples where TSC spectroscopy has been used to detect two glass transitions within the same sample, i.e. two distinct regions of amorphicity (Shmeis 2004).

1.7 RESEARCH OBJECTIVES

The major objective of the research presented in this thesis is to develop TSC spectroscopy as a novel instrumental technique for the study of LOMs; particularly in relation to secondary relaxation phenomena. The focus will be placed upon the detection and characterisation of secondary relaxations in crystalline materials; emphasising, in particular, the mechanisms and nature of secondary relaxations and their relationship to the primary transition.

CHAPTER 2: MATERIALS AND METHODS

2.1 MATERIALS

Details of the materials used in the research reported in this thesis are as follows.

Material:	**β-Alanine**	Supplier:	BACHEM, UK
Product code:	F-1110	Lot No:	1028713
Purity/Grade:	≥ 99.5%		

Material:	**Benzamide**	Supplier:	SIGMA-ALDRICH, UK
Product code:	150762-1G	Lot No:	02716AH
Purity/Grade:	≥ 99.9%		

Material:	**D-α-Alanine**	Supplier:	BACHEM, UK
Product code:	F-1100	Lot No:	1030819
Purity/Grade:	≥ 99.5%		

Material:	**Ethanol**	Supplier:	SIGMA-ALDRICH, UK
Product code:	459828-1L	Lot No:	41696KM
Purity/Grade:	HPLC/spectrophotometric grade		

Material:	**L-α-Alanine**	Supplier:	BACHEM, UK
Product code:	E-1285	Lot No:	1029564
Purity/Grade:	≥ 99.5%		

Material:	**Paracetamol**	Supplier:	SIGMA-ALDRICH, UK
Product code:	A3035	Lot No:	051M5015
Purity/Grade:	≥ 99.5%		

Material:	**Salicylic acid**	Supplier:	SIGMA-ALDRICH, UK
Product code:	10591-0	Lot No:	S57066-059
Purity/Grade:	≥ 99.5%		

2.2 SAMPLE PREPARATION METHODS

Unless otherwise stated, all samples were used as received with the exception of light 'grinding' (section 2.2.1) or tableting for TSC analysis (section 2.2.2).

2.2.1 Light 'grinding'

The term 'grinding' is applied loosely as it generally conveys the idea of harsh treatment of a material. In this instance extreme care and caution was taken during the 'grinding' process to ensure minimal pressure was applied to the material; negating any negative effects on the sample. Light 'grinding' by hand was used in an attempt to homogenise samples which contained large 'lumps' or crystals to improve sample homogeneity (in terms of morphology) and therefore sample contact (with sample vessel) and/or for ease of tableting. Rather than being ground to a fine powder, sample 'lumps' were carefully 'broken up' to achieve a visually uniform, morphologically homogeneous sample.

2.2.2 Tableting for TSC analysis

A tablet press (MTCM-1 manual tablet compression machine (Globe Pharma, USA)) was used to prepare tablets of 8 mm in diameter, ~1.5 mm in thickness (accurately measured using a digital calliper) and 50.0 mg in mass. A force of 1000 kPa was applied for 30 s.

2.2.3 Preparation of physical mixtures

The required amount of each component was placed in a glass vial. If necessary, large 'lumps' or crystals were broken up using the method described in section 2.2.1. A lid was then placed on the glass vial before being secured onto a head-over-head wheel mixer for 24 hours. After 24 hours a clean spatula was used to mix the sample and remove any deposits from the side of the glass vial before being placed back in the mixer for a further 24 hours.

2.2.4 Preparation of the salicylic acid/benzamide co-crystal (CC)

The CC was prepared using the 'co-crystallisation via slow evaporation' method previously reported by Elbagerma et al., (2010). A 1:1 molar ratio mixture of salicylic acid (500 mg) and benzamide (428.50 mg) was dissolved in 75 mL of ethanol with slight warming until dissolution was complete. The filtered solution was then allowed to slowly evaporate at room temperature.

2.3 INSTRUMENTAL METHODS

The following section outlines the instrumental methods used, details of the instruments and the methods used for calibration. The experimental methods section gives an overview of the type of experiments used and the experimental variables. Details of the exact experimental conditions are given in the relevant experimental chapter for ease of reading/reference.

2.3.1 TSC spectroscopy

2.3.1.1 Instrument details

Instrument:	TSCII, Thermally Stimulated Current Spectrometer
Manufacturer:	SETARAM Instrumentation, France
Electrometer (internal):	6517A electrometer/high-resistance meter (Keithley, UK)
Cooling system (external):	900 series LN2 microdosing system (Norhof, Netherlands)
Software:	TSC/RMA software (SETARAM Instrumentation, France)

Cooling system

The liquid nitrogen (LN_2) cooling system pumps LN_2 from an LN_2 reservoir (aluminium Dewar) into the TSC instrument and around the exterior of the furnace housing. The microdosing system is controlled by a combination of outlet temperature (as LN_2 flow exits the instrument) and pressure (inside the Dewar). As a general rule the outlet temperature is set to 50°C below the lowest experimental temperature, T_o.

Flushing system

Upon introducing a sample the analysis chamber is flushed and filled with helium (He) gas via the use of a vacuum pump (external) and a compressed He supply (external). The chamber is evacuated and filled three times. The final fill stops at a pressure of *circa.* 1000 mbar. He is considered the ideal gas for TSC analysis as it has a suitable thermal conductivity coefficient over the temperature range of interest (-196 to 400°C).

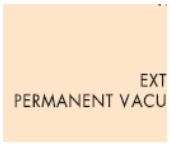

Figure 2.1 Cross-section of TSCII instrument (reproduced from TSCII user manual).

Electrode types

Three types of electrode are available for the TSCII.

Point and disc electrode-for use with tablets, discs and films (Figure 2.2). A pointed electrode attachment is used in combination with a disc containing a shallow hole on the top. This allows the surface area of the electrode to be increased and to maintain contact with flat samples. Sometimes the thin insulating sheets of poly(tetrafluoroethene) (PTFE) are used above and below the sample to maintain better contact and reduce artefacts which arise from poor sample-electrode contact.

Liquid/powder electrode-for use with liquids or powdered samples (Figure 2.3); this electrode consists of the point and disc electrode used in combination with a specially designed sample holder. The sample holder consists of two gold discs which sandwich a hollow ring of PTFE. The liquid or powdered sample is contained within the PTFE ring,

Calibration electrode-for use during calibration using indium. Consists of a disc electrode with a 'recess' and a PTFE cup. As the indium melts it contracts into the recess of the electrode to maintain contact.

Figure 2.2 Point and disc electrode used in combination with thin sheets of PTFE when analysing a tablet sample.

Figure 2.3 Liquid/powder electrode (inset: with lid removed to view PTFE ring and powdered sample).

2.3.1.2 Calibration

Calibration of the TSC spectrometer is undertaken experimentally using an indium reference material (supplied with instrument) and the calibration electrode (section 2.3.1.1.3). The objective of the calibration is to calculate a set of offset values to compensate for differences in temperature between the thermocouple and the sample area upon heating and cooling. To achieve this, the reference material is melted (upon heating) and crystallised (upon cooling).

The calibration method is outlined in Figure 2.4 and a typical calibration output is shown in Figure 2.5.

The experimental calibration data is automatically analysed by the TSC/RMA software such that the calibration offset values are calculated and automatically stored within the instrument. The calibration process is highly heating/cooling rate dependent and so is often repeated for a minimum of three different heating and cooling rates to obtain a range of offset values which are applicable to a range of heating and cooling scenarios.

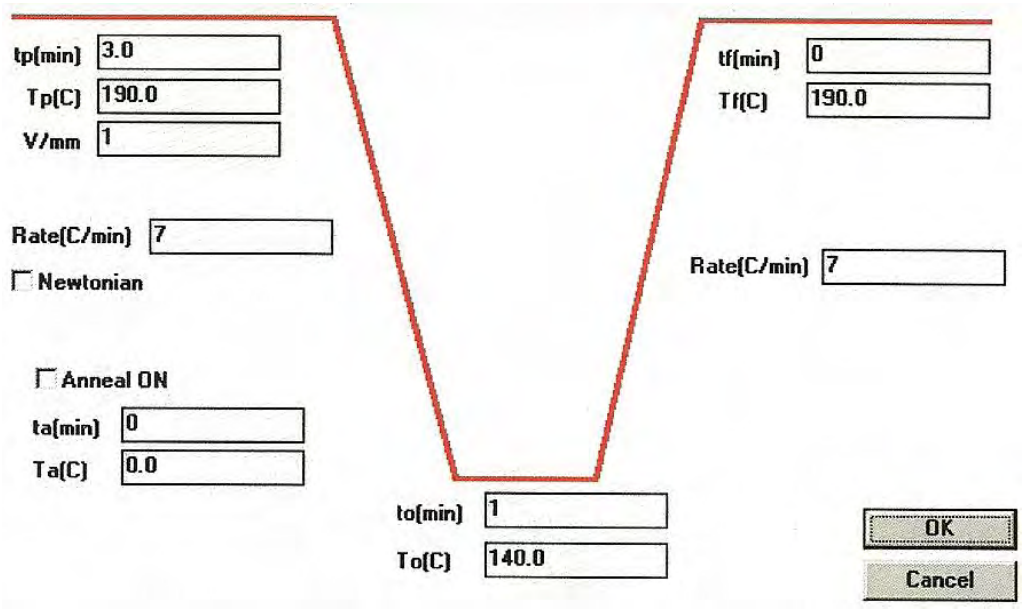

Figure 2.4 Calibration method (reproduced form the TSCII user manual).

2.3.1.3 Experimental methods

There are various types of TSC spectroscopy experiments. These experiments differ mainly by when the electrical field (E_p) is applied (if at all), and at which point the current is measured. Descriptions of the four most common TSC experiments are given in sections 2.3.3.1-2.3.1.3.4. Table 2.1 gives a guide to the experimental variables used in TSC experiments.

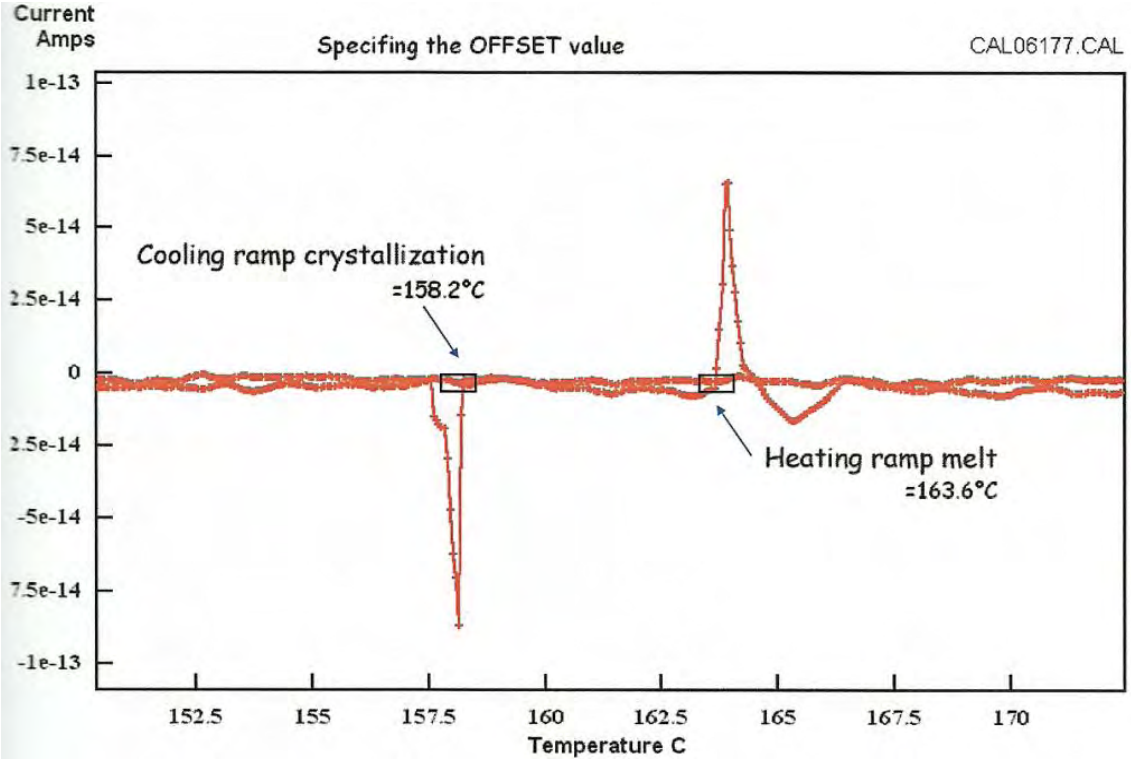

Figure 2.5 Typical TSC calibration output (reproduced from the TSCII user manual).

Table 2.1 Experimental variables for TSC spectroscopy methods.

Term	Meaning	Typical unit
E_p	Applied electrical field	V/mm
q	Heating rate (linear)	°C/min
q_c	Cooling rate (linear)	°C/min
T_a	Annealing temperature	°C
t_a	Time at T_a	min
T_f	Final experimental temperature	°C
t_f	Time at T_f	min
T_o	Lowest experimental temperature	°C
t_o	Time at T_o	min
T_p	Temperature of polarisation	°C
t_p	Time at T_p	min
T_w	Thermal window	°C
t_w	Time of thermal window	min

Spontaneous Depolarisation Current (SDC)

During an SDC experiment the sample is heated at a defined rate with no applied electrical field. This experiment is designed to assess the 'natural' motion of molecules within the

sample as a function of temperature and without external influence. A schematic of an SDC/TSPC experiment is outlined in Figure 2.6.

Experimental variables: T_o, t_o, q and T_f

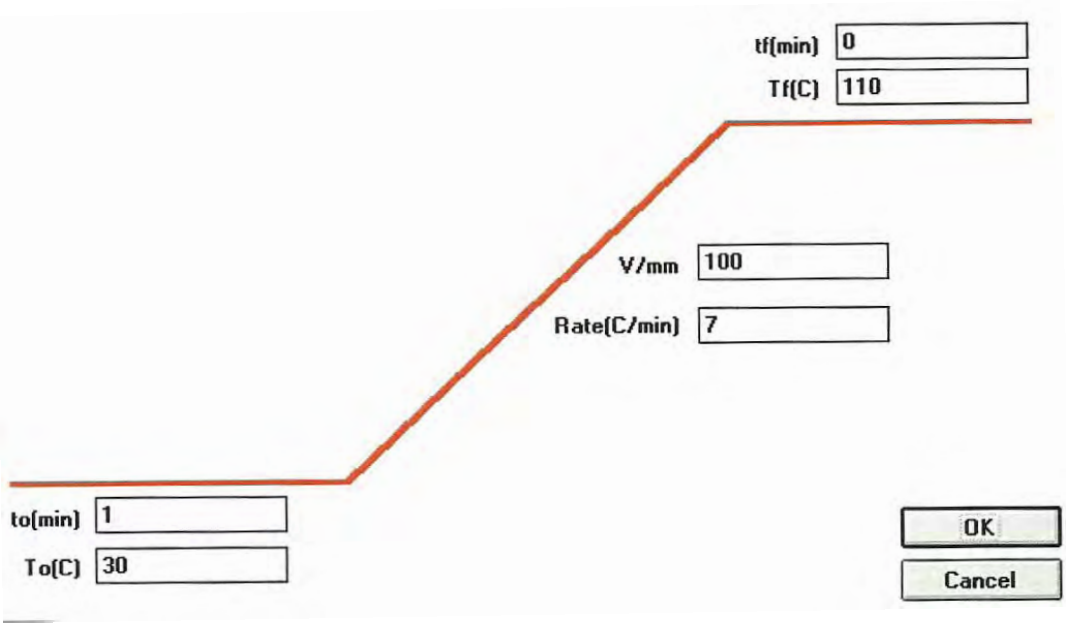

Figure 2.6 Schematic representation of an SDC/TSPC method. SDC involves no application of E_p whereas TSPC involves a constant application of E_p from T_o to T_f (reproduced from the TSCII user manual).

Thermally Stimulated Polarisation Current (TSPC)

A TSPC experiment is very similar to an SDC experiment (Figure 2.6) with the exception that an electrical field is applied after t_o at T_o and maintained throughout the duration of the experiment. TSPC experiments are designed to assess the influence of a constant electrical field on the motion of molecules.

Experimental variables: T_o, t_o, q, T_f and E_p

Thermally Stimulated Depolarisation Current (TSDC)

The theory of the TSDC experiment has already been mentioned in Chapter 1 (section1.4.2). From a practical point of view a TSDC experiment (Figure 2.7) involves initial polarisation of the sample, cooling of the sample to 'freeze in' the polarisation, and then release of the stored polarisation upon heating (i.e. depolarisation). TSDC experiments are designed to assess the influence of a previously applied electrical field to assess the

molecular mobility of the sample upon subsequent heating. TSDC is the most common form of TSC experiment. An additional annealing temperature and time can be incorporated into the TSDC method.

Experimental variables: t_p, T_p, E_p, q_c, t_a, T_a, t_o, T_o, q and T_f

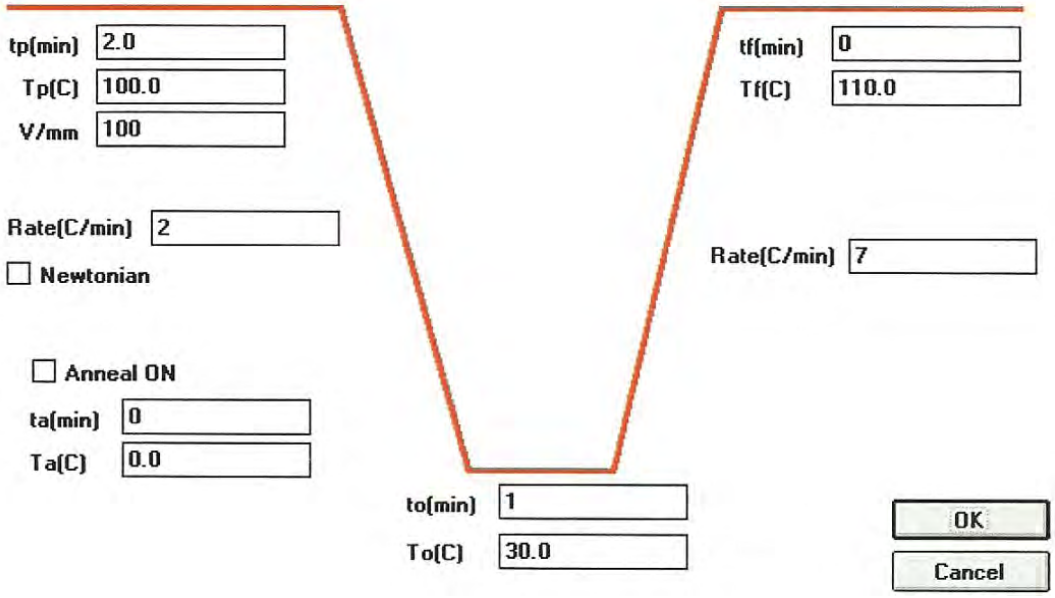

Figure 2.7 Schematic representation of a typical TSDC experiment (reproduced from the TSCII user manual).

Thermal Windowing (TW)

Thermal windowing (TW) is an advanced approach for analysing a TSDC peak in more detail. The global TSDC spectrum is a summation of each individual relaxation process and their distributions. TW consists of partial polarisation of samples and several 'steps' of isothermal depolarisation. It is essentially the same as the TSDC method with the addition of an early depolarisation step prior to cooling. In TW a sample is polarised at T_p for t_p and then cooled to T_d (isothermal depolarisation temperature). The sample is then depolarised at T_d for t_d and then cooled again to T_0. Temperatures T_p and T_d are usually quite close, 2-5^oC apart. The resulting depolarisation curve will (theoretically) represent a single, narrow distribution mode isolated from the global spectrum. This method of experimental deconvolution allows each separate process to be analysed as a single relaxation process using Arrhenius type expressions.

Repetition of the TW technique across the temperature range of the global TSDC peak allows for an entire series of deconvoluted spectra to be obtained (Figure 2.8). The data can then be processed using relaxation map analysis (RMA), an advanced software approach for analysing TW data.

A TW experiment is similar to a TSDC with the addition of a T_w after the polarisation stage (Figure 2.9). The T_w is usually small (1-5°C) and lasts typically 1-5 minutes. Prior to t_o, E_p is switched off and so the sample is allowed to depolarise at T_p - T_w. This is often the reason why TW experiments are referred to as partial polarisation or fractional polarisation experiments. The aim of a TW experiment is to experimentally observe those molecules polarised over a narrow temperature window; with the intention of experimentally observing a process with a single relaxation time. TW experiments are undertaken as a series of experiments rather than a single experiment; covering the temperature range of a known process which represents a distribution of relaxation times. The intention is to experimentally deconvolute the global transition into a series of elementary 'Debye-like' relaxation curves which (theoretically) represent a single relaxation time. These relaxation curves can then be analysed by the advanced technique of relaxation map analysis (RMA). Experimental variables: t_p, T_p, E_p, T_w, t_w, q_c, t_a, T_a, t_o, T_o, q and T_f.

Figure 2.8 Example of data obtained from a series of TW experiments. Solid lines represent TW relaxation curves. Dashed line represents data from the global TSDC experiment (reproduced from Correia, 2000).

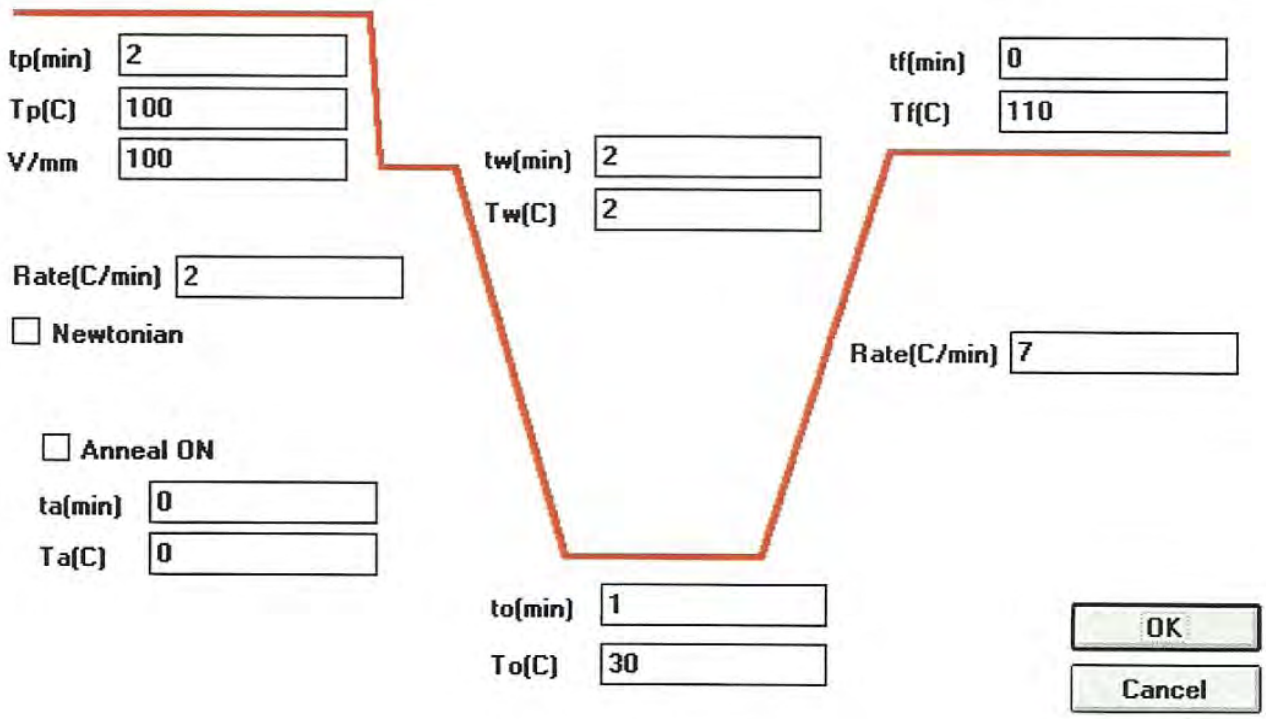

Figure 2.9 Schematic representation of a typical TW experiment (reproduced from the TSCII user manual).

2.3.2 ThermoGravimetric Analysis (TGA)

TGA is used to measure the mass of a sample as a function of temperature and/or time under a controlled atmosphere. This allows for mass loss/gain data to be collected during a controlled temperature/time experiment (Craig and Reading 2007). Mass loss can be due to evaporation, sublimation, desolvation and/or degradation processes, to name a few, whereas mass gains are commonly associated with oxidation or solvation processes (Hulse et al. 2009). TGA experiments are commonly undertaken under 'inert' atmospheres using nitrogen, helium or argon gas; unless oxidation or solvation is the intended aim where pure oxygen, 'dry/wet' air or steam is used (Rus et al. 2012).

A typical experimental TGA curve is shown in Figure 2.10. A thermogravimetric (TG) output is typically plotted as the first derivative *i.e.,* dTG *v* temperature in order to identify, more

easily, the number of mass loss processes and the temperature range over which they occur. From a pharmaceutical perspective, TGA is most commonly used to determine solvent content (via forced desolvation) or chemical degradation (via heating to high (relative) temperatures). The loss of volatiles via such processes is of paramount importance, particularly on an industrial scale (large loss of volatiles is a safety hazard), and on a smaller scale when interpreting data from other thermal techniques such as DSC (Craig and Reading 2007).

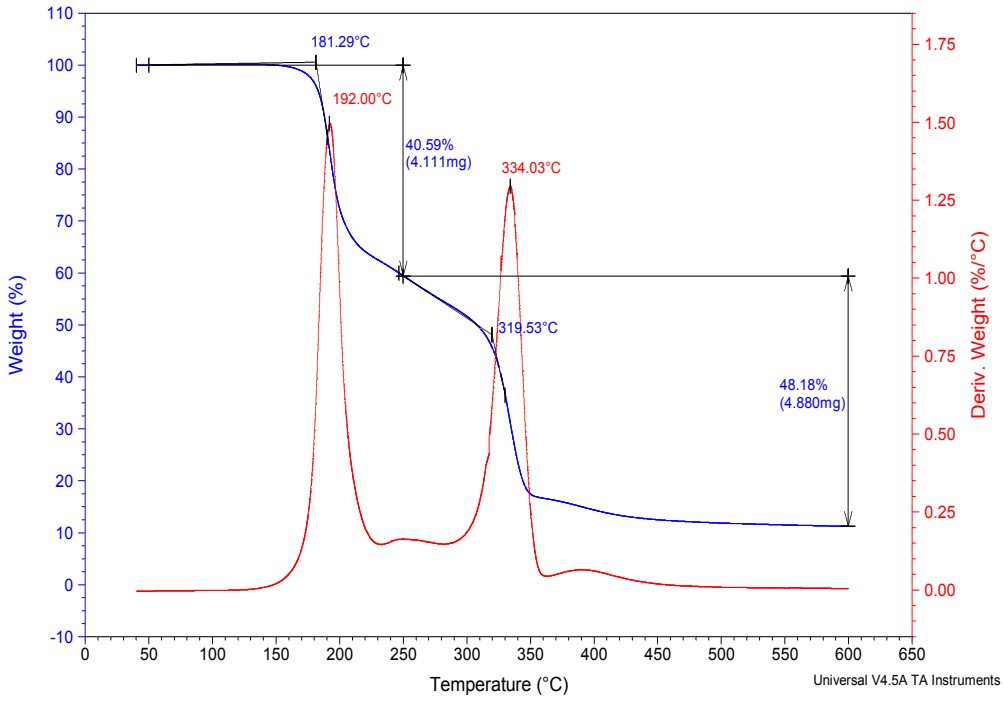

Figure 2.10 Typical experimental TGA output; TG curve (blue), dTG curve (red).

2.3.2.1 Instrument Details

Instrument:	TGA Q5000-IR ThermoGravimetric Analyser
Manufacturer:	TA Instruments, UK
Cooling system (internal):	Compressed air cooling/water circulator
Software (control):	TA Q Series (TA Instruments, UK)
Software (analysis):	TA Universal Analysis (TA Instruments, UK)

2.3.2.2 Calibration

Both TGA systems are calibrated for temperature using the Curie point method whereby a magnet is used to increase the apparent mass of a certified Curie point reference material. At

the material(s) Curie point a sharp apparent mass loss is observed and the extrapolated onset temperature calculated. This process is repeated for two reference materials (alumel and nickel (supplied with the instrument)). Onset values are entered into the software where the calibration offsets are automatically calculated and stored. The TGA(s) is also calibrated for mass using certified Class I reference weights.

2.3.2.3 Experimental methods

Samples are introduced to the instrument in aluminium sample pans (open or capped). An inert atmosphere is achieved via purging of the system with nitrogen gas.

2.3.3 Differential Scanning Calorimetry (DSC)

DSC measures the difference in heat flow rate between a sample and an inert reference as a function of temperature (and time). The inert reference is generally an empty, and identical, pan to that used to contain the sample. DSC essentially measures changes in heat flow (endothermic or exothermic) of the sample (Gabbott 2008). A typical DSC output is shown in Figure 2.11. Common exothermic events include phase changes upon heating (melt, evaporation, and sublimation), desolvation, and degradation; whereas common endothermic events include phase changes upon cooling (crystallisation, solidification) and re-crystallisation upon heating. Another common event observed by DSC is a 'step-change' in the baseline. This is indicative of a material passing through the glass transition and is caused by a change in sample heat capacity (Schick 2009; Braga et al. 2011).

DSC is the second most common solid-state technique employed within the pharmaceutical industry (Chieng et al., 2011) and as such instrumental development and associated theory is well developed and readily accessible. When combined with TGA, events observed by DSC can easily be defined as involving no, or some, loss of mass making assigning a particular process to an experimental thermal event much easier. However, if there is no loss of mass over the same temperature range as an experimental DSC transition, it is often difficult to assign a process without perhaps, visualising the sample as it is heated (e.g., by HSM).

2.3.3.1 Instrument details

Instrument:	DSC Q2000 Differential Scanning Calorimeter
Manufacturer:	TA Instruments, UK
Cooling system (external):	RCS90 Refrigerated Cooling System

Software: TA Universal Analysis (TA Instruments, UK)

2.3.3.2 Calibration

The DSC is calibrated for a 'cell constant' using an indium certified reference material (supplied with each instrument). The reference material is heated at a defined linear rate through its melting point. The experimental melting peak is analysed for the onset temperature and integral value of the peak. Inputting these values into the software allows calculation of the temperature offset and cell constant.

2.3.3.3 Experimental methods

DSC experiments utilise a pair of identical sample pans which are generally capped (or sometimes hermetically sealed). A sample is placed in one of the pans whilst the other is left empty. Both pans and sample are accurately weighed using an analytical balance. Advanced DSC software and the use of a cooling system allows for the use of elaborate experimental methodologies.

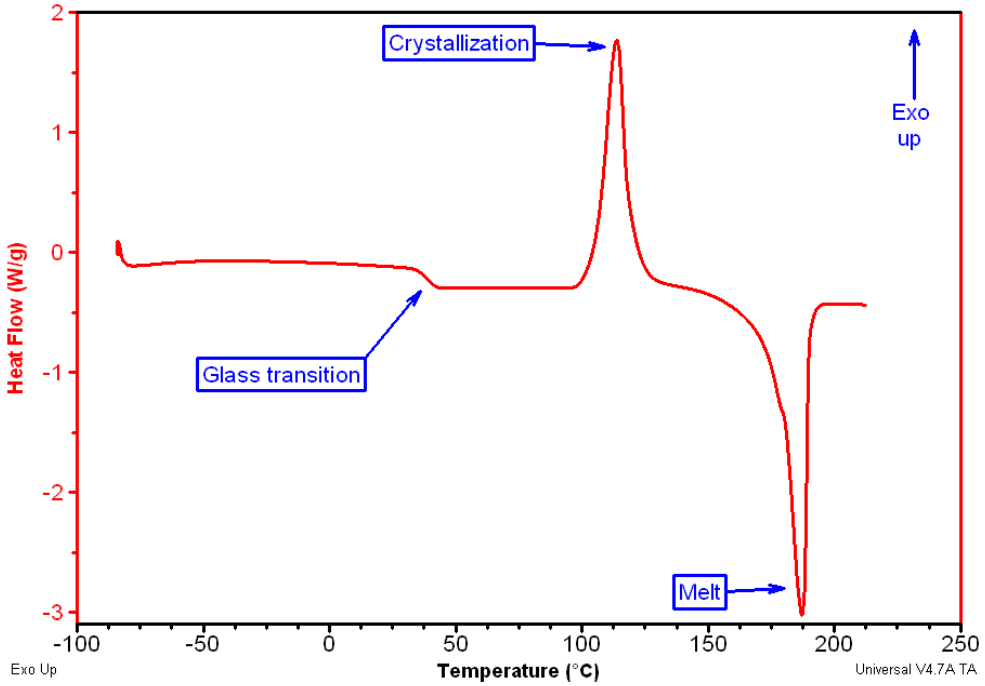

Figure 2.11 Typical DSC output (reproduced from TA Instruments user manual).

2.3.4 Hot-Stage Microscopy (HSM)

HSM is an imaging technique which allows the user to visualise a sample as it subjected to a temperature program. This is achieved via the use of a conventional microscope (and commonly a camera) with a 'hot-stage' (a small furnace with a viewing window). The use of HSM within the pharmaceutical arena is concentrated into two main areas. The first is as mentioned in the previous section using imaging to assign the peaks of a DSC experiment to a particular thermal process. The second is crystallisation studies. Often HSM is combined with plane polarised light filters to distinguish liquids from solids and between different crystalline forms (Craig and Reading 2007).

2.3.4.1 Instrument details

Hot-Stage:	FP82HT (Mettler Toledo, UK)
Controller/processor:	FP90 (Mettler Toledo, UK)
Microscope:	DME Model 13595 (Leica Microsystems, China)
Camera:	PL-A622 Firewire camera (PixeLINK, Canada)
Software (video capture):	Studio Capture 3.1 (Studio86Designs, UK)

2.3.4.2 Calibration

The hot-stage is calibrated for temperature difference between the thermocouple and the sample platform via the use of a certified calibration material which melts upon heating. Upon melting the material exhibits a large increase in transparency which is quantified via the light intensity readings from the microscope camera. A temperature offset is calculated and stored within the processing software. The microscope is calibrated for size using a reference graticule (supplied).

2.3.4.3 Experimental methods

Due to the lack of a cooling accessory, HSM experiments generally only involve controlled heating experiments with cooling often observed but at a slow rate. The sample is placed on a glass slide and housed within the furnace of the hot-stage.

CHAPTER 3: α-ALANINE

3.1 INTRODUCTION

α-Alanine (α-Ala) is the lowest molecular weight, naturally occurring chiral amino acid and, in the crystalline solid-state, adopts a zwitterionic form ($^{+}NH_3$-C_2H_4-COO). α-Ala exists in two stereoisomeric forms: D-α-Ala (D-Ala) and L-α-Ala (L-Ala). Both forms occur naturally and are found extensively throughout nature where they play important roles in the biology of almost all living organisms (Kumar et al. 2008).

Despite the abundance of Ala in nature, and its immense importance in biology, publications in the scientific literature pertaining to the analysis of Ala in the solid-state are sparse. A reasonable amount of literature relating to thermal studies of L-Ala exists, but no data are currently available in relation to the thermal analysis of D-Ala.

For L-Ala, only a single thermal degradation involving 95 to 100% mass loss over the investigated temperature ranges (-50 to 1200°C) is reported. TGA studies report degradation to occur over the temperature range 216 to 357°C (Table 3.1). As is evident from the data in Table 3.1 there is a discrepancy over which temperature range degradation occurs. This is most likely due to differences in instrumental design and/or sample preparation.

Table 3.1 TGA decomposition temperatures for L-Ala (from the scientific literature).

Decomposition temperature range (°C)	Reference
290 to 310	Caroline et al., 2009
216 to 357	Rodante et al., 1992

DSC studies report degradation to occur between 295 to 301°C (peak temperatures; Table 3.2).

A manuscript published in 2004 highlighted a surprising result in that the authors report a 'micro-transition' or 'breather' in L-Ala (a small change in specific heat capacity; less than 0.01 W/g) in the temperature range -30 to -27°C as reported by DSC (Barthes et al. 2004). This result was discounted in 2008 as it was not repeatable in a similar experiment (Kumar et al. 2008).

Table 3.2 DSC peak temperatures for the decomposition of L-Ala.

Peak Temperature (°C)	Reference
295	Caroline et al., 2009
299	Suriya Kumar et al., 2008
301	Rodante et al., 1992
295	Olaffson and Bryan, 1970
297	Olaffson and Bryan, 1970

Despite the publications concerning the solid-state thermal analysis of L-Ala, no such publications were found relating to D-Ala. It can only be assumed that this is because L-Ala is the more common stereoisomer, is easier to source, and from our current understanding the physical properties of stereoisomers in the solid-state should not differ (unless studied by techniques sensitive to chirality).

The rationale for the research reported in this Chapter was to utilise TSC spectroscopy as a novel technology in the hope of detecting secondary relaxations in α-Ala. Should they be detected, advanced TSC methodologies would be utilised to fully characterise the relaxation. Samples of both stereoisomers were selected for analysis, on the *premise* they should be identical in their physicochemical properties.

3.2 EXPERIMENTAL

3.2.1 Materials

α-Ala was purchased at a purity of ≥ 99.5% (Bachem, UK) and used as received. The identity of α-Ala ($C_3H_7NO_2$; α-aminopropanoic acid) was confirmed via elemental and $^{1}H/^{13}C$-NMR analysis and its purity by using MS-MS analysis.

3.2.2 TGA

TGA studies were conducted using a TGA Q5000-IR instrument (TA Instruments) calibrated via the Curie point method using Alumel and nickel certified reference materials. A nitrogen atmosphere at a flow rate of 25 mL/min was employed. Samples of ca. 1.5 mg were heated from 30 to 600°C at a scan rate of 10°C/min.

3.2.3 DSC

DSC experiments were undertaken using a DSC Q2000 instrument (TA Instruments) calibrated using an indium certified reference material. A nitrogen atmosphere at a flow rate of 50 mL/min was used. Accurately weighed samples of ca. 1.5 mg in standard "TZero" aluminium pans were heated from -90 to 600°C at a scan rate of 10°C/min.

3.2.4 HSM

HSM experiments were undertaken using a FP82HT hot stage instrument (Mettler Toledo, UK), FP90 controller (Mettler Toledo, UK) and a DME model 13595 microscope (Leica Microsystems, China). Studio Capture 3.1 software (Studio86Designs, UK) was used for image/data acquisition. Samples were placed on glass slides, covered with a glass cover slide and heated from ambient temperature to 350°C at a scan rate of 10°C/min.

3.2.5 TSC spectroscopy

TSC experiments were undertaken using a TSCII spectrometer (Setaram, France). Samples were introduced as freshly prepared tablets. The sample chamber was evacuated and flushed with helium three times prior to analysis to create an inert atmosphere and to improve thermal transfer throughout the cell. Experimental parameters used were as follows: T_o (lowest experimental temperature) = -100°C, t_o (time at T_o) = 120 s, T_f (final temperature) = 200°C, E_p (polarising electrical field) = 200 V/mm, $q_{(heat)}$ (dynamic heating rate) = 10°C/min, $q_{(cool)}$ = 'Newtonian', T_p (temperature of polarisation) = 140°C, t_p (time at T_p) = 120 s. Thermal windowing was undertaken over the temperature range of 80 to 180°C; T_w (thermal window) = 5°C, t_w (time of thermal window) = 120 s.

3.2.6 Optical rotation

Specific rotation measurements for D- and L-Ala were undertaken using a type AA-(6)5 polarimeter (Optical Activity Ltd., UK). Analyses were undertaken using D- and L-sucrose in deionized water as calibrants. The $\alpha \frac{20}{D}$ values were found to be -14.2 for D-Ala and +14.2 for L-Ala (c=2%) indicating that they were >99.5% pure enantiomers (in accord with literature values).

3.3 RESULTS

3.3.1 Thermal Analysis

Conventional thermal analysis utilising TGA, DSC and HSM was undertaken in an attempt to reproduce previously reported results and to study D-Ala in the solid state. The thermal gravimetric (TG) curves, and their derivatives with temperature (dTG), are presented in Fig. 3.1. L- and D-Ala exhibit very similar behaviours and it was not possible to differentiate the stereoisomers by TGA. The single process observed by TGA is characterised by an extrapolated onset temperature of 295°C (± 2°C), a peak temperature of 305°C (± 2°C) and a mass loss of 97.50% (± 0.5%). DSC analysis (Fig. 3.2) complements TGA results, where a single endothermic peak is realised at very similar temperatures to the mass loss event characterised by TGA (DSC extrapolated onset: 298°C (± 2°C), peak: 300°C (± 2°C)). No other thermal events were observed by DSC in the -90 to 600°C temperature range. HSM analysis of D- and L-Ala samples provided complementary information as it identified no melting takes place during the transition at *ca.* 295°C; implying a solid-state degradation or possible sublimation. This event is termed the 'primary transition' in α-Ala.

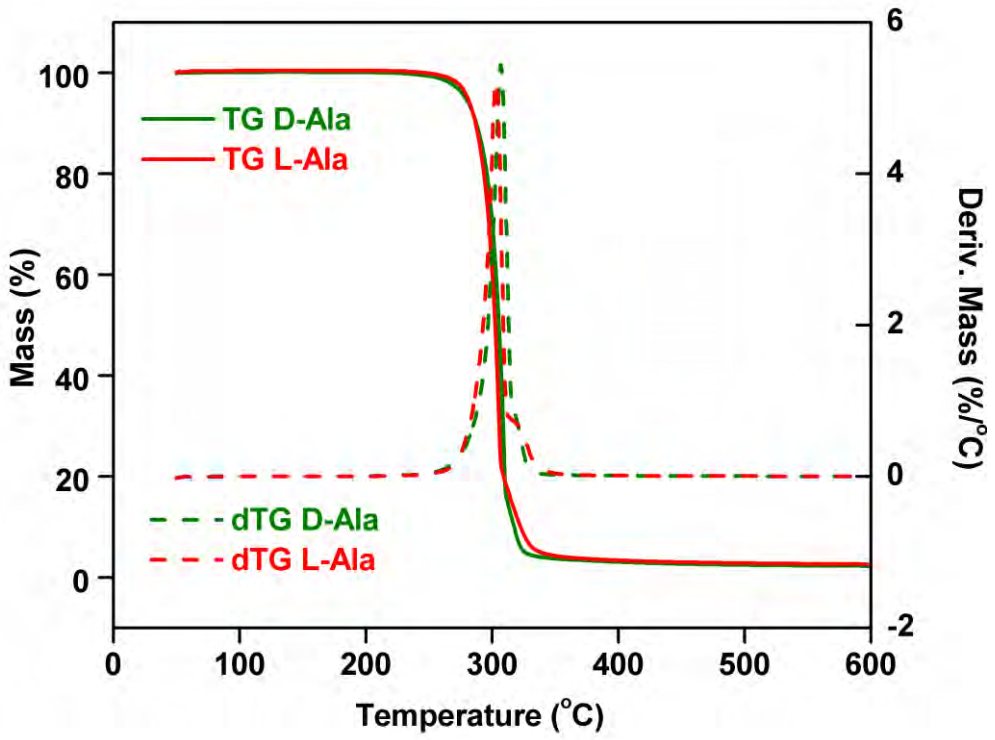

Figure 3.1 TGA outputs for α-Ala.

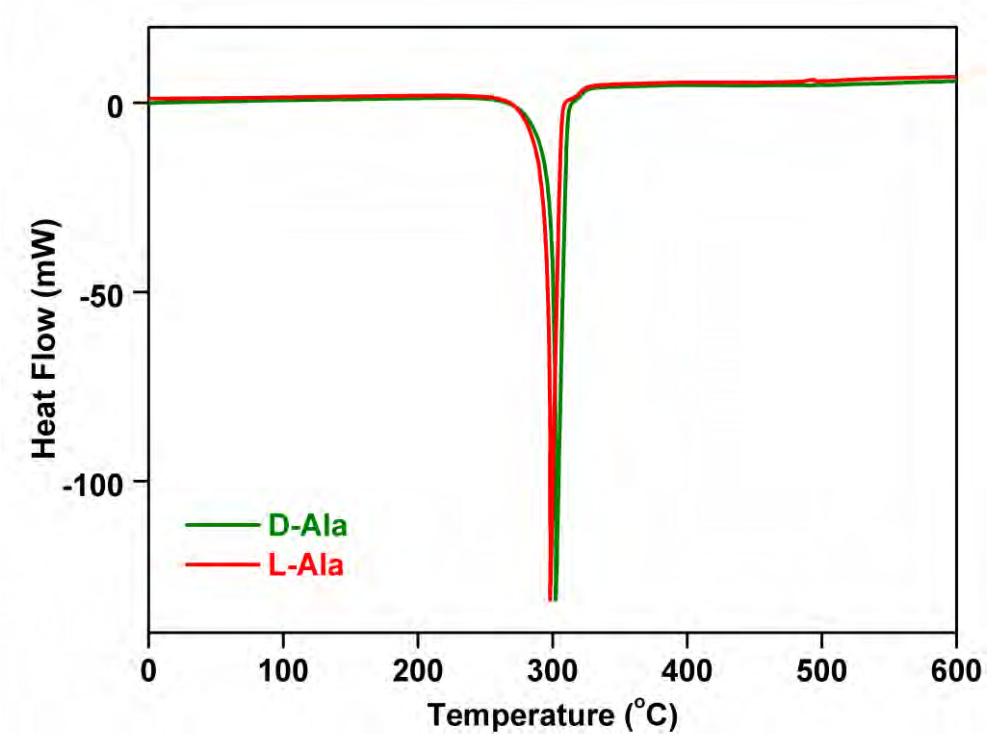

Figure 3.2 DSC thermograms for α-Ala.

3.3.2 TSC spectroscopy

Based on the results from thermal analysis an upper temperature limit of 200°C was imposed upon TSC experiments to protect against loss of volatiles during the primary transition. TSC spectroscopy was used to probe for secondary relaxations below 200°C and if any were found, to characterise them fully. Results of SDC experiments are presented in Fig. 3.3 where there is a deviation from the baseline at 125°C indicating a possible transition. Very interestingly, SDC experiments tentatively suggest stereoisomers can be differentiated; in this case D-Ala gives a positive, and L-Ala a negative, current signal. This trend was not realised in TSPC experiments (Fig. 3.4); where a similar process beginning at 125°C was identified. However, this is not unexpected as TSPC is essentially a 'driven' technique whereby a stimulus is applied throughout the experiment; forcing molecules to align with the field rather than displaying their natural motion (as they would in an SDC experiment).

TSDC experiments (Fig. 3.5) were undertaken using polarisation temperatures just above the start of the transition observed by SDC/TSPC (T_p = 140°C) where global relaxation peaks at T_{max} = 145°C (± 3°C) were realised; differentiation of stereoisomers was not possible.

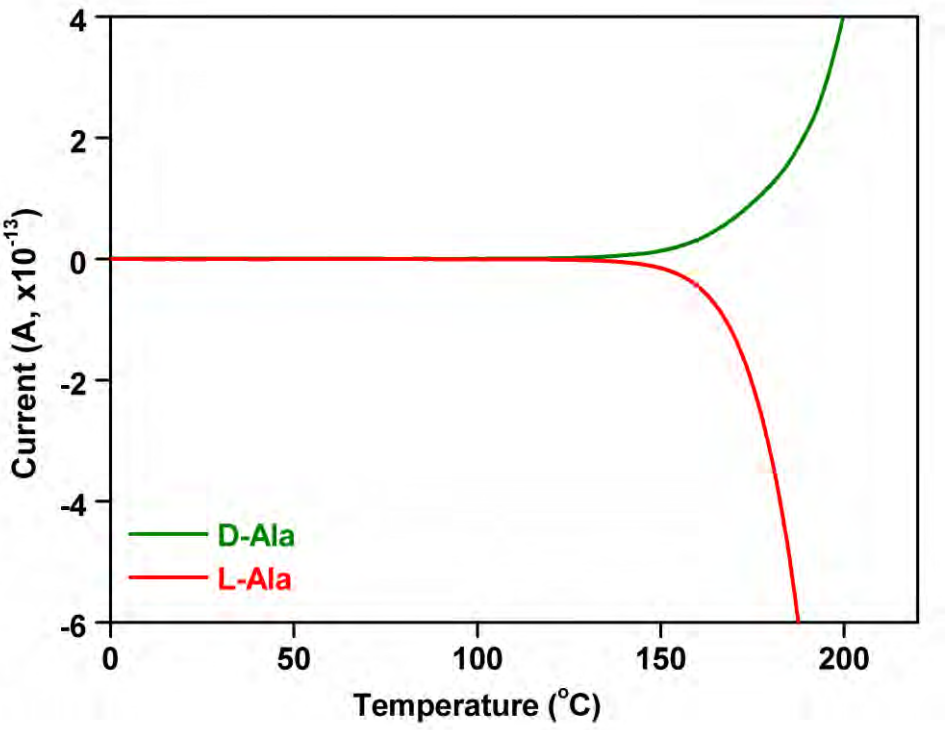

Figure 3.3 SDC curves for α-Ala.

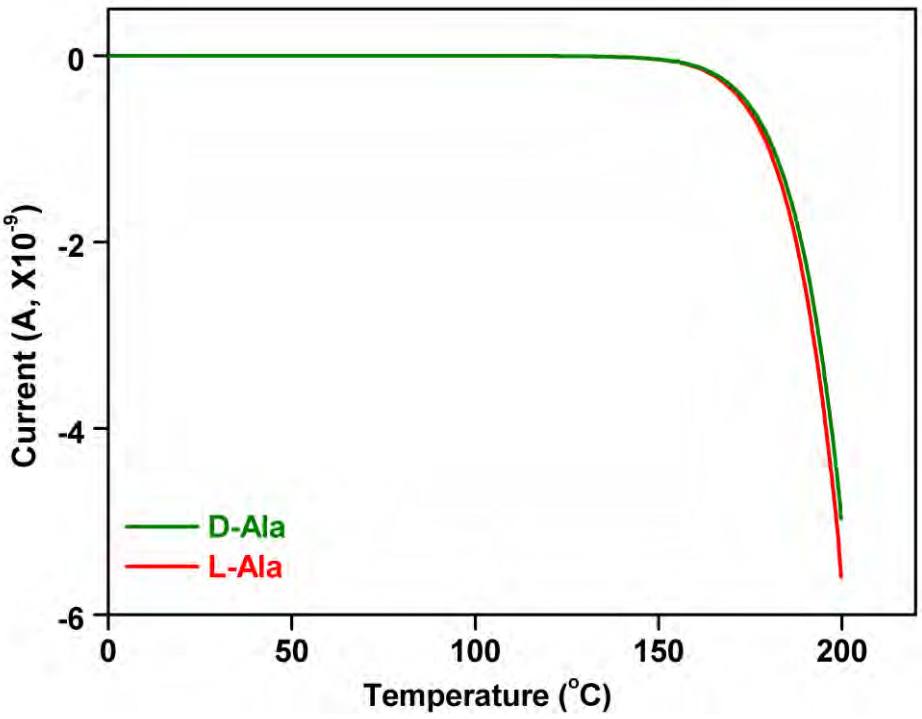

Figure 3.4 TSPC curves for α-Ala.

TSDC experiments utilising different polarisation electrical field strengths (Figs. 3.6, 3.7) were undertaken to identify whether the transition is a true dipolar relaxation or an anomalous current caused by space-charge or Maxwell-Wagner-Sillars type phenomena (Diogo et al. 2007; Antonijevic et al. 2008). The relationship between normalised applied electrical field (E_f (V/mm)) and the magnitude of the maximum current (I_{max}(A)) is linear for a dipolar process (Williams 1975; Vanderschueren and Gasiot 1979). Plots of I_{max} *vs.* E_f show linear relationships with R^2 values of 0.999 for both D- and L-Ala; proving that the process observed by TSC arises from dipolar motion and is not an artefact of sample discontinuity or poor sample-electrode contact.

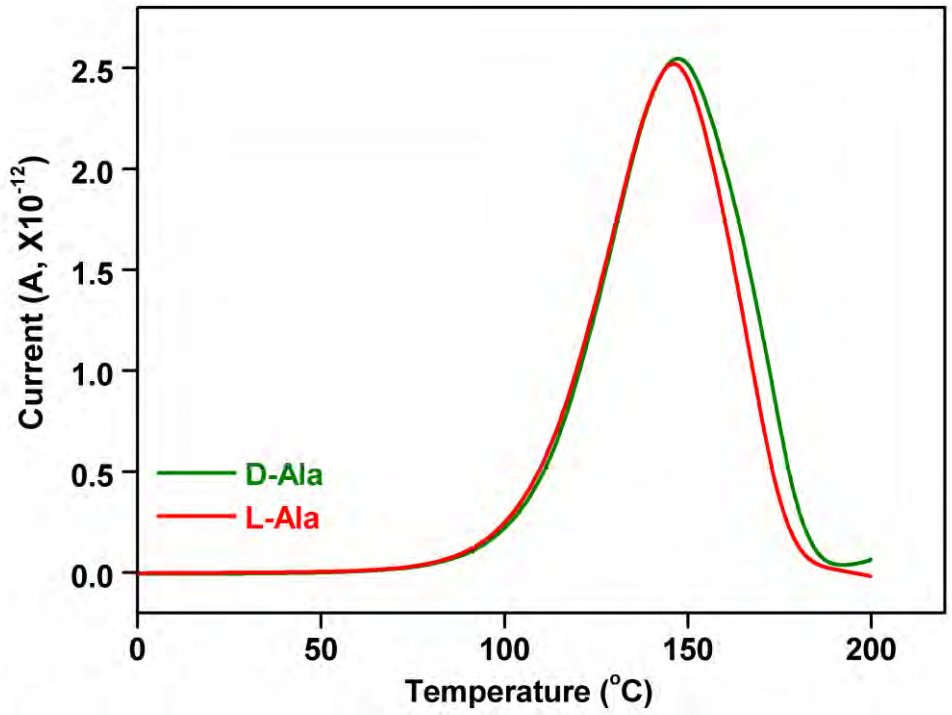

Figure 3.5 TSDC curves for α-Ala (T_p = 140°C).

TSC spectroscopy can therefore, definitively, be used to detect a secondary relaxation in α-Ala; beginning at about 40°C with a T_{max} of 145°C (± 3°C). TSC data has also hinted that the technique *may be* stereoselective; this is evident in SDC experiments (Fig. 3.3) and also in TSDC experiments (Fig. 3.5, post 180°C).

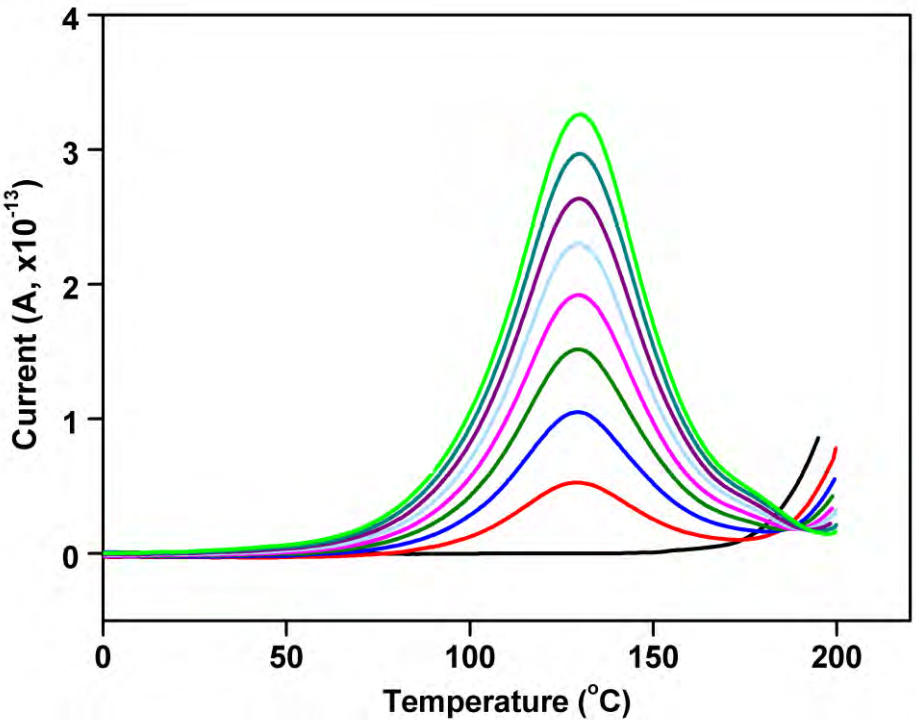

Figure 3.6 TSDC curves for D-Ala at different strengths of E_f (T_p = 120°C).

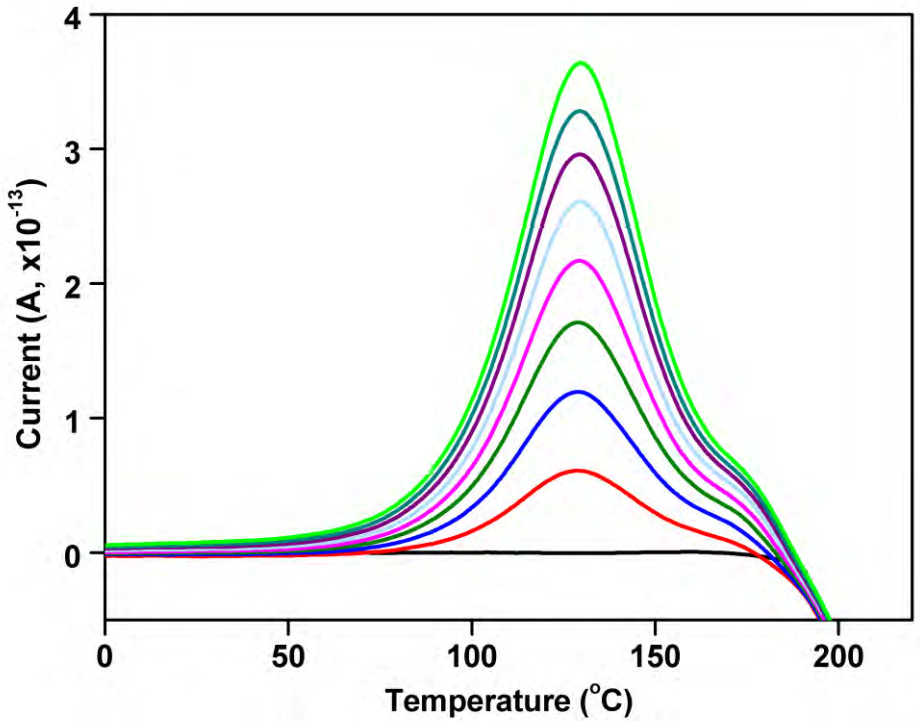

Figure 3.7 TSDC curves for L-Ala at different strengths of E_f (T_p = 120°C).

3.3.3 Thermal windowing and compensation analysis

The global relaxation process identified by TSDC is likely to be the result of many underlying motions each with its own single, or a narrow distribution of, relaxation time(s). The thermal windowing (TW) methodology utilises a series of narrow temperature windows of polarisation (5°C) to experimentally deconvolute a global relaxation process into elementary relaxation spectra. Theoretically, each TW relaxation curve represents a process with a single relaxation time; in reality, a narrow distribution of relaxation times (Correia et al. 2000). TW data is shown in Fig. 3.8 and the associated 'Bucci plot', generated by relaxation map analysis (RMA) (Williams 1975) is presented in Fig. 3.9. The results of the TW experiments shows some differences in the relaxation behaviour of D- and L- forms of Ala; notably in the intensity of the current signal. The foregoing suggests the secondary relaxation of D-Ala involves a larger displacement of dipole moments compared to L-Ala.

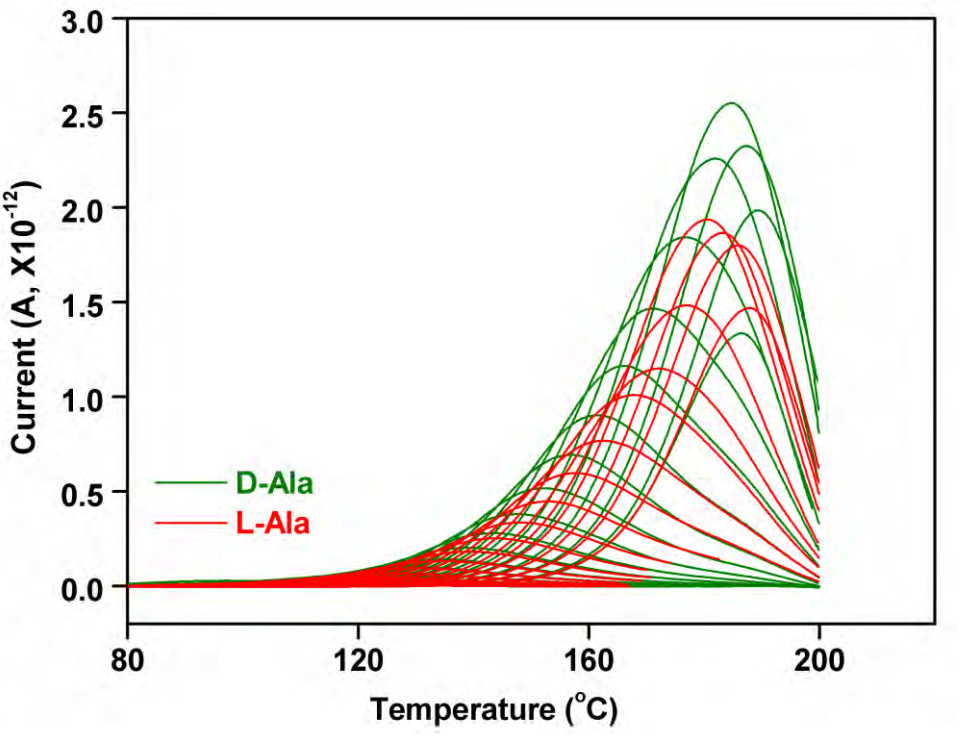

Figure 3.8 TW curves for α-Ala.

Many experimental parameters can be elucidated using RMA including dielectric, thermodynamic and kinetic data. Of notable contemporary interest is the compensation behaviour observed in LOMs (Neagu and Neagu 2003; Moura Ramos et al. 2007; Moura Ramos et al. 2008) a phenomenon widely observed and reported, but still undefined in its

behaviour and origin (Ferrante and Gorski 2012; Meloun and Ferenčíková 2012; Remizov and Skochilov 2012; Starikov and Nordén 2012).

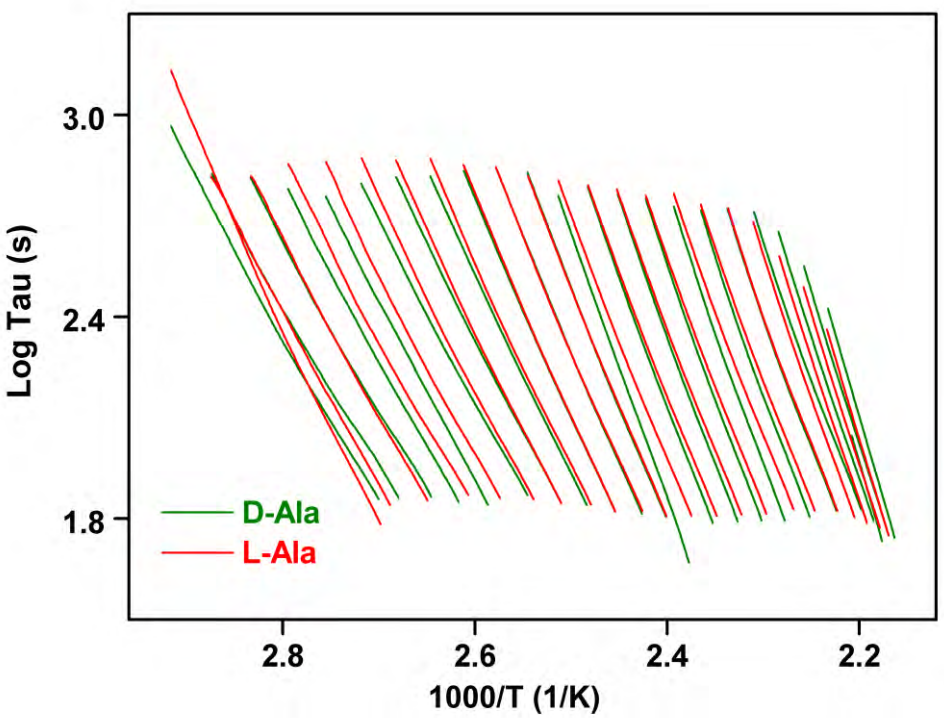

Figure 3.9 'Bucci plot' presenting relaxation curves for α-Ala.

Compensation analysis (Fig. 3.10) identified two distinct groupings of compensation points resulting in two compensation domains, A and B. The parameters for each compensation domain are presented in Table 3.3; there are some clear distinctions between stereoisomers. Compensation domain A shows very different compensation temperatures (T_c) for D- and L-Ala (greater than 50°C difference) and very different relaxation times at the compensation point (L-Ala is an order of magnitude faster than D-Ala). Similarly, the degree of disorder (DOD) values of 48-54 suggests moderate disorder and a scenario where molecular mobility is likely to be hindered by interactions with neighbouring molecules (Ibar 1991). Via compensation analysis it is possible to reproducibly and distinctly differentiate stereoisomers of α-Ala. Compensation domain B shows a similar trend to A whereby the T_c of D-Ala is significantly lower (*ca.* 20°C) than that of L-Ala, and the relaxation time of L-Ala is much faster than D-Ala. DOD values are slightly smaller for domain B and suggest the system may be less disordered at the lower compensation temperature of domain B.

The significance of the compensation temperatures is not fully understood, and is tentatively linked to the primary transition. All calculated T_c values are in the region of 214 to 300°C

and fall within the experimentally (TGA/DSC) observed transition region of 240 to 350°C; where values below 240°C are plausibly representative of potential onset values during isothermal experiments.

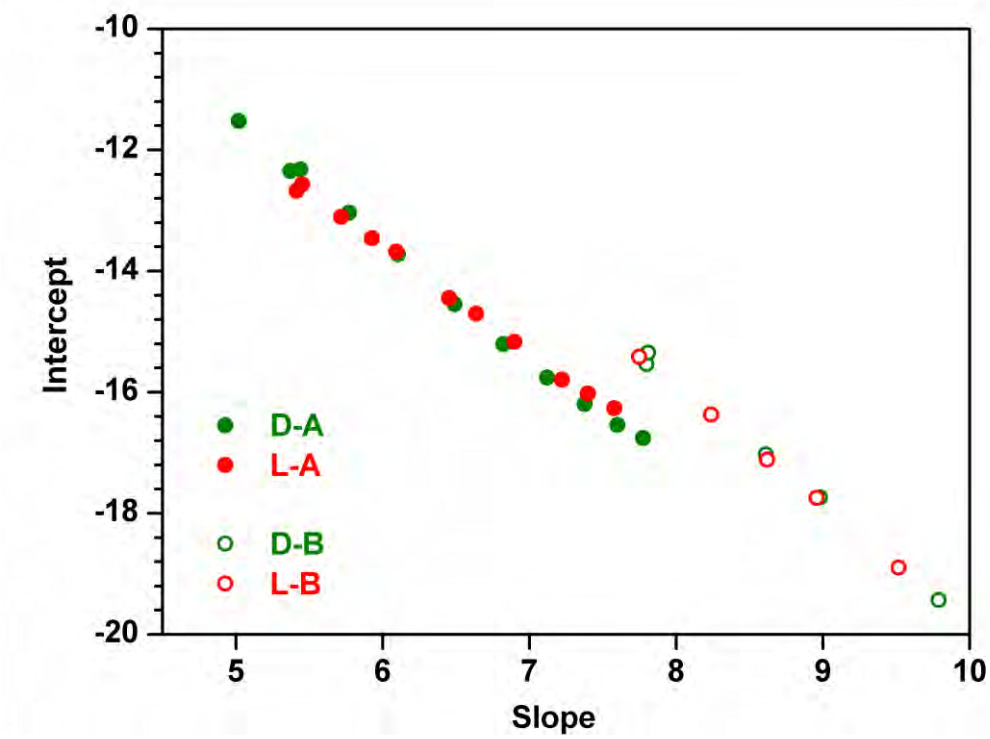

Figure 3.10 Compensation plot for α-Ala.

Table 3.3 (A) Compensation parameters for domain A (T_p = 80 to 130°C)

(B) Compensation parameters for domain B (T_p = 160 to 180°C)

(A)	D-Ala	L-Ala
R^2	0.998	0.999
T_c (°C)	243	300
τ (s)	0.0271	0.0018
DOD	48	53

(B)	D-Ala	L-Ala
R^2	0.999	0.999
T_c (°C)	214	236
τ (s)	4.5604	0.6397
DOD	37	41

Figs. 3.11 and 3.12 show thermodynamic parameters determined from RMA experiments, where classic linear relationships among Gibbs free energy and enthalpy/entropy changes are apparent (Neagu and Neagu 2003). This type of behaviour is fairly common and is a prerequisite for enthalpy/entropy compensation behaviour. A plot of ΔH *vs.* T_m (Fig. 3.13) shows that the calculated data points for compensation domain A lie close to the zero entropy prediction indicating non-/low-cooperative relaxations, considered to arise from local motions (Correia et al. 2000). The cooperativity increases with T_m, to a point where the relaxation may be considered cooperative. Compensation domain B deviates from the zero entropy prediction at all temperatures and may be considered to arise from cooperative motions.

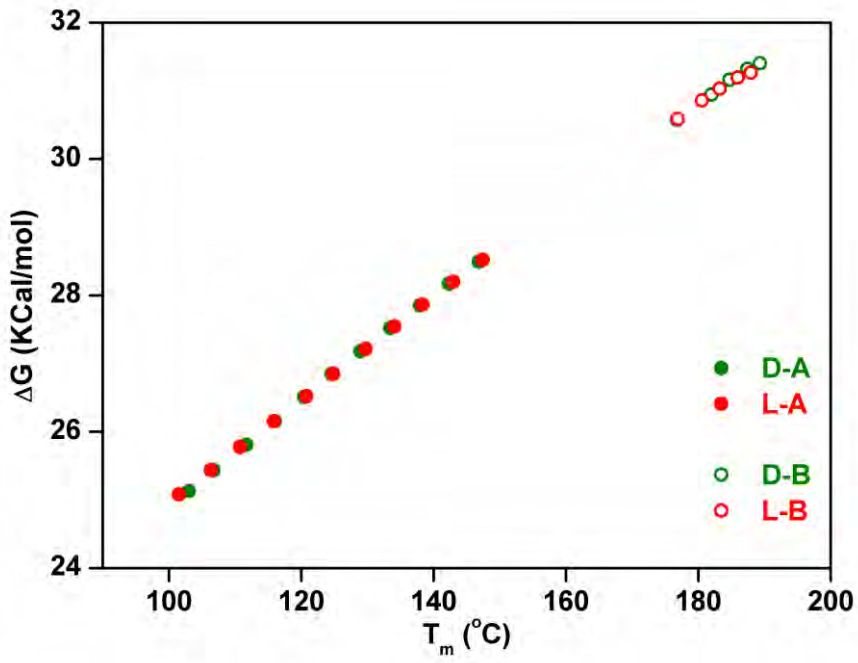

Figure 3.11 Gibbs free energy as a function of peak temperature for α-Ala.

The data presented above identifies how experimental and computational TSC methodologies may be utilised to not only detect secondary relaxations, but to use the knowledge derived from them to understand the nature of the secondary relaxation and its intrinsically linked relationship with other thermal events, such as the primary transition. It is suggested that molecular mobility in the solid-state begins with localised, non-cooperative motions at lower temperatures (represented by compensation domain A, Fig. 3.13, 95 to 120°C, points below the zero entropy prediction), leading to a gradual increase in cooperativity (represented by compensation domain A, Fig. 3.13, 120 to 150°C), until a fully cooperative region is

achieved (represented by compensation domain B, Fig. 3.13, 170 to 190°C, points above the zero entropy prediction).

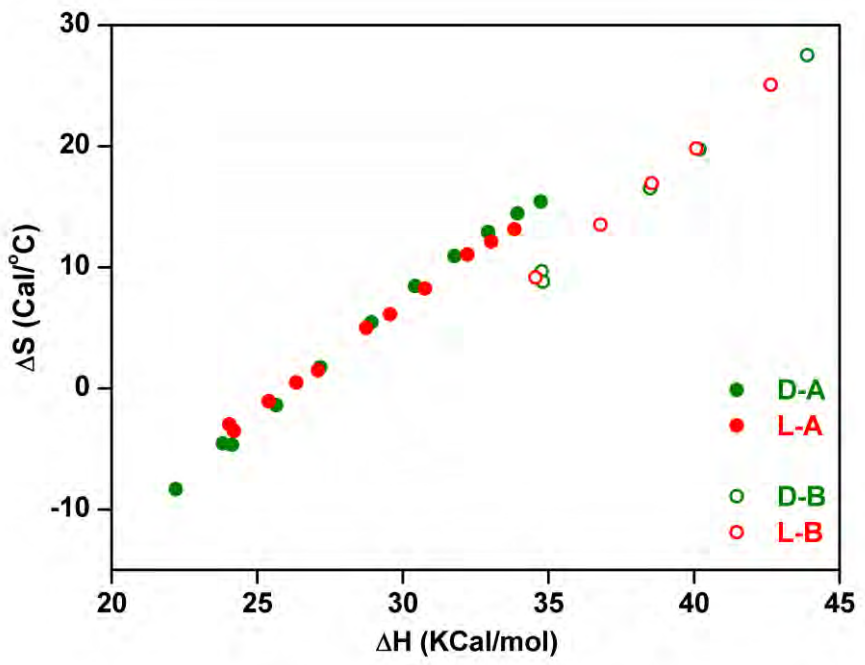

Figure 3.12 Enthalpy/entropy plot for α-Ala.

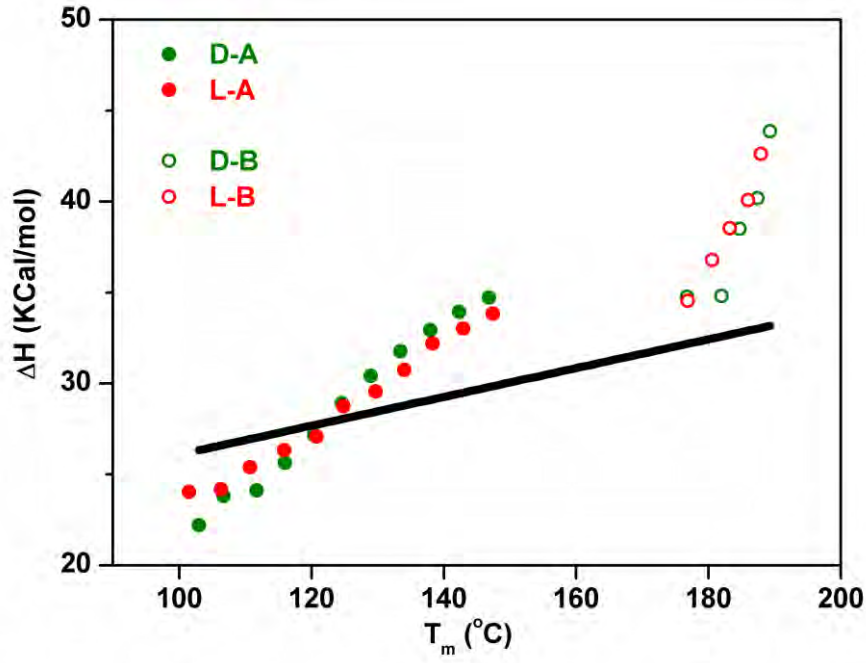

Figure 3.13 Activation enthalpy as a function of peak position for α-Ala. The black line denotes the zero entropy prediction.

Fig. 3.14 presents activation energy (E_a) plots derived from an Arrhenius analysis of the relaxation curves; where a steady increase in activation energies in line with maximum temperatures is apparent. Neagu and Neagu (2003) propose such a trend to be a prerequisite for compensation behaviour; a significant, non-linear, increase in E_a with T_m was shown to be essential. An E_a minima is present within each relaxation domain, for both D- and L- forms of Ala ($E_{a(min)(D\text{-}A)}$ = 98.41 kJ/mol @ 119°C, $E_{a(min)(L\text{-}A)}$ = 97.45 kJ/mol @ 116°C, $E_{a(min)(D\text{-}B)}$ = 149.48 kJ/mol @ 181°C, $E_{a(min)(L\text{-}B)}$ = 148.20 kJ/mol @ 180°C). Interestingly, the temperatures of activation energy minima correspond to the transition from non-cooperative to partially cooperative motion in domain A ($E_{a(min)(A)}$ = 118°C), and to the transition from partially cooperative to fully cooperative motion in compensation domain B ($E_{a(min)(A)}$ = 180°C).

In summary, molecular mobilities within compensation domain A appear to share a prerequisite relationship with molecular mobilities present in domain B. Domains A and B both share a prerequisite relationship with the primary transition, as defined by their compensation temperatures. It is hypothesized that secondary relaxations are pre-cursor motions to primary transitions and dictate a chain of events essential for the primary process to initiate. Acting similarly to mechanisms that may be found in reaction chemistry, each secondary relaxation compensation domain represents a transitional state to the next, in tandem with an increase in cooperativity until, finally, cooperative motion is achieved and the primary transition begins.

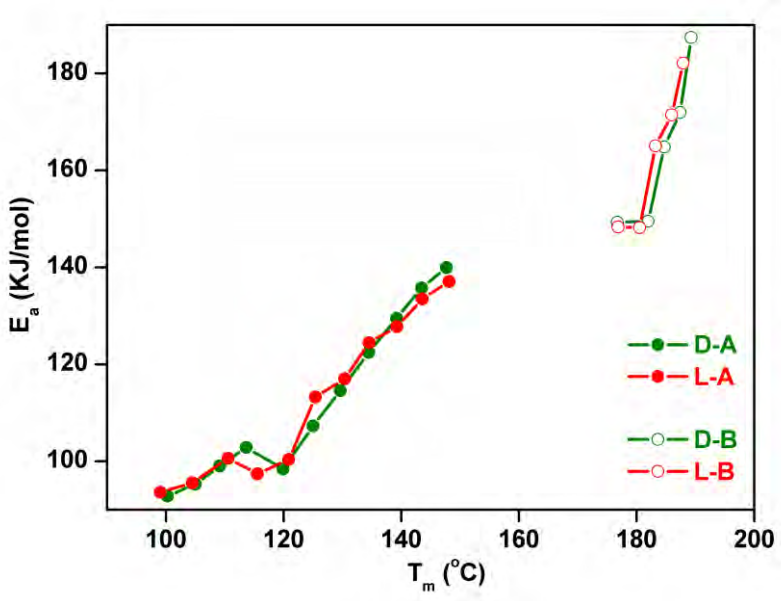

Figure 3.14 Plot of activation energy (E_a) *vs* maximum temperature (T_m) for α-Ala.

3.4 CONCLUSIONS

TSC spectroscopy (a novel technique in this field) has been utilised to detect a previously unreported secondary relaxation in α-Ala in the 40 to 195°C temperature region; representing new knowledge in relation the solid-state molecular mobility at temperatures below the primary transition.

Via experimental deconvolution (TW) and data processing methodologies (RMA) the properties of the secondary relaxation have been characterised. Results suggest that the lower temperature secondary relaxations in α-Ala are precursor motions for higher temperature primary transitions (in this case degradation), and that the secondary relaxation itself is complex, formed of transitional states, each essential for the next process to be initiated. Such a hypothesis is significant in terms of our perception of stability in solid-state materials. Generally, storage temperatures are decided as 'X'°C below the temperature of the primary transition (often the lowest temperature event detectable by conventional thermal analysis techniques). However, it is evident that, in this case, via the use of TSC experiments, molecular mobility can be identified at temperatures significantly lower than what one would consider to be 'stable' storage temperatures. Importantly, it has been demonstrated that these molecular mobilities are initiating a chain of events, ultimately leading to a physical change in (or degradation of) the material. The initiation of molecular relaxation, ultimately resulting in degradation of α-Ala begins at 40°C; 255°C below the experimentally observed onset temperature of degradation.

The TSC data for L-and D-Ala indicate that the technique may be sensitive to chirality, and/or, chirality itself has an influence on the solid-state properties of materials (most likely from a dielectric perspective). Further consideration of these results, and a number of repeatable experiments, is required to elucidate the phenomena of stereoselective TSC spectra presented herein.

CHAPTER 4: β-ALANINE

4.1 INTRODUCTION

β-alanine (β-Ala) is the simplest possible β-amino acid, having no substituent's at its central two-carbon bridge and is - on the basis of current knowledge - the only naturally occurring β-amino acid endogenous to mammals (including humans). In α-amino acids, the carboxylic and amino termini are separated by a 2.5 Å one carbon bridge; in β-amino acids the carboxyl and amino termini are separated by a 5.1 Å two carbon bridge (Figure 4.1).

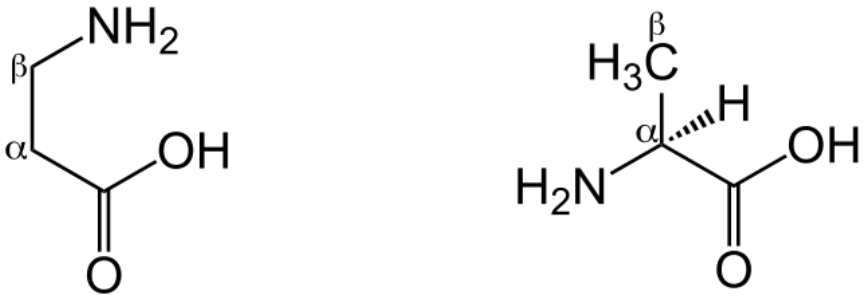

Figure 4.1 Comparison of the schematic chemical structures of β-alanine (left) and L-α-alanine (right).

Unlike its normal counterpart, α-Ala, β-Ala has no stereocenter. To date, β-Ala - a non-essential amino acid - has not been found in naturally occurring proteins. A diverse number of chemical, enzymatic and tandem chemo-enzymatic routes have and are being explored for the challenging, contemporary synthesis of enantiomerically pure β-amino acids. It is noteworthy that the foregoing is not only of interest from an intrinsic knowledge base point of view but also in relation to the use of β-amino acids as building blocks for peptidomimetics and a variety of pharmaceutically important compounds, such as antimicrobials. Furthermore, β-amino acid derivatives are excellent building blocks for versatile chemical transformations, e.g. multi-component reactions resulting in β-lactams, syntheses of 1,3-heterocycles and diaminopyrimidine derivatives or the formation of peptides containing e.g. an H12 helix. β-Ala has been used as a reactant in synthetic biomimetic chemistry in an attempt to understand the underlying molecular mechanism of neuropathy (axon atrophy or swelling) due to n-hexane which is mediated *in vivo* by 2,5-hexanedione (Peil et al. 2007).

In vivo, β-Ala is produced via three main biosynthetic pathways: a product of L-aspartate decarboxylation by gut microbes, a by-product of the interchangeable reaction of pyruvate to L-Ala as well as a product of deamination and carboxylation of the pyrimidine uracil (Hayaishi et al. 1961). β-Ala exists in many mammalian tissues such as adrenal glands, atria, aorta, bronchi, kidney, liver, pancreas and ventricles, not to mention the central nervous system (Decker et al. 1995). In non-neural tissues, it occurs in multiple forms: as a free amino acid, as part of the pantothenic acid moiety of coenzyme A, as a product of L-aspartate and uracil metabolism, and as a by-product of aspartic acid decarboxylation by gut microbes (Hayaishi et al. 1961). Within muscle, β-alanine exists as a component of the di-amino acid peptide carnosine (β-alanyl-histidine). The most common natural dietary sources of β-Ala are believed to be obtained by ingesting the β-Ala containing di-amino acid peptides: carnosine, anserine and balenine. β-Ala is used as a supplement by athletes and a high-potency artificial sweetener, suosan, is derived from β-Ala. Interestingly, it has been proposed that β-Ala biochemistry is compatible, in mammals, with many of the pre-requisite criteria for being a neurotransmitter.

β-Ala, therefore, has a significant number of applications/research interests and it is important to characterise the solid-state physicochemical properties of such a material which, to date, appears to be lacking in the published scientific literature. A publication dating back to 1974 reported the elucidation of the products of degradation at 220°C by mass spectrometry; where it was reported that β-Ala undergoes a complex degradation at this temperature, leading to a large number of degradation products (Lien and Nawar 1974).

Herein TSC spectroscopy - in combination with a range of other analytical techniques - is used to characterise the thermal properties of β-Ala; particularly in the pre-primary transition temperature region.

4.2 EXPERIMENTAL

4.2.1 Materials

β-Ala (stated purity of ≥ 99% (Bachem, UK) was used as received (with the exception of light grinding by hand or compression into tablets). The identity of β-Ala ($C_3H_7NO_2$; β-aminopropanoic acid) was confirmed via elemental and $^{1}H/^{13}C$-NMR analysis and its purity by using MS-MS analysis.

4.2.2 TGA

TGA studies were conducted using a TGA Q5000-IR (TA Instruments) instrument calibrated using the Curie point method by the use of alumel and nickel certified reference materials. A nitrogen atmosphere, at a flow rate of 25 mL/min was employed. Samples of *ca.* 1.5 mg were heated from 30 to 600°C at a scan rate of 2°C/min in non-isothermal experiments. Similar size samples were held at 80, 100, 120 and 140°C for isothermal experiments. Experiments were undertaken in triplicate.

4.2.3 DSC

DSC experiments were undertaken using a DSC Q2000 (TA Instruments) instrument calibrated using an indium certified reference material. A nitrogen atmosphere (flow rate of 50 mL/min) was used. Accurately weighed samples of *ca.* 1.5 mg in standard "Tzero" aluminium pans were examined. One set of samples was heated from -90 to 600°C at a scan rate of 2°C/min and the other set of samples were cycled (cooled then heated) three times from -90 to 120°C at a scan rate of 10°C/min. Experiments were undertaken in triplicate.

4.2.4 HSM

HSM experiments were undertaken using a FP82HT hot stage (Mettler Toledo, UK), FP90 controller (Mettler Toledo, UK) and a DME model 13595 microscope (Leica Microsystems, China). Studio Capture 3.1 software (Studio86Designs, UK) was used for image/data acquisition. Samples were placed on glass slides, covered with a glass cover slide and heated from 25 to 350°C at a rate of 10°C/min.

4.2.5 TSC spectroscopy

TSC experiments were undertaken using a TSCII spectrometer (Setaram, France). Samples were examined as freshly prepared tablets. The sample chamber was evacuated and flushed with helium three times prior to analysis to create an inert atmosphere and to improve thermal transfer throughout the cell. Experimental parameters used were as follows: T_o (lowest experimental temperature) = -100°C, t_o (time at T_o) = 120 s, T_f (final temperature) = 120°C, E_p (polarising electrical field) = 200 V/mm, q_{heat} (dynamic heating rate) = 10°C/min, q_{cool} = 'Newtonian', T_p (temperature of polarisation) = 40, 50, 60, 70, 80°C, t_p (time at T_p)= 120 s. Thermal windowing was undertaken over the temperature range of 10 to 56°C; T_w (thermal window) = 2°C, t_w (time of thermal window) = 120 s.

4.3 RESULTS AND DISCUSSION

4.3.1 Thermal Analysis

The thermal gravimetric (TG) output and its derivative with respect to temperature (dTG) are presented in Figure 4.2; upon heating, β-Ala exhibits a distinct two-stage mass loss profile. The first mass loss process begins at 72°C, based on the point of first mass loss (extrapolated onset 181°C), peaks at 191°C and involves a 65% loss of mass. The second mass loss process begins at 335°C (extrapolated onset), peaks at 344°C (dTG peak) and involves a 31% loss of mass.

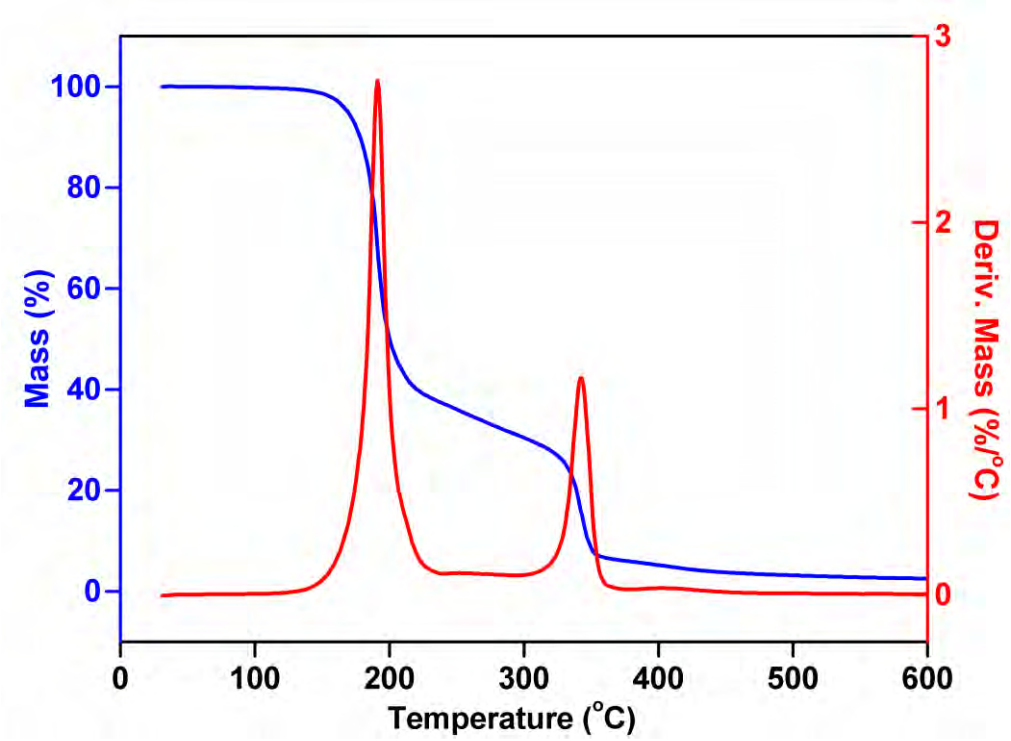

Figure 4.2 TG (blue) and dTG (red) outputs for β-Ala.

DSC (heating only) experiments (Figure 4.3) show two temperature areas of interest. The first process, beginning at 195°C, is a sharp endothermic transition followed by a multitude of small shoulder transitions (indicative of degradation), possibly overlapping with a melt. The second process beginning at 331°C is an enthalpically much smaller and 'cleaner' endothermic transition.

HSM analysis (see Appendix) identified a melt process between 200 to 210°C inferring a possible melt-degradation or melt-evaporation. The apparent solidification/crystallisation of

the sample (within the previously melted liquid) begins at 240°C and is followed by melting of the newly formed solid at 330 to 335°C.

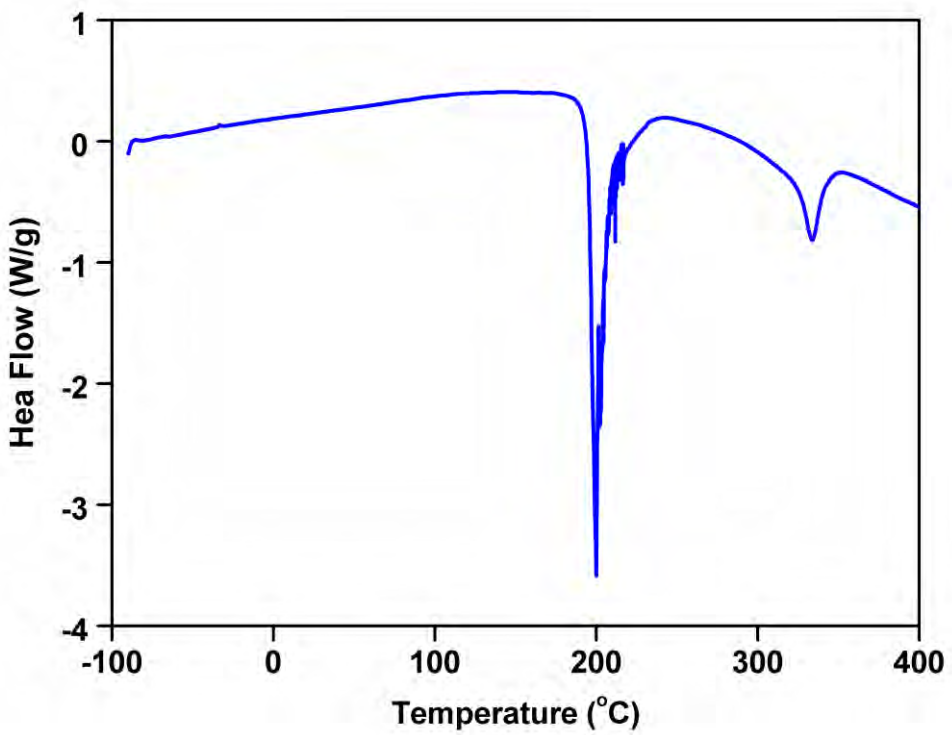

Figure 4.3 Normalised DSC heat flow *vs*. temperature thermogram for β-Ala.

The temperatures of the processes identified in the TGA, DSC and HSM experiments are very similar and consolidation of the information obtained from all three complimentary techniques permits characterisation of the solid-state thermal behaviour of β-Ala. On heating from low to high temperatures, the first distinct process begins at 72°C and peaks at *ca.* 190°C. This process is attributed to a complex melt-degradation/evaporation, with a mass loss of 65%. The second distinct process occurs at *ca.* 330°C and is attributed to the melt of a solid formed in the time/temperature region between the first and second processes.

Further DSC studies were undertaken in the search for a lower temperature relaxation/transition which would, perhaps, not be noticeable in the previous DSC experiments or only become apparent upon multiple heating. Results of cyclic DSC experiments (Figure 4.4) clearly show no DSC-detectable relaxations/transitions in the -90 to 120°C temperature region; a similar temperature region to that probed by TSC experiments (-100 to 120°C). In the absence of any lower temperature transitions the complex melt-degradation/evaporation process beginning at 72°C is, therefore, considered the primary (α) transition in β-Ala.

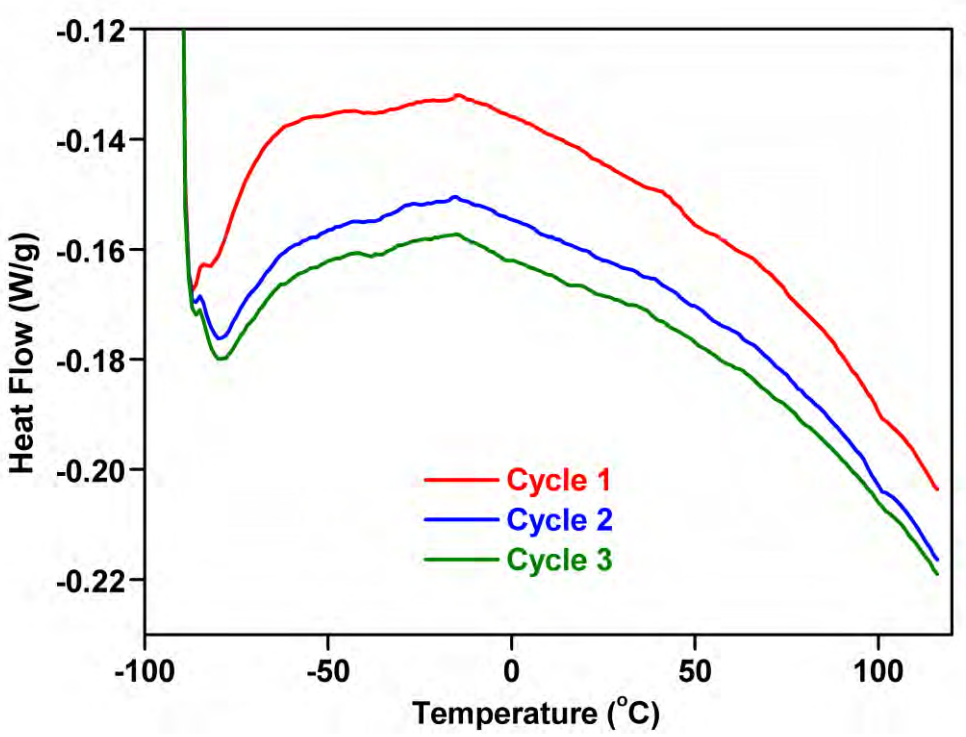

Figure 4.4 Cyclic (heat-cool-heat) DSC curves for β-Ala. Repeated for three cycles. Only the final heating scan for each cycle is shown.

4.3.2 TSC Spectroscopy

With the primary transition identified by thermal analysis, TSC experiments were used to identify any secondary relaxation processes. Only a small number of research groups have reported secondary relaxations in crystalline materials with notable TSC specific examples being reported by Moura Ramos et al. (2005), Shmeis and Krill (2005), Diogo et al. (2007, 2008) and Chamarthy and Pinal (2008). As is the case for glass-forming materials, some research groups (e.g. Johari and Goldstein (1970, 1971) using dielectric studies, have reported that secondary relaxations are related to/influence the primary transition i.e. secondary relaxations are claimed to be pre-cursor (or preparative) motions which are essential for the primary transition to occur.

The results of spontaneous depolarisation current (SDC) experiments are presented in Figure 4.5. There is a clear discrepancy between the first heating (SDC 1) and the second heating (SDC 2). This phenomenon is well documented in freshly prepared sample tablets and is the result of stress relaxation arising from the tableting process (Galop and Collins 2001); the first SDC curve can therefore be ignored. Analysis of curve 'SDC 2' elucidates a process

beginning at *ca.* 70°C. This spectral profile, showing a sudden deviation from the baseline and no apparent return to the baseline, is usually indicative of space-charge or Maxell-Wagner-Sillars phenomena (Diogo et al. 2007; Antonijevic et al. 2008). However, it may also be attributed to the start of a dipolar relaxation peak and therefore a 'real' molecular mobility process. In this instance, the latter scenario is believed to be true, and the process beginning at *ca.* 70°C is attributed to the onset of the primary transition.

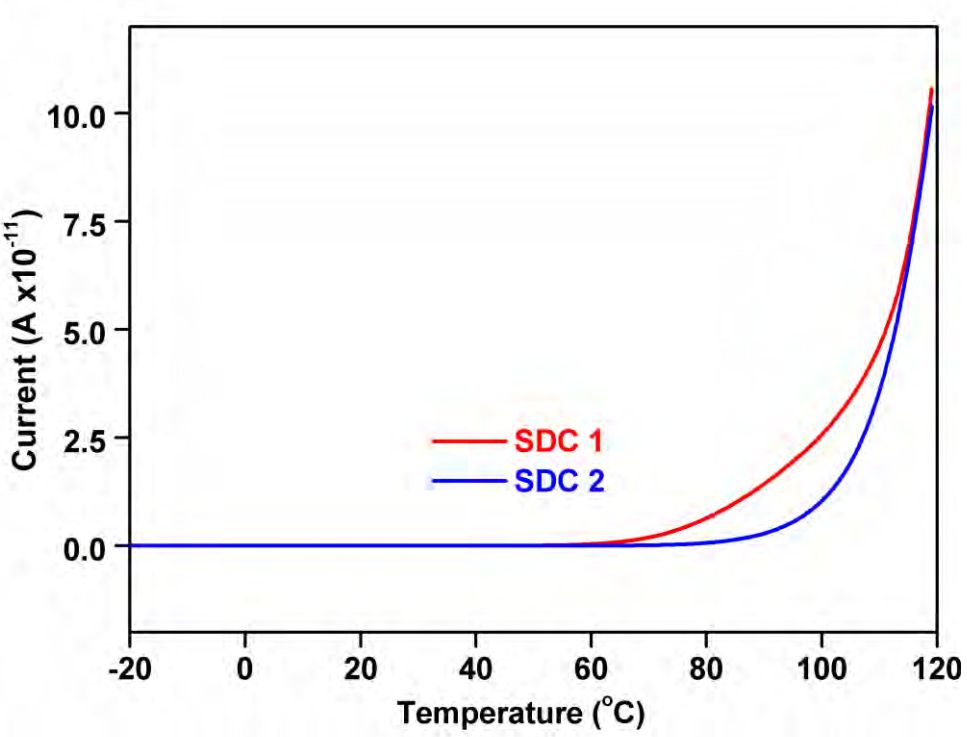

Figure 4.5 SDC curves for β-Ala. 'SDC 1' indicates first heating, 'SDC 2' second heating of the same sample.

Results of a thermally stimulated polarisation current (TSPC) experiment (Figure 4.6) highlight similar behaviour to that exhibited by SDC analysis. A signal of $1x10^{-6}$ A is particularly intense and represents a temperature region of significant molecular motion.

Results of TSDC experiments using different values of T_p (Figure 4.7) identify a thermal event occurring over the temperature range of 0 to 60°C, peaking at 42 to 48°C; closely followed by the onset of the primary transition. This secondary relaxation appears to be relatively uninfluenced by the chosen T_p values, with only a small deviation in peak position and intensity occurring with increasing polarisation temperatures.

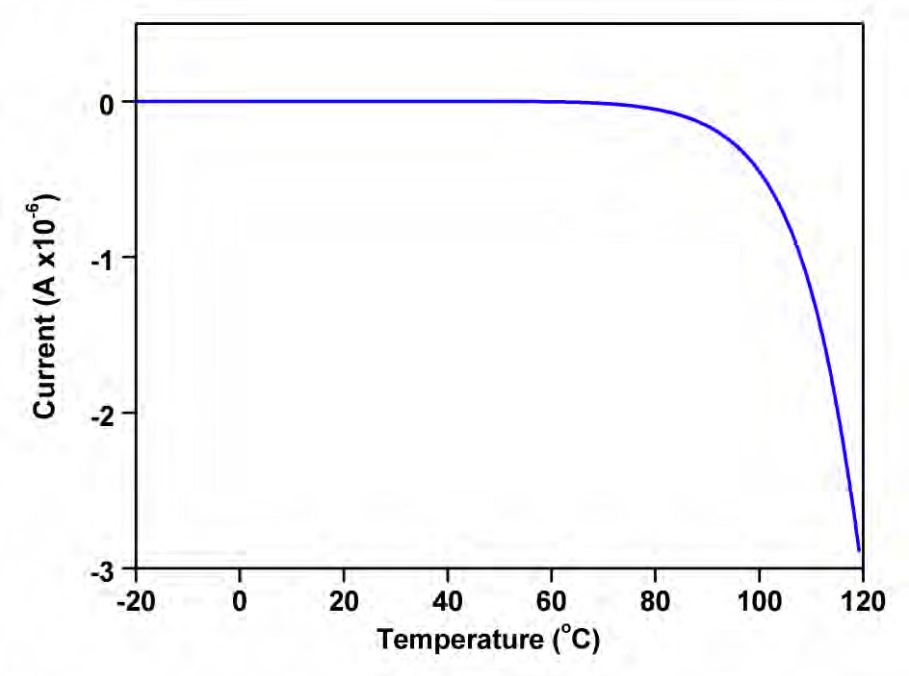

Figure 4.6 TSPC curve for β-Ala

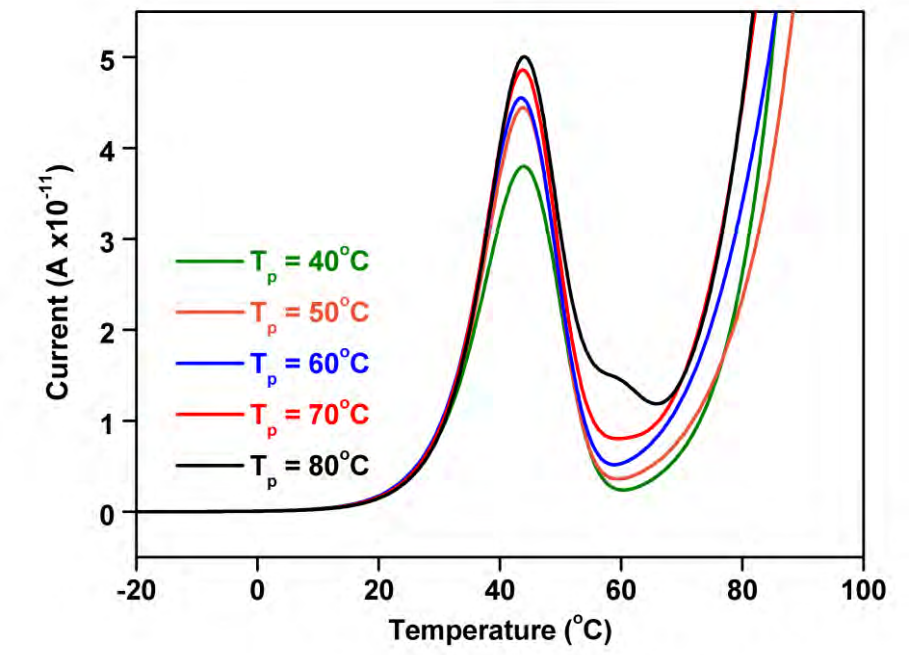

Figure 4.7 TSDC curves for β-Ala at different polarisation temperatures (T_p).

It is sometimes the case that the peaks/signals in TSC spectra do not arise from the movement of molecules within the sample, but originate from discontinuities in the sample or poor sample-electrode contact. Such anomalous phenomena is often referred to in dielectric

literature as space-charge or Maxell-Wagner-Sillars type phenomena (Diogo et al. 2007; Antonijevic et al. 2008) and can produce a peak which looks very similar to a 'true' motional process. It is therefore advisable to perform additional verification experiments to distinguish an 'anomalous' peak from a 'real' peak when dealing with TSC data. In TSDC experiments the intent is to monitor changes in, and influence, the motion of molecules by the processes of measuring dipolar depolarisation and actively polarising dipoles by the application of static electrical fields. Such is the nature of dipolar (de)polarisation, that the magnitude of the depolarisation is uniformly related to the magnitude of the prior polarisation. The relationship between normalised applied electrical field (E_f (V/mm)) and the magnitude of the maximum current (I_{max} (A)) is linear for a dipolar process (Williams 1975; Vanderschueren and Gasiot 1979). No other polarisation mechanisms exhibit such behaviour.

The results of TSDC experiments using different electric field strengths are shown in Figure 4.8. An increase in I_{max} with increasing electrical field strength is apparent, and when plotted (Figure 4.9) shows a linear relationship (R^2 = 0.996). The foregoing results prove that the secondary relaxation process found for β-Ala by TSC experiments does indeed arise from dipolar motion (and therefore molecular motion/relaxation) and is not an artefact of sample discontinuity or poor sample-electrode contact. No breakdown of the sample or deterioration of data quality at higher electrical fields is apparent; suggesting excellent sample-electrode contact is maintained throughout the experiments and that the electrical field at 200 V/mm does not have a deleterious effect on the sample.

4.3.3 Thermal windowing and compensation analysis

The global relaxation process identified by TSDC is likely to be the result of many underlying motions each with its own single, or a narrow distribution of, relaxation time(s). The TW methodology utilises a series of narrow polarisation temperature windows (1 or 2°C) in order to experimentally deconvolute a global relaxation process into elementary relaxation spectra. Theoretically, each TW relaxation curve should represent a process with a single relaxation time; in practice, it may reflect a narrow distribution of relaxation times (Correia et al. 2000). The TW data for β-Ala and the associated 'Bucci plot', generated by RMA (Williams 1975) are shown in Figures 4.10 and 4.11, respectively.

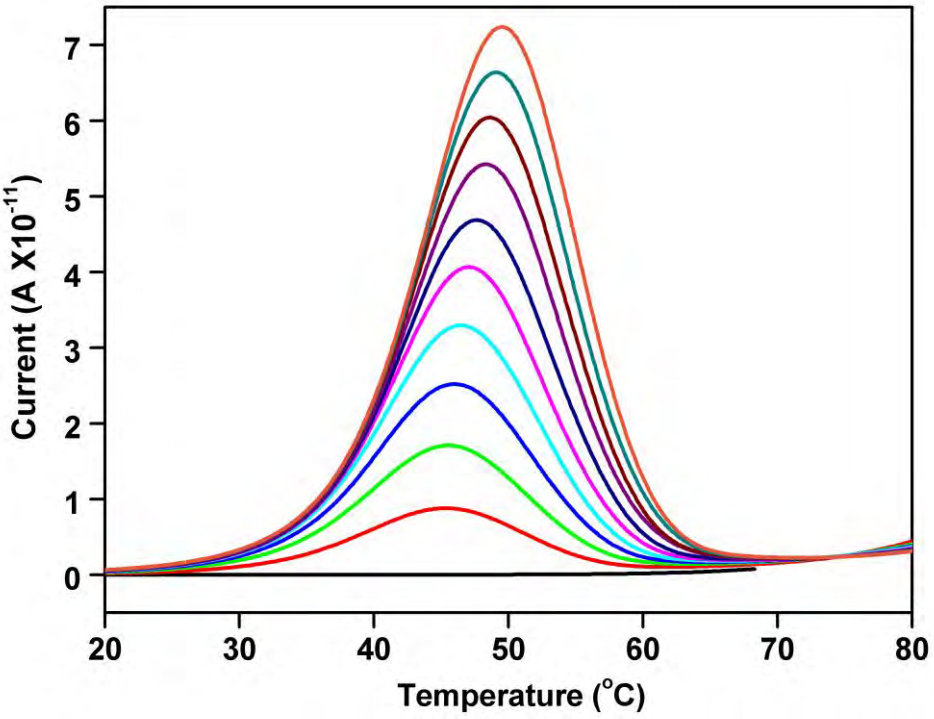

Figure 4.8 TSDC curves for β-Ala at different electrical field strengths (E_f). T_p = 50°C.

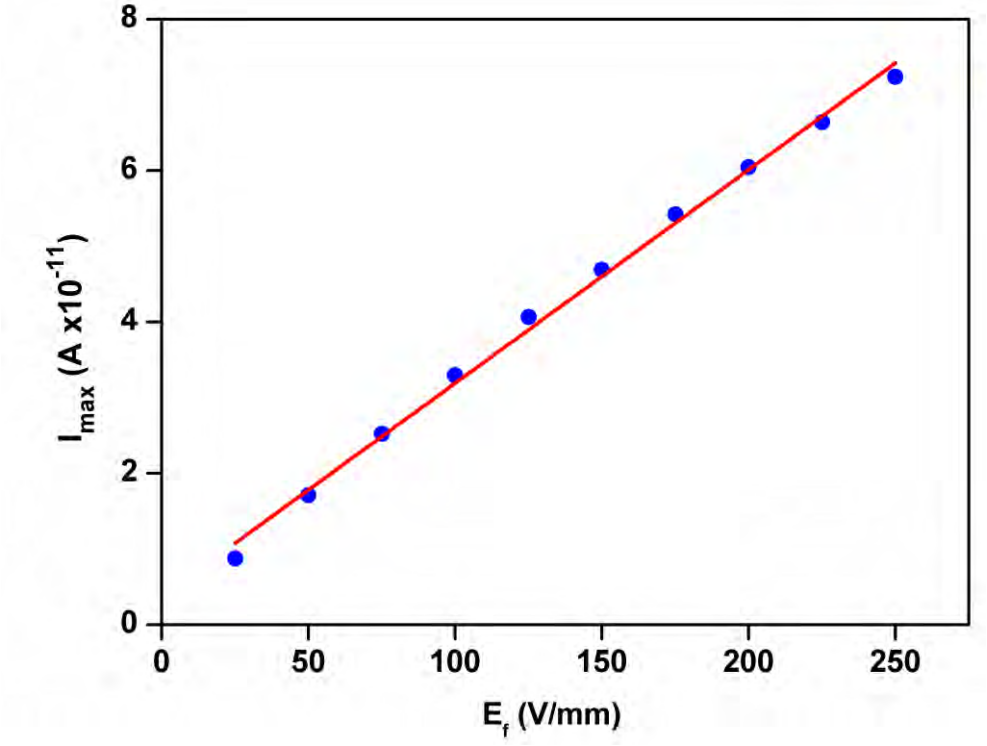

Figure 4.9 Plot of electrical field strength (E_f) *vs*. maximum current (I_{max}).

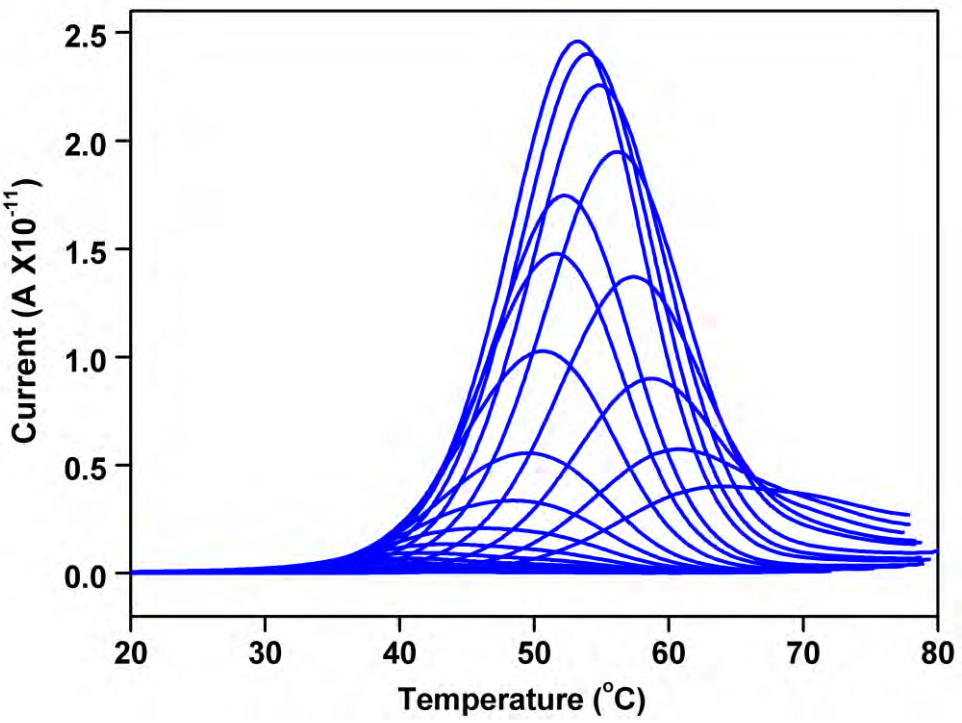

Figure 4.10 Thermal windowing curves for β-Ala.

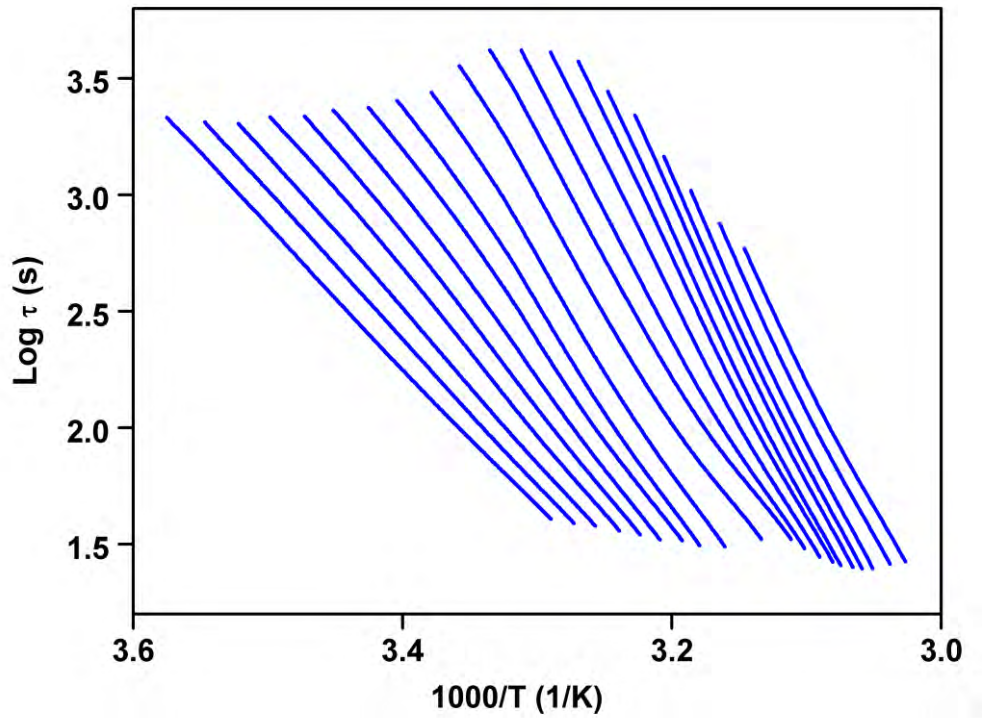

Figure 4.11 'Bucci plot' showing relaxation curves generated from β-Ala TW curves.

Once the TW data has been collected many experimental parameters can be elucidated using RMA, including dielectric, thermodynamic and kinetic data. Of notable contemporary interest is the phenomenon of compensation observed in LOMs (Neagu and Neagu 2002; Moura Ramos et al. 2007; Moura Ramos et al. 2008). The phenomenon is widely observed throughout chemistry and biology and attracts substantial contemporary research interest (Ferrante and Gorski 2012; Meloun and Ferenčíková 2012; Remizov and Skochilov 2012; Starikov and Nordén 2012). Compensation analysis can be undertaken using the RMA software where, notably, the temperature of compensation (T_c) can be elucidated and used to link secondary relaxations to primary transitions. This phenomenon is sometimes observed in glass-forming LOMs, but rarely in the crystalline state.

Compensation analysis of β-Ala (Figure 4.12A) exhibits two compensation points: A and B. Both compensation points are distinct, with well separated compensation temperatures, which suggest an overlap of two distinct molecular relaxation domains. Compensation domain A has the parameters: T_c = 74°C, τ_c = 0.1042 s, R^2 = 0.997, degree of disorder (DOD) = 45 and T_p values between 10 and 40°C. Compensation domain B has the parameters; T_c = 23°C, τ_c = 1.5790 x 10^5 s, R^2 = 0.997, DOD = 17 and T_p values between 42 and 56°C.

Both compensation domains exhibit the classic linear compensation relationship between the change in enthalpy and entropy as dipolar relaxation progresses (Figure 4.12B). A plot of the change in the Gibbs free energy against peak position (T_m) (Figure 4.12C) highlights a linear relationship for both domains across most of the T_m region. However, there is an obvious discrepancy in the 52 to 58°C region; this is attributed to overlap of the two relaxation domains at these temperatures.

The data shown in Figure 4.12D demonstrates the change in enthalpy in comparison to the zero entropy prediction. Points on (or close to) the zero entropy prediction highlight non-cooperative or low cooperativity relaxations; often considered to arise from local motions, uninfluenced by neighbouring molecules (Correia et al. 2000). In the case of β-Ala, all molecular motions in the secondary relaxation temperature region deviate significantly from the zero entropy prediction; suggesting a situation of cooperative motions and interaction with neighbouring molecules. The relaxations of compensation domain A increase in cooperativity with increasing T_m; whereas the relaxations of compensation domain B become less cooperative.

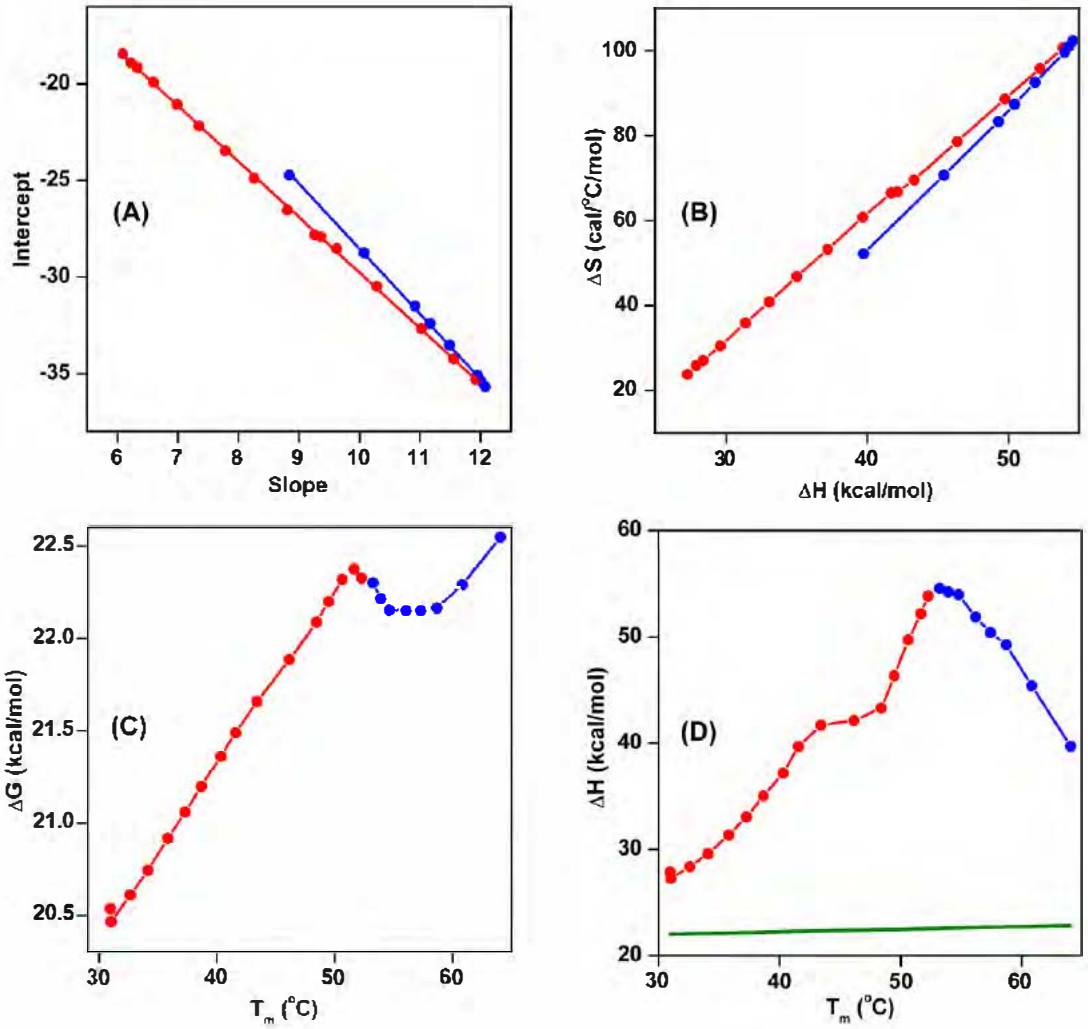

Figure 4.12 **(A)** compensation analysis of β-Ala, **(B)** change in enthalpy against change in entropy, **(C)** change in Gibbs free energy against peak position, and **(D)** activation enthalpy against peak position in comparison to the zero entropy prediction (green line). For A-D compensation domain A (red) and compensation domain B (blue).

In summary, compensation domain A has a compensation temperature of 74°C. This is very close (within 2°C) to the onset of the primary transition found by TGA at 72°C. This evidence strongly suggests that the secondary relaxation of β-Ala is connected in some way to the primary transition. A relaxation time of 0.1042 s shows the relaxation to be relatively fast; although the speed of dipolar relaxation varies dramatically from 10^{-10} s to infinity (i.e. longer then the experimental time-frame) (Vanderschueren and Gasiot 1979). A deviation from the zero entropy prediction suggests a cooperative relaxation where there is likely to be interactions with neighbouring molecules. This is supported by a DOD value which falls within the expected range of 30 to 70; where a value of 45 suggests low to moderate disorder

and implies a scenario where molecular mobility may be hindered by interactive inter-/intra-molecular forces (Ibar 1991). The nature of the crystalline state dictates a situation where molecules are closely packed together and where intermolecular interactions are numerous and often strong. A scenario of cooperative relaxation with inter-molecular interaction is, therefore, plausible.

Compensation domain B has a compensation temperature of 23°C. Interestingly, this compensation temperature relates to a temperature region before the relaxations of domain B occur and suggests a relationship with the onset of the entire secondary relaxation (Figure 4.12) at the same temperature. The relaxation time for this process is 44 hours; a high value, but one that is to be expected as the relaxations at lower temperatures are likely to have slower relaxation times.

The origin of, and theoretical explanations for, secondary relaxation processes in the crystalline state at the molecular level is, currently, unknown. Any motion within the crystalline state is unlikely to be isolated and should, seemingly, always involve interaction with neighbouring molecules. The cooperative behaviour of relaxations in the crystalline state observed herein for β-Ala is therefore, to be expected. It is my strong belief that secondary relaxations are often related to a primary transition. As observed here, the secondary relaxation of β-Ala has been shown, via compensation analysis, to be directly related to the start of the primary melt-degradation/evaporation process elucidated by other thermoanalytical methods. The secondary relaxation is likely to be a pre-cursor motion in readiness for (and possibly a necessity for) the primary transition to begin.

4.3.4 Further TGA experiments

To test our hypothesis and to further examine the relationship between the secondary relaxation and the primary transition, additional isothermal TGA experiments were undertaken. Samples were held at 80°C (close to the experimentally observed onset and the compensation temperature), 100°C, 120°C and 140°C for 24 hours. Results are presented in Figure 4.13 where total mass losses over 24 hours were determined as 0.3%, 0.7%, 3.7% and 31.3% at 80, 100, 120 and 140°C, respectively. These experiments show that the mass loss for the primary transition is occurring at temperatures as low as 80°C (albeit at an extremely slow rate) and that the compensation temperature determined from the secondary relaxation observed by TSC is indeed related to the onset of the primary transition.

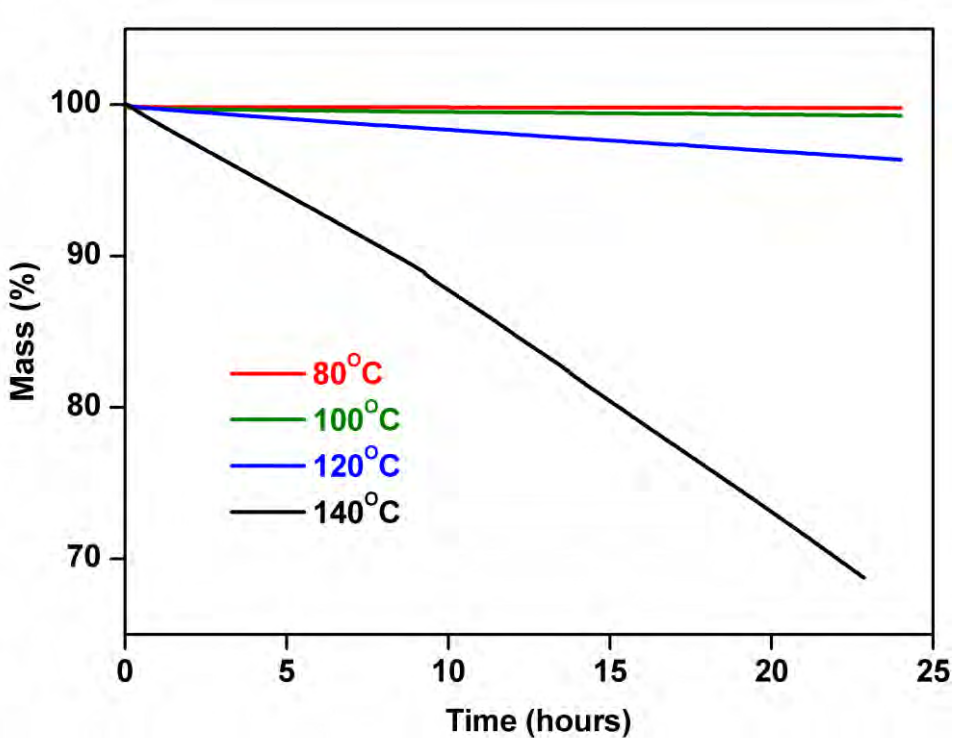

Figure 4.13 Isothermal TGA plots for β-Ala at 80, 100, 120 and 140°C.

Kinetic analysis was undertaken where a plot of conversion fraction (α) vs. time (t) gave a linear reaction profile. Such a reaction profile indicates an order based (F) model; where a linear reaction profile indicates a zero-order (F0/R1) reaction model (Khawam and Flanagan 2006). Via integration the reaction constant can be calculated and its natural logarithm plotted against reciprocal temperature to determine the activation energy from the slope of the linear plot (Vyazovkin et al. 2011). The activation energy was calculated to be 112.48 kJ/mol; large enough to indicate a high temperature dependence of the reaction rate. A plot of reaction constant against temperature yielded a linear slope where the temperature intercept was determined to be 72.85°C; representing the temperature at which the reaction constant is 0 (i.e. the start of the process). Once again this value correlates favourably with the onset temperatures observed by TGA/DSC/HSM and predicted by compensation analysis from the TSC data. A zero-order reaction denotes a situation where the rate is independent of the concentration of reactant and occurs when a material that is required for the reaction to proceed (i.e. a surface) is saturated by the reactants, i.e. a surface limited process. It also exemplifies the situation where the reaction is yet to reach completion as a linear time-conversion profile cannot be infinitely sustained; eventually reactants will be depleted and the profile will 'tail-off'.

Based on the cumulative evidence from all the techniques used we conclude the process beginning at 70-74°C is sublimation. A typical surface limited process, which when forcibly heated by non-isothermal methods (i.e. TGA/DSC/HSM) and therefore restricted in time and the amount of material that can leave the surface, results in the 'bulk' of the material reaching a higher temperature than it would when not restricted; resulting in degradation before it has the chance to reach the surface and sublime or evaporate.

4.4 CONCLUSIONS

The solid-state properties of β-Ala (a typical LOM) have been characterised by thermal analysis and TSC experiments. The primary transition in β-Ala has been characterised; beginning at 70°C and continuing through many stages to beyond 600°C. TSC spectroscopy was used to identify a secondary relaxation process in the 0 to 60°C temperature region; peaking between 45 and 50°C.

Experimental (TW) and computational (RMA) methodologies were employed to fully characterise the secondary relaxation process; including its compensation, thermodynamic and kinetic behaviour. Compensation analysis identified two distinct compensation domains with the following compensation point parameters: domain A: T_c = 74°C, τ_c = 0.1042 s, R^2 = 0.997, DOD = 45 and T_p values between 10 and 40°C. Domain B: T_c = 23°C, τ_c = 1.5790x105 s, R^2 = 0.997, DOD = 17 and T_p values between 42 and 56°C.

The compensation phenomenon of domain A represents a relationship between the secondary relaxation process and the primary transition. The compensation phenomenon of domain B represents an alliance between the lower and higher temperature regions of the secondary relaxation temperature region. This highlighted an interdependence of two distinct relaxation modes.

The thermodynamic parameters of free energy, enthalpy and entropy were determined where the activation enthalpies and entropies were used to elucidate the cooperativity of the relaxation process. A significant rise in cooperativity occurs within domain A followed by a peak in activation enthalpy at the transition region between the compensation domains. A slight decrease in cooperativity is observed during domain B, but overall, a net increase in cooperativity occurs throughout the relaxation process.

This is the first time the secondary relaxation in β-Ala has been detected. Crucially, the relaxation process has been shown to be related to the onset of the primary transition; providing further evidence of the theorised pre-requisite relationship between primary and secondary processes in the solid-state. Of equal interest is the relationship uncovered within the secondary relaxation itself. Two distinct relaxation domains were observed, each with varying properties, but related by a 'transitional state' type relationship.

The temperature region of secondary relaxation phenomena in β-Ala (0 to 60°C) is particularly interesting as this temperature region falls within the manufacturers recommended storage temperatures for β-Ala; they suggest room temperature. Whilst the material may appear to be chemically and physically stable at room temperature by other analytical techniques, it's been proven here that the material is undergoing cooperative motions at room temperature; suggesting a lower storage temperature may be more effective.

Shortly after the secondary relaxation process (which ends at ≈ 60°C) a solid-gas transition has been proven to begin at ≈ 72°C; relatively close in temperature to the secondary relaxation process. The system is cooperative by 60°C and one can assume (from extrapolation of the cooperativity plot) even more so by 72°C. This suggests a situation whereby – if a long enough time period is allowed – materials which may appear to melt at relatively high temperatures (when analysed by other non-isothermal techniques) will in fact undergo a solid-gas type transition at much lower temperatures. Plausibly, this is the result of slow molecular mobility and cooperative rearrangement in the secondary relaxation temperature region.

In conclusion, not only has a secondary relaxation in β-Ala been characterised but the TSC technique has been demonstrated to be a powerful analytical tool; capable of being used for the detection of solid-state behaviour not found by other thermal techniques. This research also has a profound effect on our perception of solid-state behaviour from a purely theoretical perspective. The identified relationships between different types of thermal process are intriguing, and they must be fully understood in order to develop a complete and coherent understanding of solid-state thermal behaviour in LOMs.

APPENDIX

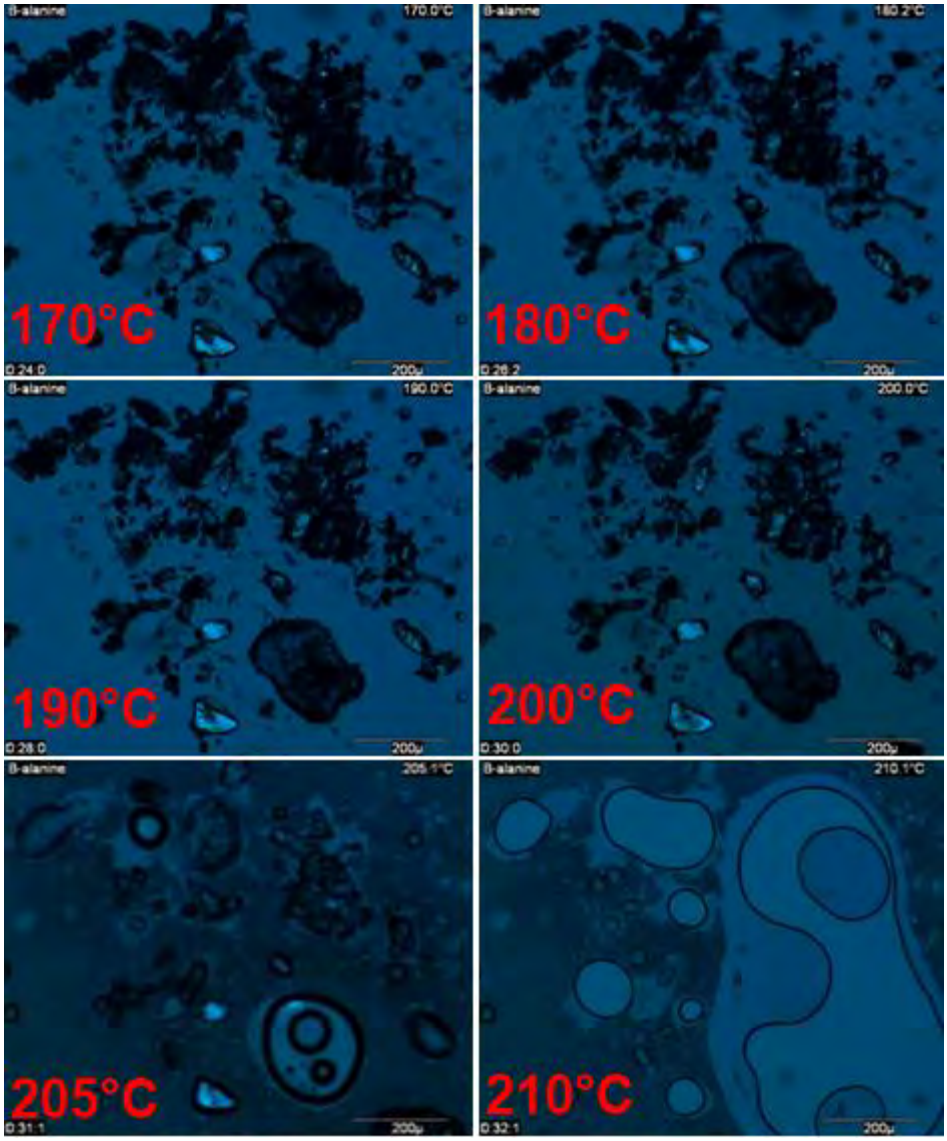
β-alanine
170.0°C
170°C
0:24.0
200µ
β-alanine
180.2°C
180°C
0:26.2
200µ
β-alanine
190.0°C
190°C
0:28.0
200µ
β-alanine
200.0°C
200°C
0:30.0
200µ
β-alanine
205.1°C
205°C
0:31.1
200µ
β-alanine
210.1°C
210°C
0:32.1
200µ

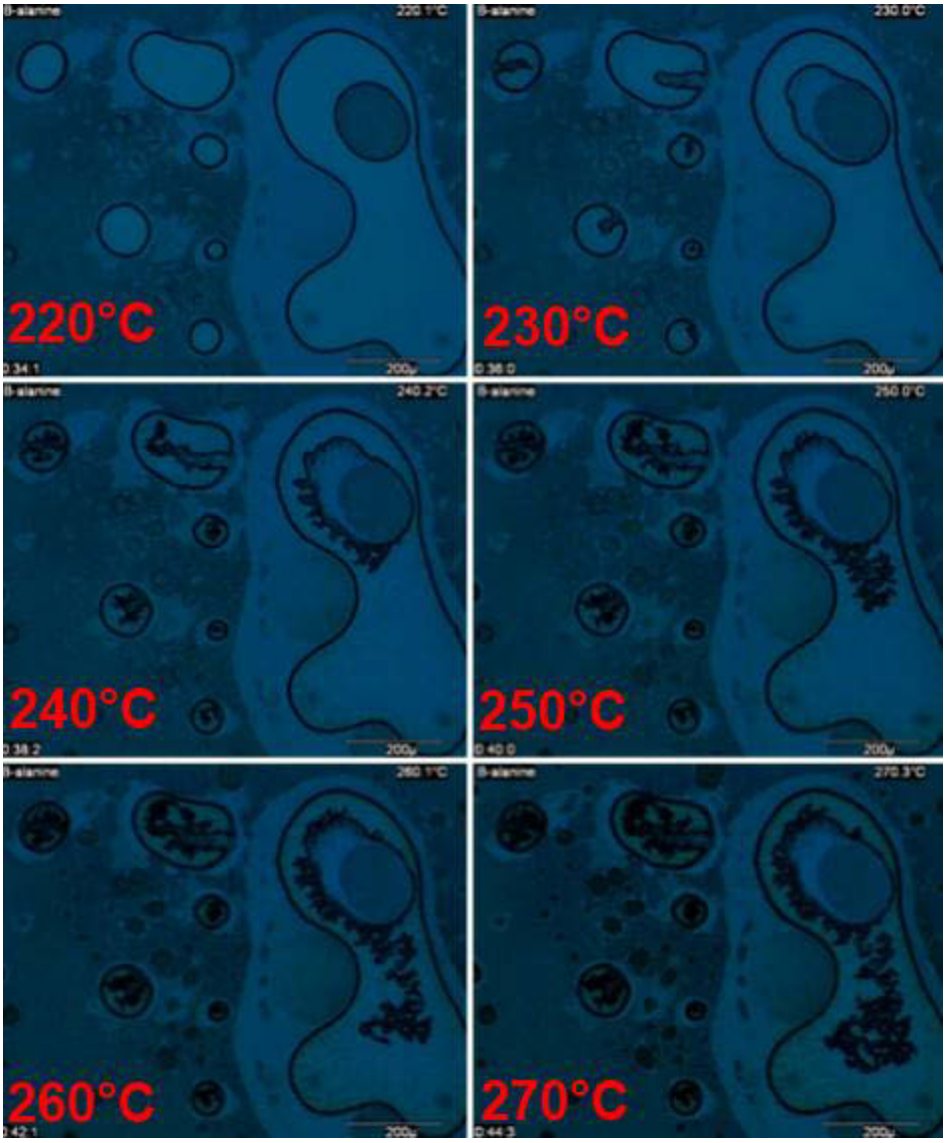
220°C
230°C
240°C
250°C
260°C
270°C

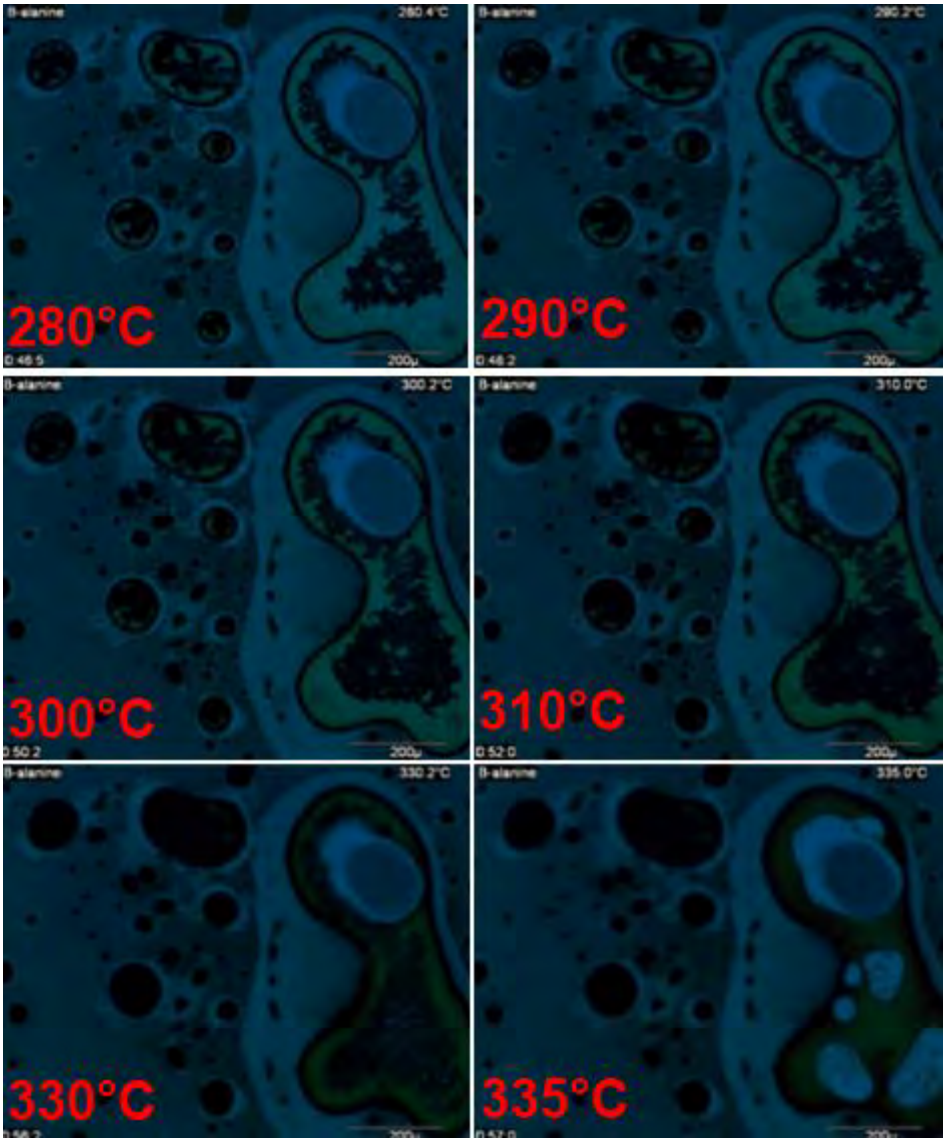

Figure 4.14 HSM snapshots of the heating of β-Ala.

CHAPTER 5: CHARACTERISATION OF A CO-CRYSTAL

5.1 INTRODUCTION

Pharmaceutically relevant co-crystals (CCs) are of increasing contemporary importance within the pharmaceutical industry as they represent a relatively unexplored class of materials. Co-crystallisation of an active pharmaceutical ingredient (API) can lead to potential improvements in the biopharmaceutical properties of the solid dosage form (Gagniere et al. 2009; Qiao 2012). Poor biopharmaceutical performance is one of the primary contributing factors as to why only 1% of APIs enter the market (Qiao et al 2012). Additionally, CCs are considered non-obvious forms of an API, and as such, can represent intellectual property (Elbagerma et al. 2010).

CCs are part of a broader family of chemically-modified crystals which also include salts, solvates and hydrates (Morissette et al. 2004). A working definition of a CC is: "a stoichiometric multi-component system connected by non-covalent interactions where all the components present are solid under ambient conditions" (Thakuria et al 2012). A recent "guidance for industry" has been issued by the US Food and Drug Administration (FDA) on the regulatory classification of pharmaceutical CCs (FDA 2011; Aitipamula et al. 2012).

Despite the potential benefits associated with CC formation no currently marketed drug product intentionally utilises CCs; the Lundbeck developed antidepressant escitalopram was formulated as an oxalate salt, but was later recognised to be a CC (Schartman 2009). The main reason for this situation may be related to uncertainty surrounding the physical and chemical stability of CCs. Pharmaceutical companies are unlikely to market a metastable CC due to the risk of product recall should the CC change in some way during its shelf-life. It is therefore imperative to characterise CC materials in as much detail as possible. Much of the research on CCs involves the synthesis and structural determination of new CC forms. Whilst this is obviously important, it is also essential to characterise the physicochemical properties of CC materials e.g. using thermal analytical techniques. Such characterisation is generally undertaken using 'conventional' thermal analysis techniques which can be used to detect and characterise a large number of processes (i.e. mass loss, melting, component interaction, degradation, etc) (Zhang et al 2012). However, less conventional thermal techniques such as TSC spectroscopy have the advantage of being able to be used to detect and characterise additional thermal processes which may be otherwise undetectable using 'conventional'

thermal analysis techniques. TSC spectroscopy is likely to be of use in studying CC systems in many ways. Detection and characterisation of molecular mobility yields information regarding physical stability, component interaction and the dielectric nature of the material. This information can then be correlated to estimate the short/long term stability of the material during processing and/or storage. Additionally, molecular mobility data gained from TSC experiments may provide some useful data to help establish the intricacies and mechanisms of CC formation.

Reports of the thermal analysis of many co-crystal systems are widely available in the published literature (Vishweshwar et al. 2006; Berry et al. 2008; Rohani 2010; Kawakami et al. 2012; Zhang et al. 2012). Recent review articles by Chieng et al. (2011), Qiao et al. (2011) and Byrn and Henck (2012) outline recently studied CC systems.

The CC system of interest in this research was recently reported as a CC of salicylic acid and benzamide by Elbagerma et al. (2010). This CC was prepared via slow evaporation from solvent (section 2.2.4) to yield a 1:1 molar ratio CC, primarily stabilised via acid-amide hydrogen-bonded dimers (Figures 5.1 and 5.2). The CC was characterised by Raman spectroscopy, NMR and x-ray diffractometry (including the single crystal structure and the XRPD). Combined with some pre-existing thermal analysis (Figure 5.3) and a relatively simple, reliable method of preparation, this system was considered to be an ideal model CC system for investigation by TSC.

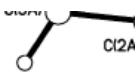

Figure 5.1 Hydrogen-bonded acid-amide dimer motifs in the 1:1 CC system of salicylic acid and benzamide (reproduced from Elbagerma et al. 2010).

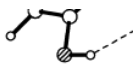

Figure 5.2 Crystal packing in the 1:1 CC of salicylic acid and benzamide viewed in orthographic projection down the a-axis of the unit cell (reproduced from Elbagerma et al. 2010).

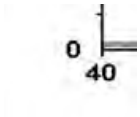

Figure 5.3 DSC melting curves of the salicylic acid and benzamide CC and its components (reproduced from Elbagerma et al. 2010).

TSC spectroscopy and a range of other thermal and non-thermal techniques are used herein to characterise the physicochemical properties of the salicylic acid-benzamide CC system. This

was achieved via the successful synthesis of the co-crystal and the subsequent analysis of the co-crystal and its components. Of particular interest is the solid-state study of the interactions between LOMs; in physical mixtures and upon co-crystallisation. Elucidation of the mechanism of co-crystal formation is of particular interest in this investigation.

5.2 EXPERIMENTAL

5.2.1 Samples

Four samples were used during this chapter/study. Refer to section 2.1 for details of the samples. A list of samples is as follows.

- Benzamide (BA)
- Salicylic acid (SA)
- 1:1 molar ratio physical mixture (PM) of BA/SA prepared via the method outlined in section 2.2.3
- 1:1 molar ratio co-crystal (CC) of BA/SA prepared via the method outlined in section 2.2.4

5.2.2 TGA

TGA experiments were undertaken using a TGA Q5000IR instrument (section 2.3.2.1). All TGA experiments used an inert atmosphere of nitrogen (flow rate of 25 mL/min). Samples of ≈2 mg were accurately weighed and heated from 50 to 600°C at a linear scan rate of 10°C/min. Experiments were repeated in at least triplicate, using a newly prepared sample each time.

5.2.3 DSC

DSC experiments were undertaken using a DSC Q2000 instrument (section 2.3.3.1). An inert atmosphere of nitrogen at a flow rate of 50 mL/min was used for all experiments. Accurately weighed samples of ≈ 5 mg were placed in 40 μL aluminium pans capped with aluminium lids with two small pinholes. Samples were heated from -50 to 600°C at a linear scan rate of 10°C/min. Experiments were repeated in at least triplicate using freshly prepared samples.

5.2.4 HSM

HSM experiments were undertaken using the equipment outlined in Chapter 2, section 2.3.4.1. HSM experiments were undertaken over the temperature range of 25 to 350°C. Samples were placed on glass slides and covered with a glass cover slide.

5.2.5 TSC spectroscopy

TSC experiments were undertaken using a TSCII (section 2.3.1.1). Samples were introduced as freshly prepared compressed tablets of 50 mg mass, 8 mm diameter and their thickness accurately measured using a digital calliper.

The sample chamber was evacuated and flushed with helium three times prior to analysis to create an inert atmosphere and to improve thermal transfer throughout the cell. Experimental parameters used were as follows: T_o = -100°C, t_o = 120 s, T_f = 70°C, E_p = 200 V/mm, $q_{(heat)}$ = 10°C/min, $q_{(cool)}$ = 'Newtonian', T_p = 40°C, t_p = 120 s. Thermal windowing was undertaken over the temperature range of -5 to 40°C; T_w = 5°C, t_w = 120 s.

5.3 RESULTS AND DISCUSSION

Of fundamental importance in the earliest stages of analysis was to ascertain the success of CC formation prepared using the methodology described in section 2.2.4. To achieve this, a combination of thermal and solid-state spectroscopic/diffractometric techniques was employed to characterise the CC in tandem with the characterisation of its constituents (BA/SA) and a physical mixture of them (PM), for comparative purposes. Confirmation of a successful CC formation would involve two key approaches. Firstly, to ascertain the presence of a new and unique chemical entity (i.e. differentiation of the CC from its constituents and/or a simple physical mixture) and secondly, to compare experimentally derived data for the prepared CC with literature reported values.

The following section is a prospective summary of relevant results specific to determining the success of CC formation. It will make reference to appendices and forthcoming sections, where the results within will be discussed in detail individually later, but not necessarily in this context.

5.3.1 Characterisation/confirmation of the prepared CC

Upon visual inspection of the prepared CC it appeared to be in the solid, crystalline state and appeared to be completely 'dry' (i.e. no evidence of residual solvent). TGA analysis (section 5.3.2) confirmed the sample was indeed void of residual solvents or moisture. The ^{13}C solid state NMR spectra for the CC and its constituents were obtained in a series of experiments (Appendix: Figure 5.1). Due to time constraints it was not possible to obtain a spectrum of the PM. NMR results confirmed the CC sample was a novel chemical entity via comparison with BA and SA. Notably, this is the first ^{13}C SS-NMR spectrum of this CC. However, further analysis and presentation was outside the scope of this research. AT-FTIR studies (Appendix: Figure 5.2 A and B) and XRPD studies (Appendix: Figure 5.3) produced a similar trend whereby the CC was distinctly and reproducibly different from its constituents and a physical mixture of them. In conclusion, the above mentioned supplementary techniques confirmed the prepared CC represented a new chemical entity in the context of its constituents; leading to the suggestion that CC preparation had been a success.

Further analysis was undertaken to compare results obtained experimentally with literature values. XRPD results reported by Elbagerma et al. (2010) were retrieved from the relevant structural database where a direct comparison with experimentally derived data from the prepared CC yielded a perfect match. XRPD analysis therefore confirmed the CC to not only be a new chemical entity, but to be the intended 1:1 molar ratio CC. This was also confirmed via analysis of the CCs physical properties by DSC analysis (see 5.3.2). An experimentally obtained DSC melting point for the CC of 118°C was in agreement with the literature reported value of 118°C reported by Elbagerma et al. (2010).

In conclusion, the preparation of a 1:1 molar ratio CC of BA:SA was successful. The same batch of CC was used for all studies presented in this Chapter.

5.3.2 Thermal Analysis

A range of thermal analysis techniques were employed to assess the physicochemical properties of the CC and its constituents prior to TSC analysis. Of utmost importance was the safety of the TSC instrumentation; physical and/or chemical changes in any samples must be well characterised in advance. Melting, sublimation, desolvation, glass transitions and degradation are the key physical and chemical processes of interest when planning TSC methodologies. Naturally, identification and characterisation of such transitions/processes are

also of equal significance in achieving comprehensive characterisation of the CC. Ultimately, the search for secondary relaxations is paramount to this research. This may be achieved by thermal analysis alone, but it is unlikely. TSC will be the focus in this context. However, without the knowledge gained from 'conventional' analysis the interpretation of TSC data, and the intrinsic understanding of material properties, is detrimentally limited.

TGA analysis (Figure 5.4, Table 5.1) allowed for the determination of mass loss processes in the materials. The extrapolated onset temperatures rate the thermal stability by mass loss as SA (180.3°C) < CC (202.8°C) < PM (207.9°C) < BA (226.9°C). The nature of the mass loss is unclear at this stage but can be defined in all samples as a singular (single dTG peak), (relatively 'steep' TG curvature) and complete (total mass losses of > 99%) transition from the solid to gaseous state.

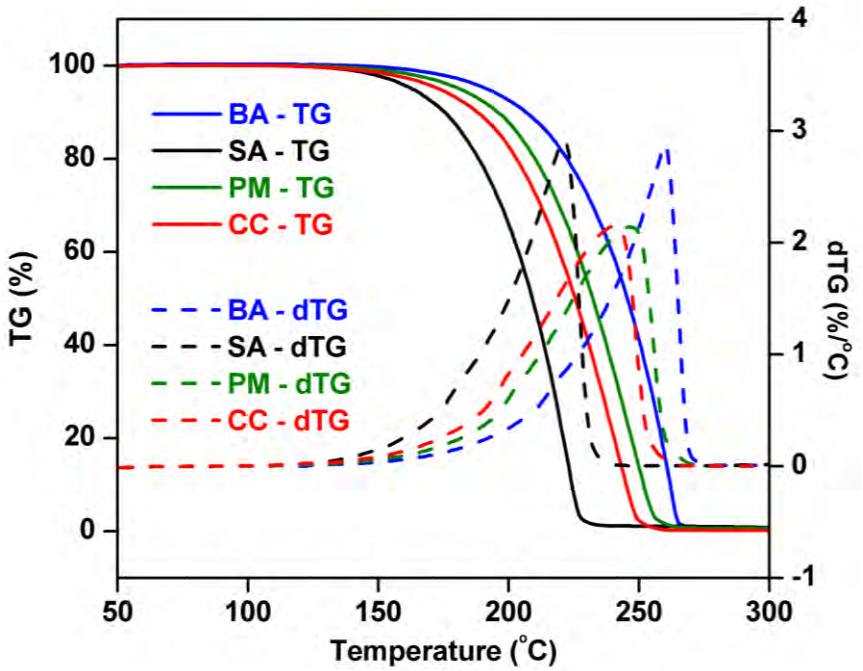

Figure 5.4 TG (solid lines) and dTG (broken lines) curves for BA, SA, PM and CC.

Table 5.1 Experimental parameters for the CC obtained from TGA analysis.

Sample	TG Onset (°C)	dTG Peak (°C)	Mass Loss (%)
BA	226.9 ± 0.7	258.7 ± 0.3	99.6 ± 0.1
CC	202.9 ± 0.9	241.3 ± 0.8	99.7 ± 0.1
PM	207.9 ± 1.2	247.1 ± 0.1	99.1 ± 0.1
SA	180.3 ± 1.6	220.8 ± 0.6	99.4 ± 0.1

DSC analysis (Figure 5.5, Table 5.3) presents fairly 'textbook' behaviour for BA, SA and CC. A sharp endothermic transition followed by a broad and shallow endotherm is indicative

of a melt - evaporation process (Craig and Reading 2006) and was confirmed by HSM analysis (not presented) to be the case. DSC rates thermal stability by melting point onset as CC (118.2°C) < BA (126.3°C) < SA (158.8°C). The broad endothermic events at 180°C coincide with the mass loss processes observed by TGA and HSM and are attributed to evaporation of the melt. There were no other thermal transitions (at lower or higher temperatures) detected for BA, SA or CC (by TGA, DSC or HSM), and so the melting points described above are considered the primary transitions in these three samples. Any transitions below the melting temperature will be considered as secondary processes.

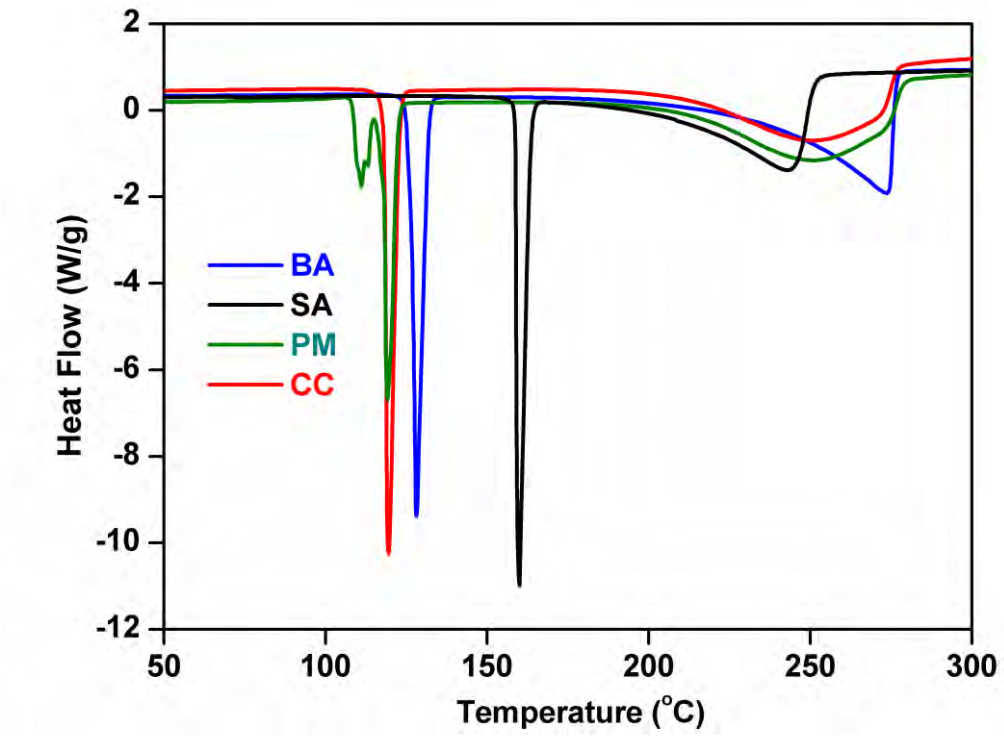

Figure 5.5 DSC curves for BA, CC, PM and SA. Note: 'exotherm up'.

Table 5.2 Experimental parameters obtained from DSC analysis of the CC system.

Sample	Onset (°C)	Peak (°C)	Peak Height (W/g)	Peak Width (°C)	Normalised Peak Integral (J/g)
BA	126.3 ± 0.3	128.0 ± 0.2	9.7 ± 0.6	3.1 ± 0.1	203.9 ± 6.5
SA	158.8 ± 0.3	159.4 ± 0.2	11.1 ± 0.5	2.7 ± 0.1	188.9 ± 5.9
PM (1^{st} peak)	108.3 ± 0.1	111.2 ± 0.3	1.8 ± 1.8	4.3 ± 1.6	40.5 ± 10.7
PM (2^{nd} peak)	118.0 ± 0.2	119.0 ± 0.2	6.6 ± 0.4	2.7 ± 0.6	200.8 ± 4.6
CC	118.2 ± 0.2	119.3 ± 0.3	10.7 ± 0.5	2.7 ± 0.6	198.9 ± 5.1

The DSC thermogram of the PM is more complex than the thermograms of the other three samples. From low to high temperatures, the first transition detected by DSC begins at 108.3°C and is a collection of multiple endothermic peaks. This is closely followed by an intense and sharp endothermic peak at 118°C (possibly a melt), which is succeeded by a broad and shallow endothermic transition (possibly evaporation). The temperature at which the second process occurs is intriguing. It occurs (for all intents and purposes) at the same temperature as the melting of the CC; thus suggesting the collective transitions before it represents a mechanism for CC formation. This process was closely followed by HSM (Figure 5.6) where softening of the sample begins at around 105°C, followed by a melting process at 111°C, immediately succeeded by crystallisation continuing until 116°C. Melting of the newly-formed crystals begins at 118°C and is complete by 120°C. It should be noted that in the case of HSM analysis some areas of the visible sample remained unchanged during analysis. This is attributed to uneven temperatures across the glass slide and lack of nucleation sites for crystallisation.

The proposed theory of CC formation via heating of PM was further confirmed by additional DSC analysis, AT-FTIR and XRPD. A DSC heat-cool-heat (HCH) protocol was developed as follows.

1. First heating from 25°C to 140°C at 10°C/min
2. Isothermal at 140°C for 30 minutes

3. Cooling from 140°C to 25°C at 10°C/min
4. Second heating from 25°C to 600°C at 10°C/min

5 mg samples were used in DSC studies. The same protocol, without step 4, was utilised to prepare 50 mg of CC for AT-FTIR and XRPD analysis. For the purpose of the remainder of this section the CC prepared by evaporation from solvent is termed CC_E, and the CC prepared via the above heating protocol is termed CC_H. It was essential to deduce whether CC_H was identical to CC_E.

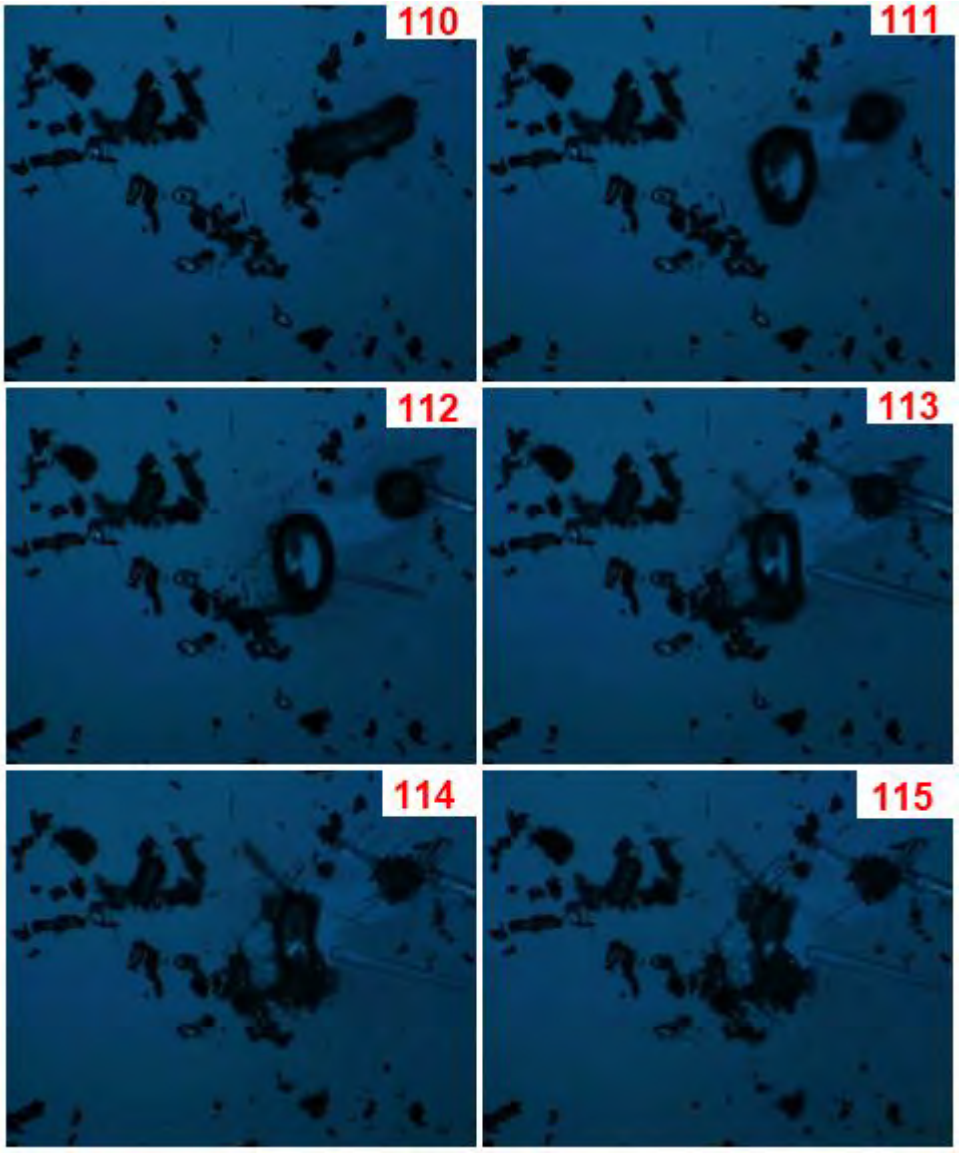

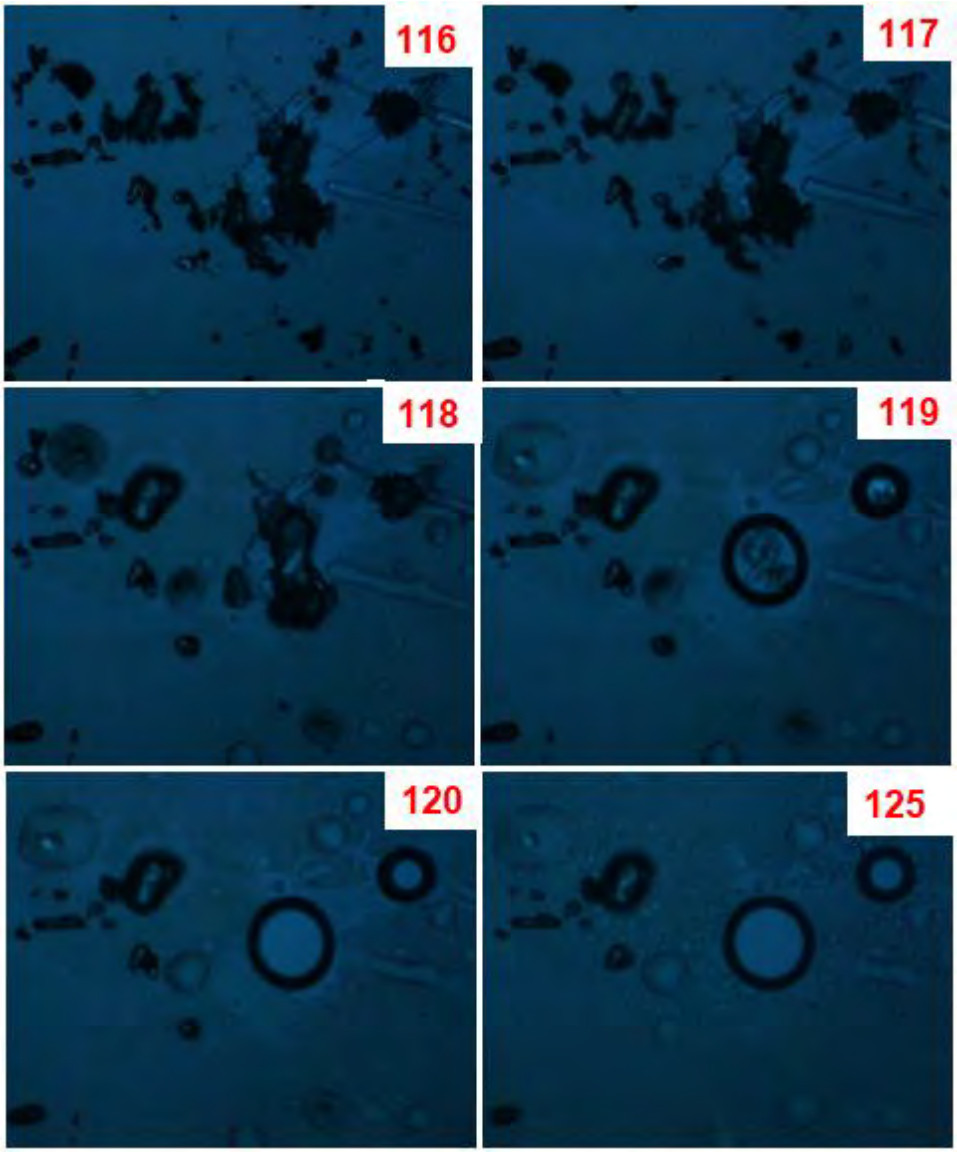

Figure 5.6 HSM snapshots of the heating of PM. Numbers in red = temperature in °C. x10 magnification.

Results of DSC heat-cool-heat (HCH; Figure 5.7) experiments demonstrate the protocol is effective for *in-situ* preparation of CC_H via heating of PM. Upon first heating a similar scenario to the original DSC study is realised. After stages 1 and 2, at 140°C, the sample is in the liquid state; where it is cooled at 10°C/min. During the cooling process, crystallisation is induced at an onset temperature of 53.8°C (peak = 52.3°C, 1°C wide, 25.85 W/g height, 202.1 J/g integral) represented by a single, intense exothermic peak. The second heating of the sample yields a single peak at 118.4°C (onset temperature), representative of the melting of CC_H.

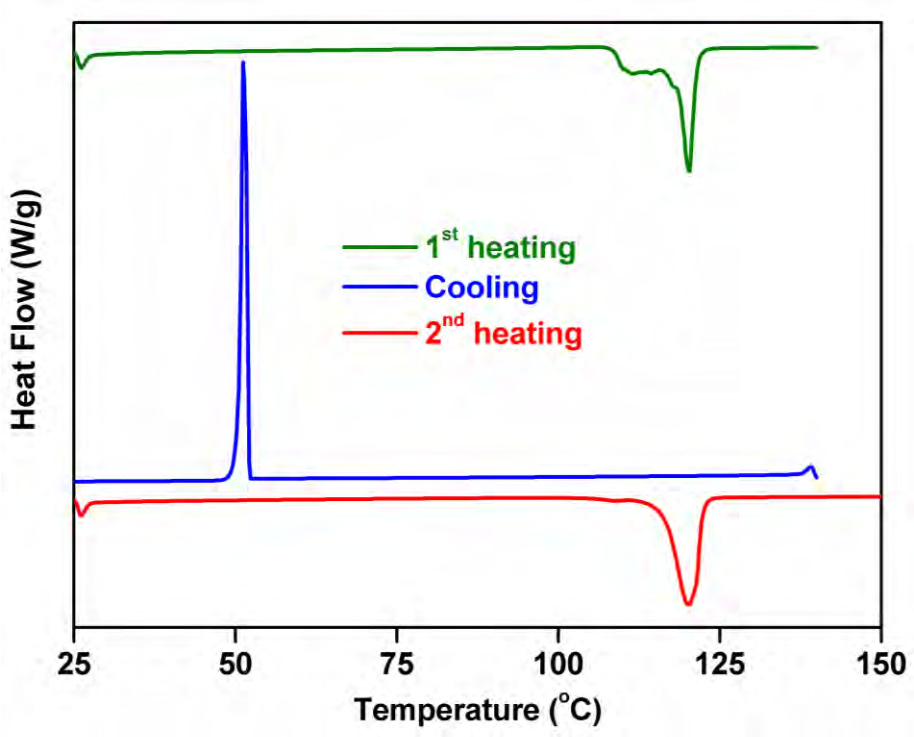

Figure 5.7 DSC thermograms representative of *in-situ* CC formation via heating of PM. Note: 'exotherm up'.

CC_H was compared by AT-FTIR and XRPD (Appendix: Figures 5.2A, B and 5.3) with the original CC_E; the data shows that the CCs are identical. Therefore, a new method of generation of the 1:1 molar ratio CC of SA/BA has been developed. This is the first reported instance of this methodology being used for the synthesis of this CC.

In the literature, this method of CC preparation is referred to as melt crystallisation, and is widely reported (Byrn and Henck 2012; Elder et al. 2012; Qiao 2012; Thakuria 2012). The SA/BA example presented here is somewhat novel in that the CC can actually be prepared *in-situ* in just one single heating step; unlike the conventional method of heating (to allow for melting of the components), and then cooling (to induce crystallisation). The SA/BA PM/CC may be considered a eutectic system as the temperature of melting and crystallisation is lower for a mixture of SA/BA than it is for any of the single components (Gabbot 2008).

In conclusion, thermal analysis has been used to detect and characterise the primary transitions in all samples. In the case of BA, SA and CC their primary transition are their melting points (126.3°C, 158.8°C and 118.2°C, respectively). For the 1:1 molar ratio PM the

primary transition is the eutectic melt/crystallisation process beginning at 108.29°C. Any processes detected by TSC experiments at lower temperatures would be considered secondary processes/relaxations. Thermal analysis also allowed for the development of a new (and possibly more efficient) methodology for preparing the 1:1 molar ratio CC via heating of a 1:1 molar ratio of the PM components. Upon scaling up of the CC preparation, by melting, it can be assumed that a larger amount of starting materials, and therefore a slower rate of cooling, would produce much larger amounts (possibly more uniform in shape and chemistry) than is achieved on the small (mg) scale used here.

5.3.3 TSC spectroscopy

To my knowledge, this is the first TSC study of a CC system. 'On paper' TSC spectroscopy has several advantages to studying such a class of materials. As mentioned, a key limiting issue with CCs is their unknown/unpredictable short and long term stability. As a technique which directly monitors molecular mobility, a process intrinsically linked to stability, TSC can potentially be used to pioneer such research efforts. Additionally, there is a justifiable need to understand the mechanisms of CC formation for the purpose of understanding why co-crystallisation occurs, by which mechanism(s) and how co-crystallisation may be predicted or controlled. TSC spectroscopy may be a unique tool to study the effects co-crystallisation has on the components of the CC and on the CC itself.

Compared to primary transitions, secondary relaxation processes generally occur in temperature regions that are more frequently accessible in real world applications. During production, storage, use and shipping, the temperature regions of the primary transition will rarely (if ever) be reached, in contrast to those of the secondary relaxations. It is therefore imperative that the secondary relaxations are detected and fully characterised as early as possible.

The 'natural motion' of molecules under the influence of heating (no electrical field) is represented by SDC experiments (Figure 5.8) where, in this case, molecular mobility is apparent after ≈ 0°C; represented by deviations from the baselines and/or peaks. The molecules in BA appear to be mobile at the lowest temperatures, followed by PM and then SA/CC at similar (but higher) temperatures. Of note is the scale at which current is being recorded; values of ± 5 x 10^{-15} A are relatively small, only an order of magnitude larger than the baseline at x10^{-16} A. This accounts for the 'noisy' signal presented here.

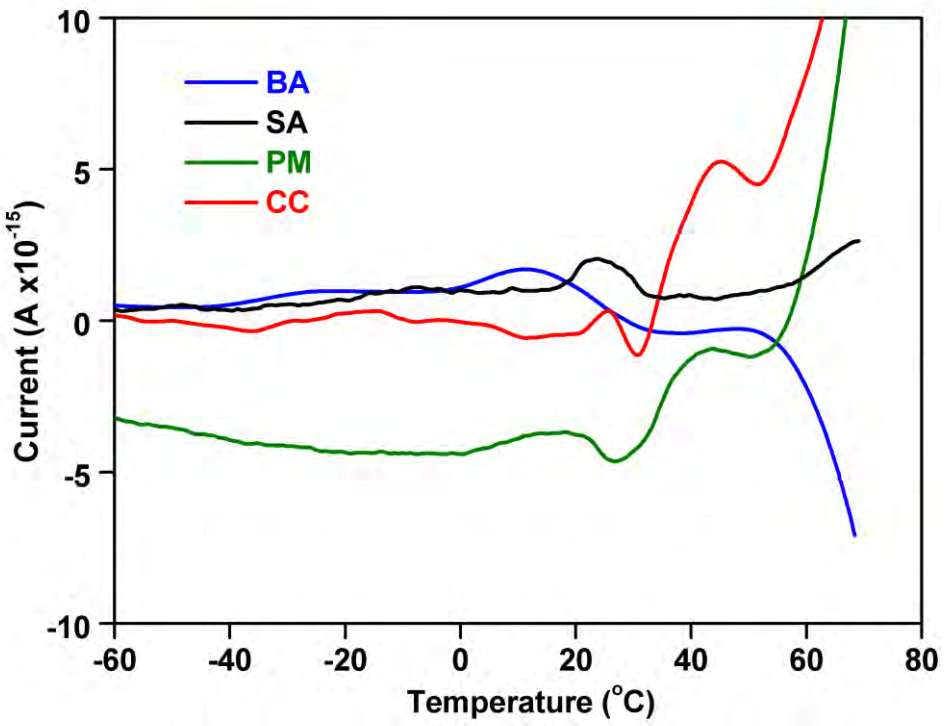

Figure 5.8 SDC curves for BA (blue), SA (black), PM (green) and CC (red). (E_p = 200 V/mm.)

Application of a constant static electrical field during TSPC experiments (Figure 5.9) can intensify the current signal by inducing a greater change in dipole moment as molecules are forced to align with the electric field as soon as energies and relaxation times are suitable. In this instance a similar scenario to SDC experiments is realised. The molecular motions of BA are the most prevalent at lower temperatures; followed by PM, CC and SA as temperatures increase. The magnitude of the currents measured here are significantly larger than those during SDC experiments.

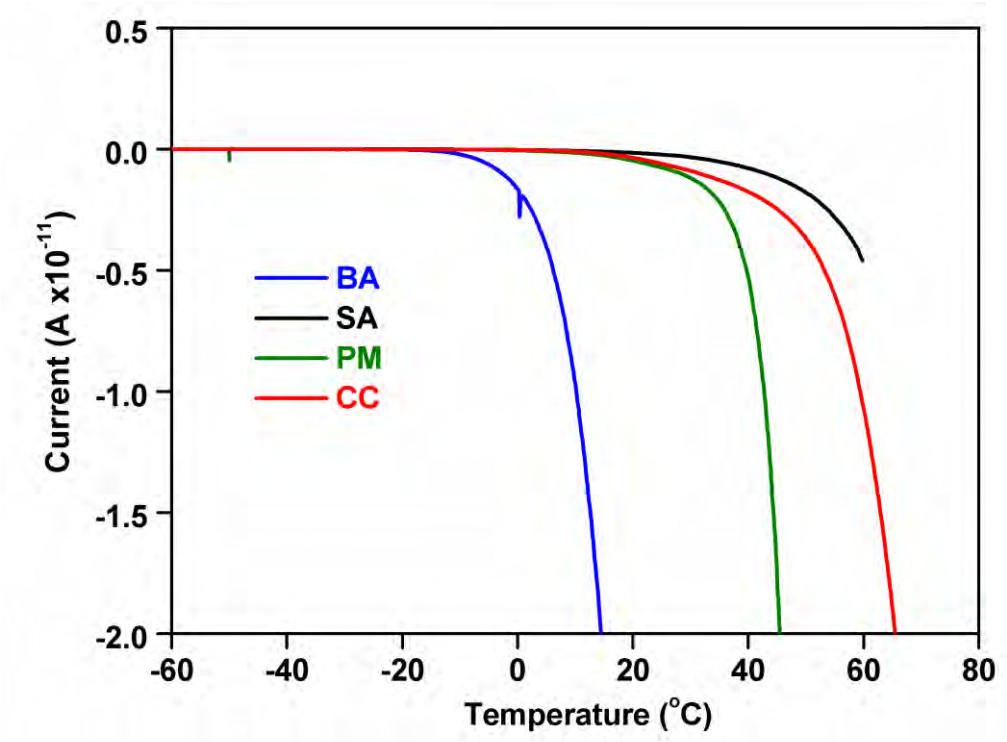

Figure 5.9 TSPC curves for BA (blue), SA (black), PM (green) and CC (red). (E_p = 200 V/mm.)

TSDC experiments (Figure 5.10) were undertaken using a polarisation temperature (T_p) of 40°C; where a single global relaxation peak for each sample was realised. Peak temperatures were: BA = 20.1°C, SA = 23.4°C, PM = 23.8°C and CC = 28.2°C. Interestingly, the TSDC relaxation profiles for all samples overlap in the same temperature region, from ≈ -30 to 50°C. This result confirms that, in the solid-state, the CC constituents share a secondary relaxation domain in the same temperature region.

Mixing of the CC constituents (represented by PM) appears to have little (or no) influence on the secondary relaxation processes. Co-crystallisation does have an effect on the relaxation process; shifting it to a slightly higher temperature. This indicates more energy is required to initialise this relaxation process, until the relaxation times of the charge carriers falls within the experimental time window utilised here. Alternatively, it can be concluded that co-crystallisation results in the relaxation domains of the constituents being less accessible at lower temperatures; slightly improving their short term stability in the secondary relaxation temperature region.

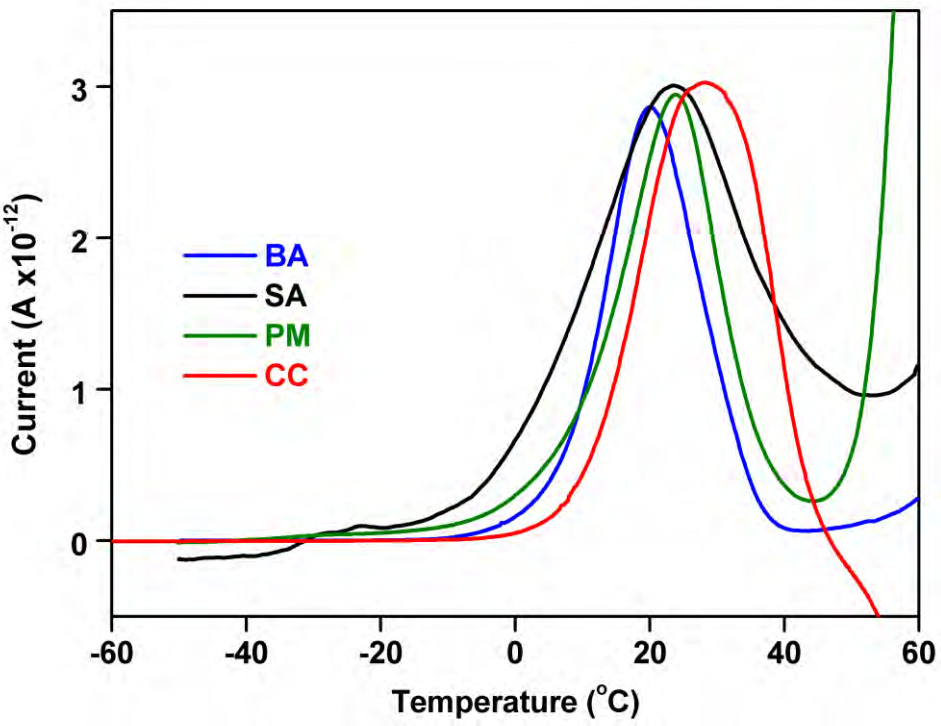

Figure 5.10 TSDC curves for BA (blue), SA (black), PM (green) and CC (red). (T_p = 40°C. E_p = 200 V/mm.)

5.3.4 Thermal windowing and compensation analysis

The global relaxation process identified by TSDC is likely to be the result of many underlying motions, each with its own single (or a narrow distribution of) relaxation time(s). The thermal windowing (TW) methodology is used to experimentally deconvolute global relaxation processes into their elementary relaxation spectra. Theoretically, each TW relaxation curve represents a process with a single relaxation time; in reality, a narrow distribution of relaxation times is obtained (Correia et al. 2000). The TW results are shown in Figure 5.11 and the associated 'Bucci plot' generated by relaxation map analysis (RMA) (Williams 1975) presented in Figure 5.12.

TW gives a more realistic and detailed representation of the relaxation behaviour of a sample compared to a standard TSC experiment, e.g. TSDC. In this instance (and in contrast to the global TSDC peaks) TW clearly highlights significant differences between the samples, whilst confirming that the relaxation domains of the samples do overlap in the same temperature region.

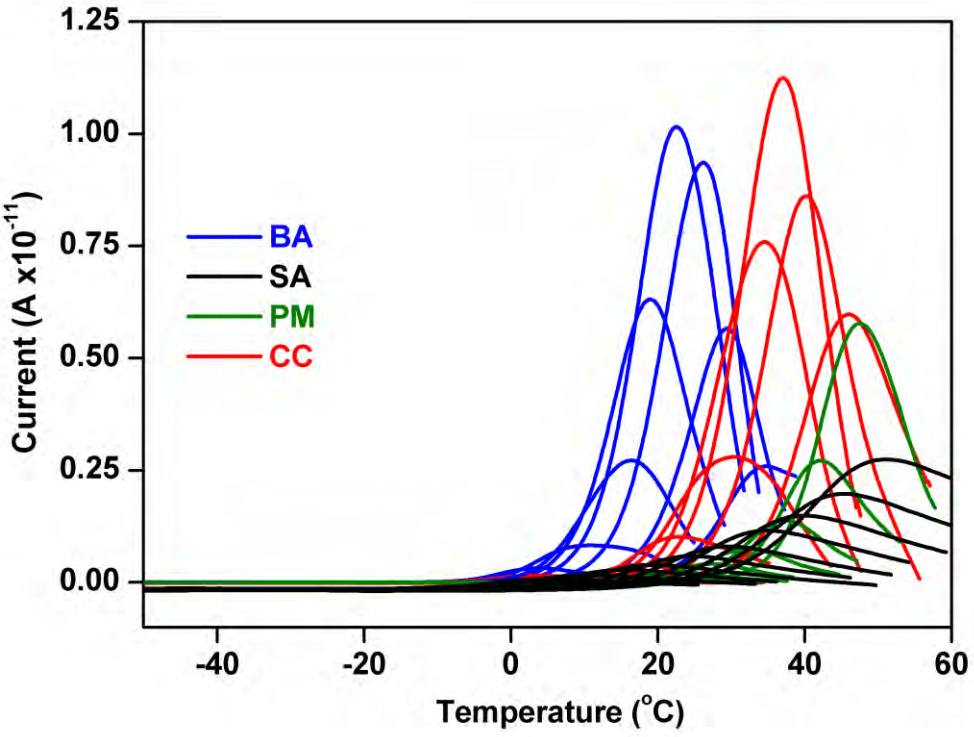

Figure 5.11 TW curves for BA (blue), SA (black), PM (green) and CC (red). (T_w = 5°C from -5 to 40°C. E_p = 200 V/mm)

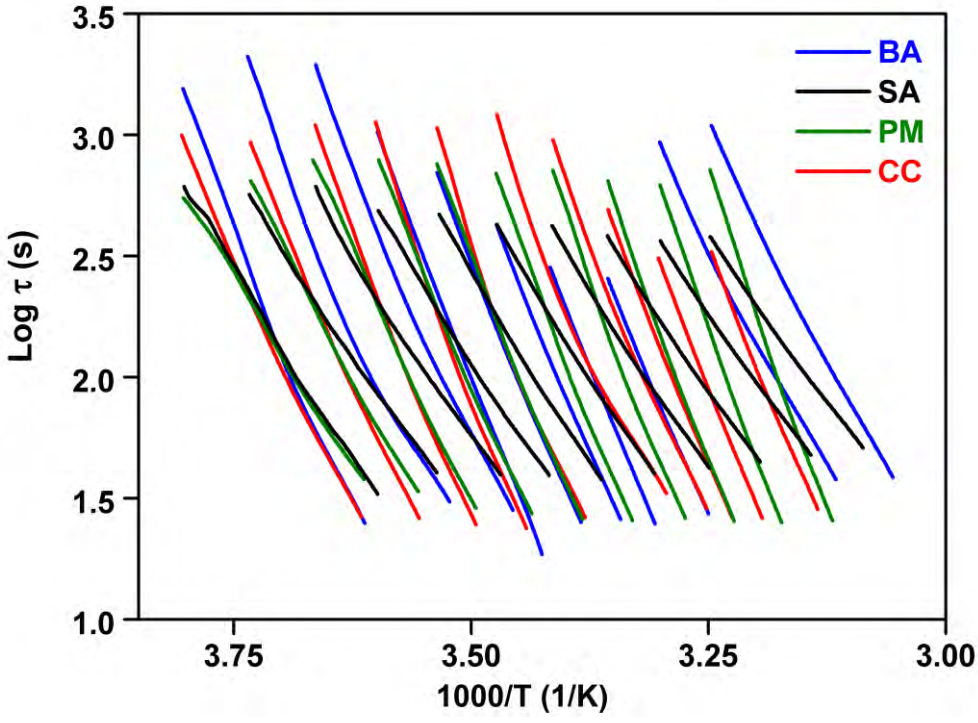

Figure 5.12 'Bucci lines' for BA (blue), SA (black), PM (green) and CC (red).

The effects of physical mixing and co-crystallisation on relaxation behaviour are more insightful in the TW representation than in the standard TSC experiments. The PM does not appear to be an aggregation of the relaxation behaviour of its constituents, but a different relaxation process altogether; suggesting an interaction between the components in this temperature region. A similar trend is also realised for the CC. The relaxation domain of the CC is clearly distinct from its constituents and a mixture thereof.

Figures 5.13 and 5.14 highlight the linear changes expected of dipolar relaxations in Gibbs free energy and peak position and temperatures of polarisation and peak position. These plots confirm that the relaxations detected are true dipolar relaxation processes (Neagu and Neagu 2003; Moura Ramos et al. 2007).

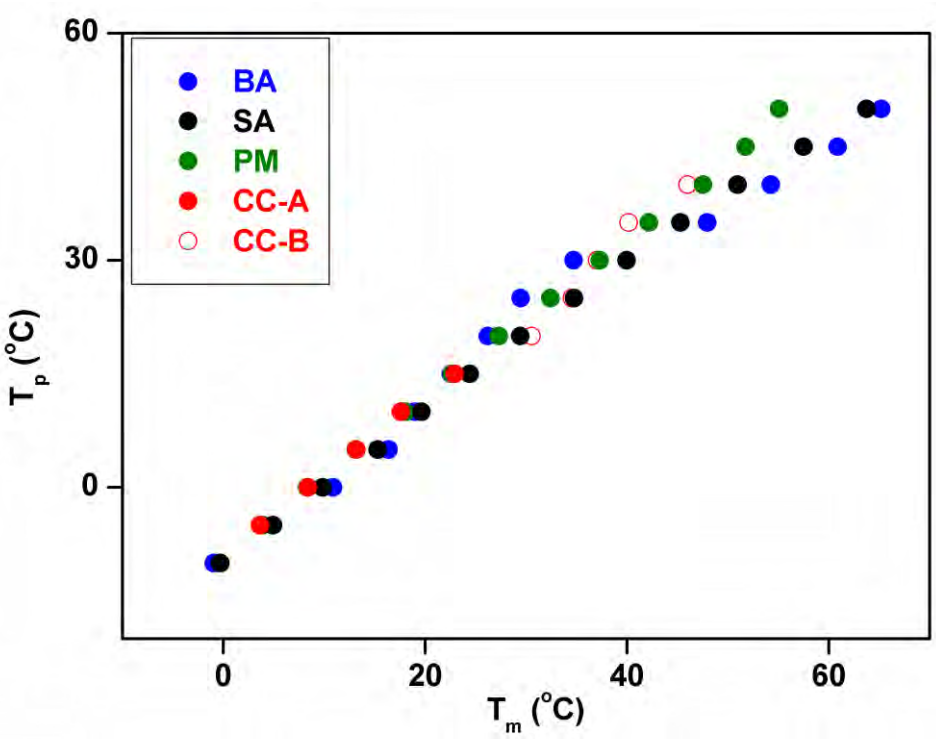

Figure 5.13 Peak position as a function of polarisation temperature for the different samples examined.

Compensation analysis (Figure 5.15) via the RMA software was undertaken on all samples. BA and SA did not show any compensation behaviour. Compensation behaviour was recognised for the PM and the CC; the compensation parameters were therefore calculated and are presented in Table 5.3. As has been mentioned in previous Chapters, the origin of compensation behaviour is currently poorly understood. However, its existence is difficult to dispute and more often than not the parameters obtained by compensation (particularly

compensation temperature) analysis correlate to temperature regions of other thermal events; suggesting a link between them.

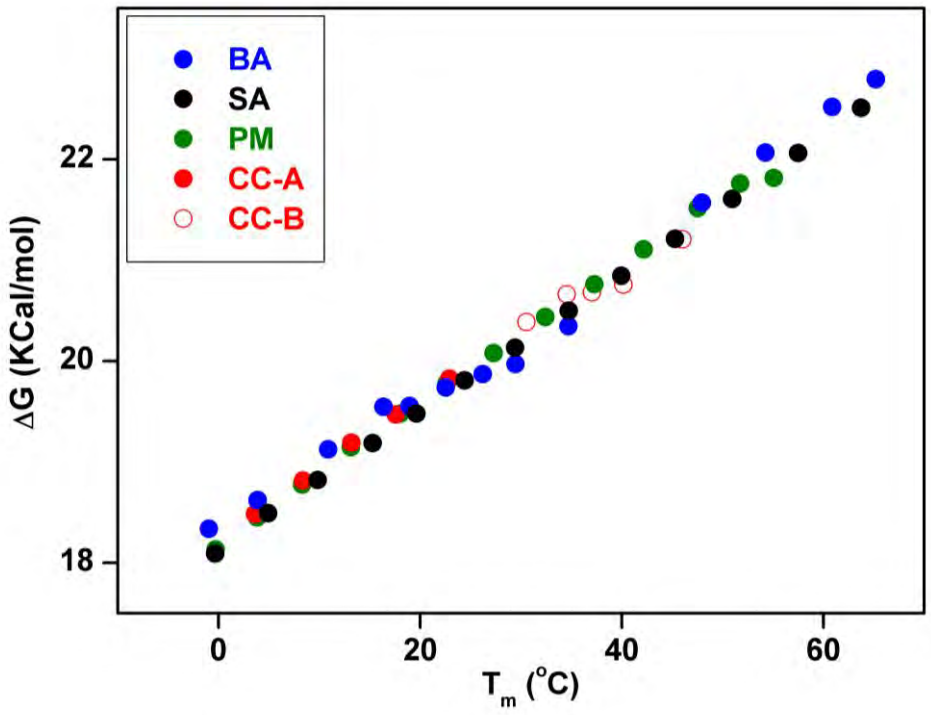

Figure 5.14 Peak temperature as a function of change in Gibbs free energy.

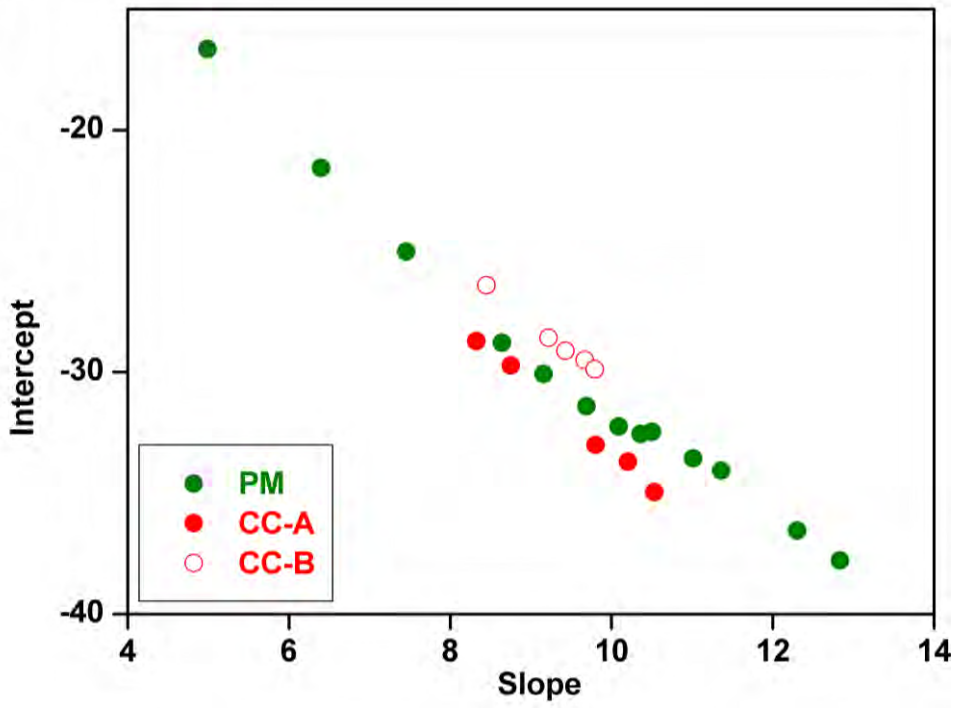

Figure 5.15 Compensation analysis of PM and CC domain A (CC-A) and CC domain B (CC-B).

Table 5.3 Compensation parameters for PM, CC domain A (CC-A) and CC domain B (CC-B).

	PM	CC-A	CC-B
R^2*	0.99	0.99	0.99
T_p range (°C)	-5 to 40	-5 to 15	20 to 40
T_c (°C)	110.51	125.71	118.58
τ at T_c (s)	6.47×10^{-6}	9.79×10^{-9}	1.67×10^{-5}
DOD	64	77	62

* Compensation correlation coefficient

The PM exhibited strong compensation correlation across the entire T_p range investigated and exhibits a compensation temperature (T_c) of 110.5°C. Referring back to DSC studies the primary transition for the PM displayed an onset of 108.3°C and a peak temperature of 111.2°C. Therefore, the T_c lies at the centre of the primary transition, providing strong evidence of a link between them. The primary transition of the PM is a eutectic transition involving the two components, which do not -on their own- possess any compensation behaviour, but do so when mixed. It is therefore apparent that the secondary relaxation observed in PM by TSC is linked (via compensation analysis) to the primary transition, and may be a subtle preparative motion in readiness for the eutectic melt of the components. It is believed this is the first reported link between a secondary relaxation and a eutectic primary transition observed in a LOM. The DOD at T_c has a value of 64.7, is high on the scale of around 25 to 75 and represents high disorder (Ibar 1991). From DSC experiments we know that at T_c the material is in, or approaching, the liquid state, and so significant disorder is to be expected. τ at T_c is also fast (6.47×10^{-6} s); again, this would be expected in a 'structurally loose' liquid or partially liquid system.

The CC also exhibited compensation behaviour which could be distinctively divided into two compensation domains A (CC-A) and B (CC-B). Once again, a clear link is found between the compensation temperatures and the primary transition. The primary transition of the CC is a melt with an onset of 118.2°C which peaks at 119.3°C. T_c values for CC are 125.7°C for CC-A (prior to the primary transition) and 118.6°C for CC-B (after the primary transition).

The DOD and τ values are representative of the state of the sample. The CC-B compensation predictions of DOD = 63 and $\tau = 1.67 \times 10^{-5}$ s at $T_c = 118.6°C$ are representative of the sample in the softened state, just about to melt. Relatively high DOD and relatively fast τ values are therefore to be expected; for the reasons explained earlier for the PM. The CC-A compensation predictions of DOD = 78 and $\tau = 9.79 \times 10^{-9}$ s at $T_c = 125.7°C$ are representative of the sample in the post-melt liquid state, where a significantly higher DOD (in comparison to CC-B) would be expected as the system will be more disordered post-melt than pre-melt. Lack or order and a 'looser' structure in the liquid state will also allow for much faster relaxation times, as indicated by a τ value several orders of magnitude greater after the melt, than before.

The conclusions drawn from compensation analysis, and therefore the links deduced between the secondary relaxation phenomena and the primary transition, are very strong in this instance. There is, undoubtedly, a prerequisite relationship between primary and secondary processes in the solid-state. As this example shows it is even possible to predict the melting points of a material from detailed analysis of their low-temperature relaxation behaviour. These types of prediction, and the fact that molecular mobility is so closely linked to stability, has profound future applications for the use of TSC spectroscopy in the assessment of, and prediction of, short and long term stabilities of pure materials and even mixtures/formulations.

As has been mentioned previously, the origins and intricacies of compensation phenomena observed in TSC experiments (and in general chemistry) are unknown. What is apparent is that the compensation phenomenon originates from a linear relationship between enthalpy and entropy or, activation energy and pre-exponential factor. This behaviour is clearly evident in this study and is presented in Figures 5.16 and 5.17. Some researchers argue that compensation in TSC spectroscopy is a consequence of the mathematical description that models the physical process of relaxation (Mano 2005); and that it arises from statistical errors. These authors only focus on the amorphous state, particularly the glass transition. This opinion has only arisen due to a lack of detailed understanding of the physical processes that occur in the solid-state. Whilst there may be some veracity in the fact that errors (mathematical or otherwise) can influence experimental TSC results, it does not account for the numerous examples of compensation phenomena which correlate to real physical processes, such as the experimentally proven links between secondary and primary processes presented here and in other Chapters of this thesis.

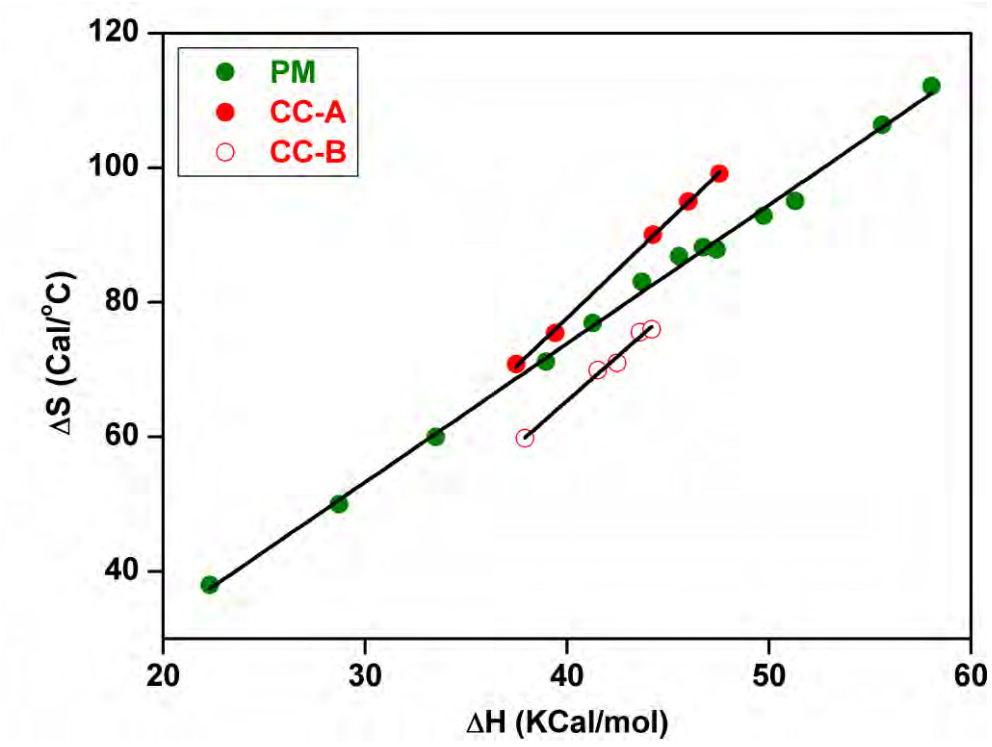

Figure 5.16 Change in enthalpy and entropy in the PM and CC.

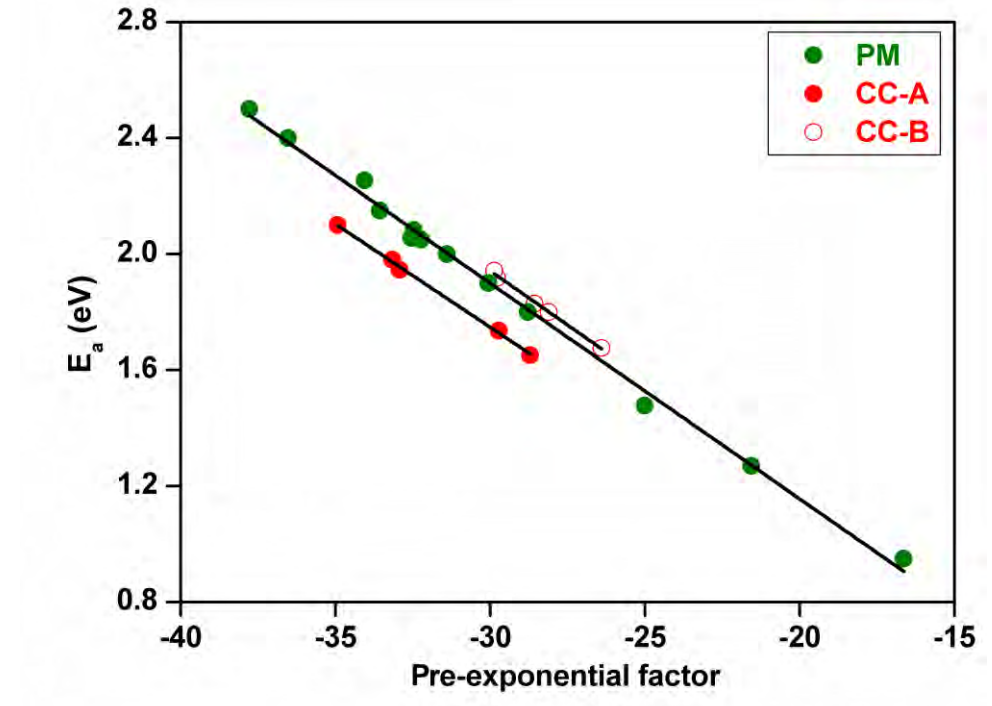

Figure 5.17 Pre-exponential factor *vs.* activation energy for PM and CC.

Further information on the relaxation processes in the CC and PM can be gained from analysis of the change in activation as a function of temperature in comparison to the zero

entropy prediction (Figure 5.18). This type of graphical representation, proposed by Starkweather (Sauer 1990; Diogo 2008), allows conclusions regarding the cooperativity of the relaxation process to be drawn. Activation enthalpies on or close to the zero entropy prediction indicate non-cooperative or low cooperative motions. Those which deviate significantly from the zero entropy prediction indicate cooperative relaxation (Correia et al. 2000).

In the case of the PM, activation enthalpy increases with peak position from close to the zero entropy prediction to a moderate deviation from it; represented by a maximum activation enthalpy of 60 kcal/mol. This suggests the cooperativity of the relaxation process is increasing with temperature. This type of behaviour is to be expected as eventually, when the primary transition temperature is reached, the process will be a fully cooperative process.

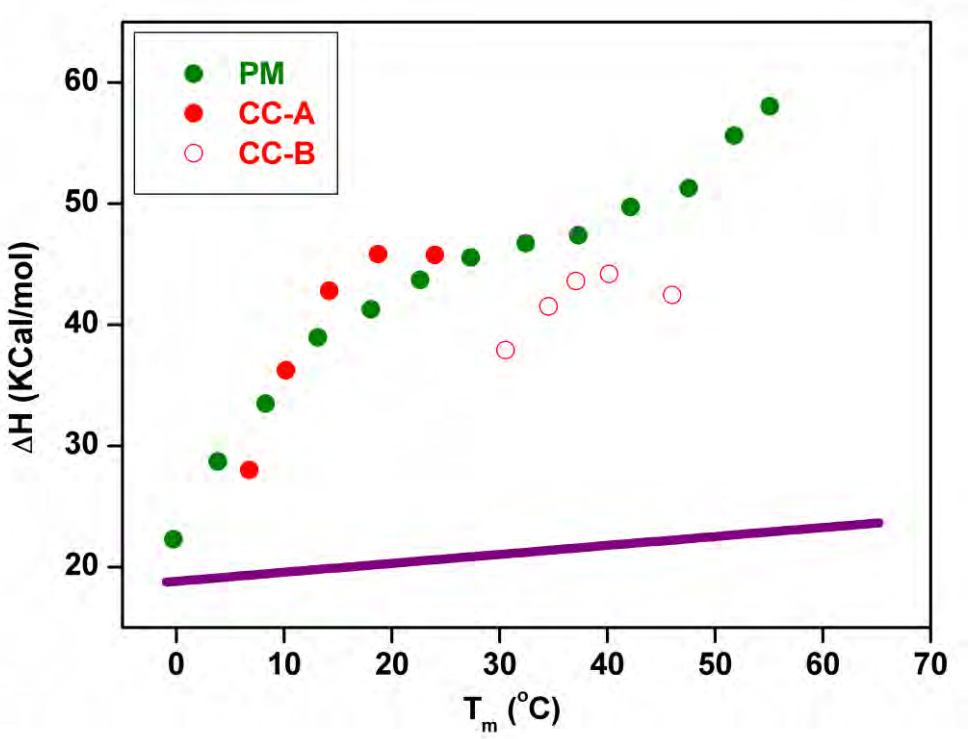

Figure 5.18 'Starkweather' plot of activation enthalpy as a function of peak position in relation to the zero entropy prediction (purple line).

For the CC, the cooperativity profile is clearly comprised of two distinct regions, relating to the compensation domains classified earlier. It is suggested that the compensation domains relate to two separate and distinct relaxation processes, accounting for many of the observations presented here including broadening of the global TSDC peak (Figure 5.1). The cooperativity of CC-A increases with peak position until a slight drop in cooperativity as the

relaxation of CC-B begins at around 25°C; represented by a similar cooperativity profile of an increase, followed by a slight decrease. Ultimately, the total cooperativity of the system is higher at the end of the relaxation process than it was at the beginning; accounting for a net increase in cooperativity with temperature.

In conclusion, the secondary relaxation phenomena in the PM and CC, as well as their constituents, have been detected and characterised via the use of experimental and computational TSC methodologies. Global relaxations at peak temperatures of BA = 20.1°C, SA = 23.4°C, PM = 23.8°C and CC = 28.2°C were detected in all samples and were ultimately all concentrated in the same temperature region of -30 to 60°C. RMA and compensation analysis were used to characterise the relaxation phenomena in PM and CC where the nature of the secondary relaxation processes were explained in relation to their compensation behaviour, their link to the primary transition and the cooperativity of the relaxation phenomenon.

5.3 CONCLUSIONS

A combination of thermal analysis, solid-state NMR, XRPD and TSC have been utilised to characterise the pharmaceutically relevant 1:1 molar ratio co-crystal system of salicylic acid and benzamide. The following conclusions can be drawn.

- Preparation of the CC from solvent was successful.
- The thermal stability by mass loss of the samples is in the order: SA (180.33°C) < CC (202.8°C) < PM (207.9°C) < BA (226.9°C) in terms of their TGA extrapolated onset temperatures. All samples showed total mass losses of > 99%.
- The thermal stability by melting of the samples is in the order: PM (108.23°C) < CC (118.2°C) < BA (126.3°C) < SA (158.8°C) in terms of their DSC extrapolated onset melting point temperatures. Melting points were identified as the primary transitions in all samples.
- The melt of the PM, at 108.3°C, was classified as a eutectic transition involving the components BA and SA.
- The eutectic transition in PM beginning at 108°C allows for the co-crystallisation of the components in the molten phase. This was confirmed by DSC and HSM. A heating, as well as a heat-cool-heat protocol was proposed for the reliable preparation

of CC without solvent; this was confirmed to be successful by solid-state spectroscopic/diffractometric studies.

- Secondary relaxation phenomena was detected in all samples and is represented by TSDC peak positions of BA = 20.1°C, SA = 23.4°C, PM = 23.8°C and CC = 28.2°C. Relaxation phenomenon in all samples is concentrated in the -30 to 60°C temperature region; possibly a reason why the components interact to form a CC (overlapping temperature regions of molecular mobility allow for favourable interactions between components).
- Mixing of the components in PM does result in a solid-state interaction in the secondary relaxation temperature region. The interaction is represented by a single (and not compound) relaxation mode in the PM, not present in either of the components.
- The aforementioned solid-state interaction in the secondary relaxation temperature region ultimately results in a eutectic transition beginning at 108°C in the primary transition region. A link between the primary and secondary processes was proved by compensation analysis by a predicted compensation temperature of 110°C. The compensation parameters of relaxation time and DOD at the compensation temperature confirm the likelihood of a melting transition, which was proved to be the case by thermal analysis.
- The secondary relaxation processes in CC were determined to comprise of two distinct relaxation modes represented by separate compensation domains (CC-A and CC-B). The compensation temperatures and parameters signify a link between the secondary relaxation process and the primary transitional melt of the CC at 118°C. Domain CC-A relates by a compensation temperature of 126°C to the post-melt condition of the CC. Domain CC-B relates by a compensation temperature of 118.6°C to the onset of the CC melt. Both domains are characterised by relatively fast relaxations and a high degree of disorder at the primary transition.
- The cooperativity of PM and CC molecular motions in the secondary relaxation temperature region was characterised by a net increase in cooperativity as a function of temperature from non-cooperative to moderately cooperative motions.

A significant amount of relevant and useful information about co-crystal systems, and this specific SA/BA CC, was gained from this study; the majority of which is attributed to the use

of the TSC technique. In relation to some of the issues surrounding the use, characterisation of and preparation of co-crystals, the information gained from and the demonstrated potential of the TSC technique in expanding such knowledge, is of significant scientific interest from an academic and industrial perspective.

On the topic of co-crystal formation: a notable feature of this particular system is that the temperature regions of molecular mobility for the components and the co-crystal overlap. This, perhaps, explains why the two components form a co-crystal in the first place; mobility at the molecular level in the same temperature region may result in favourable interactions between components leading to co-crystallisation itself, or more plausibly, subtle movements in preparation for co-crystallisation. It would be interesting to see if such a feature is present in other, or all, co-crystal systems.

A second topic of importance throughout this experimental chapter is the issue of co-crystal stability. As mentioned in the introduction to this chapter, industry may be reluctant to market a co-crystal product if they are unsure of its long term stability. A technique such as TSC which allows for the determination of several kinetic parameters may prove desirable to industry as, presumably, kinetic parameters obtained experimentally can be correlated with long term stability studies to monitor and maybe predict long term stability.

The demonstrated use of TSC spectroscopy to essentially ‘predict’ a transition (i.e. compensation analysis of PM predicted a transition at 110°C (eutectic melting point)) has potential to be utilised for the reasons mentioned in the above paragraph as well as in the study of other LOMs. Often in thermal analysis, transitions are hidden by overlapping processes, or not detectable during non-isothermal experiments (i.e. a material may degrade before its actual melting point). The ability to predict where a temperature transition may occur, by studying the material in a completely different temperature region, has significant potential in all areas of science.

APPENDICES

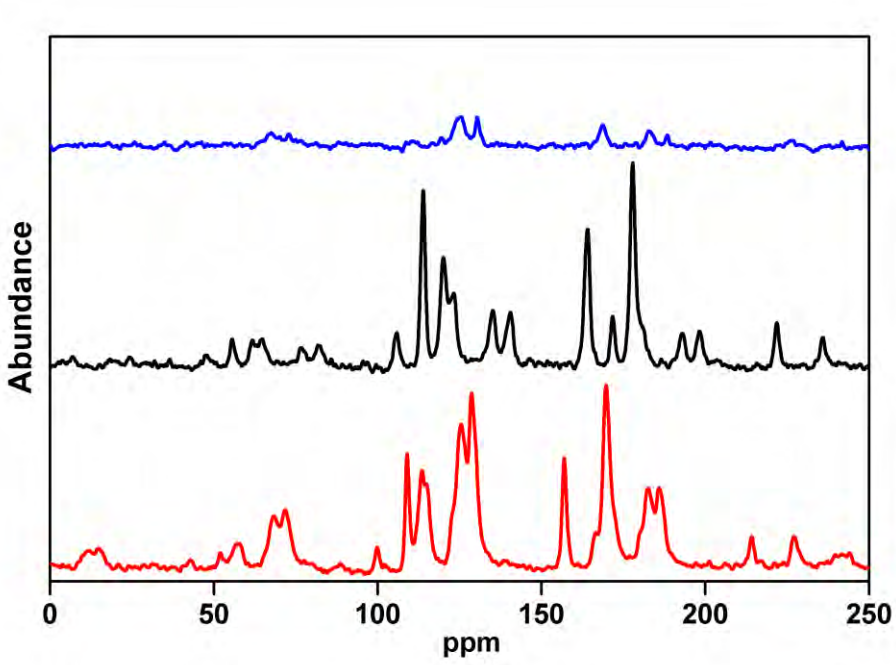

Figure 5.19 Solid-state ^{13}C-NMR spectra of BA (blue), SA (black) and CC (red).

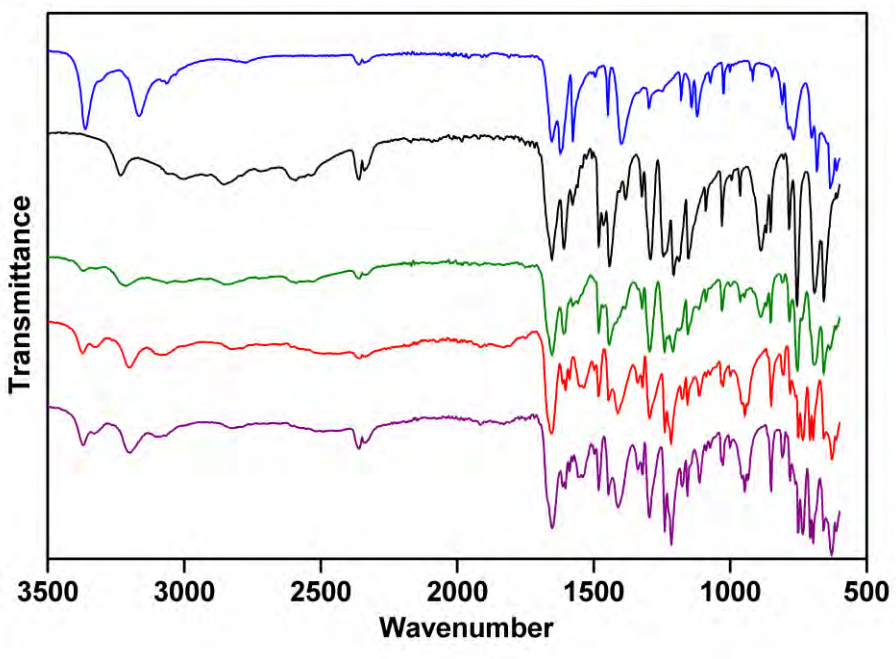

Figure 5.20 AT-FTIR spectra of BA (blue), SA (black), PM (green), CC_E (red) and CC_H (purple).

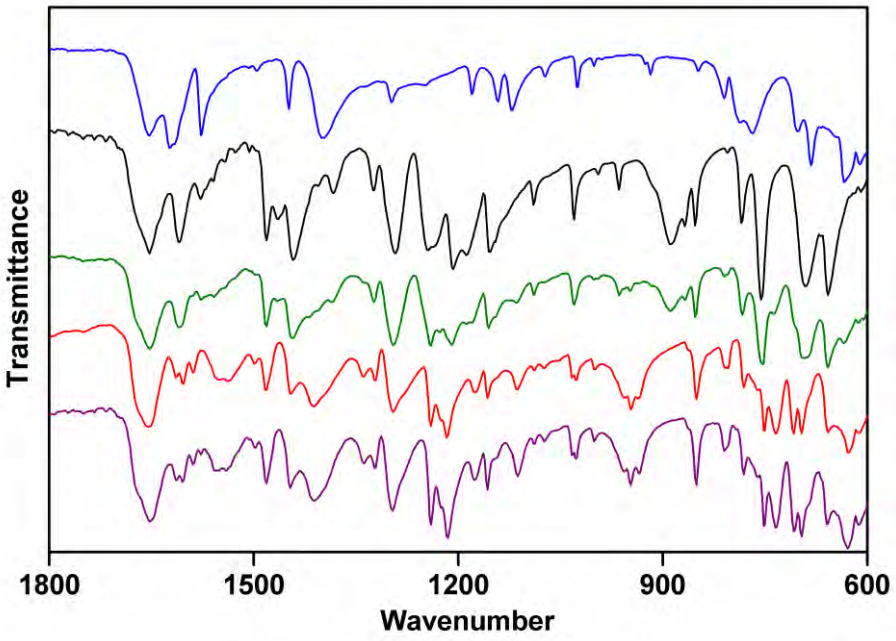

Figure 5.21 AT-FTIR spectra of BA (blue), SA (black), PM (green), CC_E (red) and CC_H (purple); expanded in the fingerprint region.

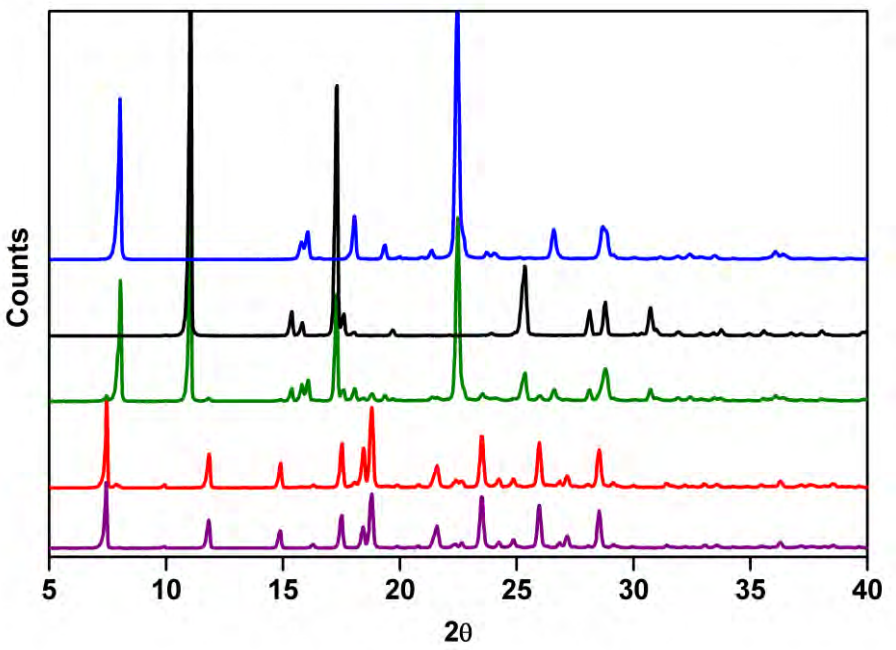

Figure 5.22 PXRD diffractograms for BA (blue), SA (black), PM (green), CC_E (red) and CC_H (purple).

CHAPTER 6: PARACETAMOL FORM I

6.1 INTRODUCTION

Paracetamol (PA; *N*-(4-hydroxyphenyl)ethanamide), also referred to as acetaminophen, (Figure 6.1) is a commercially available analgesic and antipyretic. PA exists in three crystalline polymorphic forms and an amorphous form (Kauffman et al. 2008). PA form I is a monoclinic crystal system, is the thermodynamically stable polymorph and exhibits poor compressibility. Form II is an orthorhombic crystal system, is metastable and exhibits good compressibility in relation to form I. Form II is reportedly stable for months at RT (Kauffman et al. 2008) but is difficult to prepare. Form III is a highly unstable and short lived polymorph of undefined crystal structure, and dubious physical characterisation (Gaisford et al. 2010).

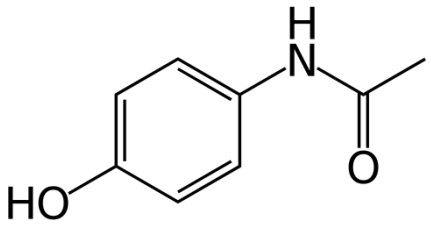

Figure 6.1 Structure of paracetamol (*N*-(4-hydroxyphenyl)ethanamide).

The three polymorphic forms can be differentiated by spectroscopic techniques used for structural elucidation, but more conveniently by melting point determination. Form I exhibits a melting point of 169-170°C, form II of 159-160°C and form III of ≈ 143°C (but often impossible to measure due to conversion of form III to II at lower temperatures; Kauffmann et al. 2008; Gaisford et al. 2010). The amorphous form can be generated by cooling from the melt and exhibits a glass transition temperature of 25°C. Upon heating of the amorphous form, a well-documented crystallisation occurs at 60-80°C (attributed to crystallisation of forms II and III) followed by a solid-solid transition at 100-120°C (attributed to conversion of form III to form II) and finally melt of form II at 159-160°C (Kauffmann et al. 2008; Gaisford et al. 2010).

Form I is available commercially at very high purity and exhibits no known transitions below its melting point (considered the primary transition). Henceforth paracetamol form I will be referred to as 'PA'.

The rationale for the work reported in this Chapter was to choose a well-known, widely used and extensively studied drug (i.e. paracetamol) and use TSC spectroscopy to demonstrate how useful it can be in the study of even the most well characterised of LOMs.

6.2 EXPERIMENTAL METHODS

6.2.1 Sample

A single sample of PA (form I, purity > 99%, analytical standard grade) was used as received. See Chapter 2; section 2.1 for details.

6.2.2 TGA

TGA experiments were undertaken using a TGA Q5000IR instrument (section 2.3.2.1). An inert atmosphere of nitrogen at a flow rate of 25 mL/min was employed. Samples of ≈ 2 mg were accurately weighed and heated from ambient temperature to 600°C at a linear heating rate of 2°C/min. Experiments were repeated in at least triplicate.

6.2.3 DSC

DSC experiments were undertaken using a DSC Q2000 instrument (section 2.3.3.1). An inert atmosphere of nitrogen at a flow rate of 50 mL/min was used for all experiments. Accurately weighed samples of ≈ 2 mg were placed in 'TZero' aluminium lidded pans. Samples were heated from -90 to 180°C at a linear heating rate of 10°C/min. Experiments were repeated in at least triplicate.

6.2.4 TSC spectroscopy

TSC experiments were undertaken using a TSCII (section 2.3.1.1). Samples were introduced as freshly prepared compressed tablets of 50 mg mass, 8 mm diameter and their thickness accurately measured using a digital calliper. The sample chamber was evacuated and flushed with helium. Experimental parameters: T_o = -100°C, t_o = 120 s, T_f = 130°C, E_p = 200 V/mm, $q_{(heat)}$ = 10°C/min, $q_{(cool)}$ = 'Newtonian', T_p = 50, 75, 100, 125°C, t_p = 120 s. Thermal windowing was undertaken over the temperature range of 25 to 100°C; T_w = 5°C, t_w = 120 s.

6.3 RESULTS AND DISCUSSION

The results for the thermal analysis of PA (TGA and DSC) are shown in Figure 6.2. A single stage mass loss process was detected with a TG extrapolated onset temperature of 259.75 ± 0.2°C, a dTG peak temperature of 289.44 ± 0.6°C and a total mass loss of 98.61 ± 0.3%. A single DSC transition was observed over the -90 to 180°C temperature range; PA exhibited a sharp endotherm with the following parameters: onset temperature = 169.2 ± 0.6°C, peak temperature = 169.8 ± 0.4°C, peak width = 1.01 ± 0.2°C and normalised integral = 209.2 ± 10.6 J/g. The DSC transition is attributed to the melt of PA form I and the DSC parameters obtained are in agreement with literature values (Lin et al. 2000; Kauffmann et al. 2008; Gaisford et al. 2010). The TGA mass loss transition represents evaporation of the melt. The melting transition in PA is considered the primary transition as no lower temperature transitions were detected (down to -90°C), or have been reported previously.

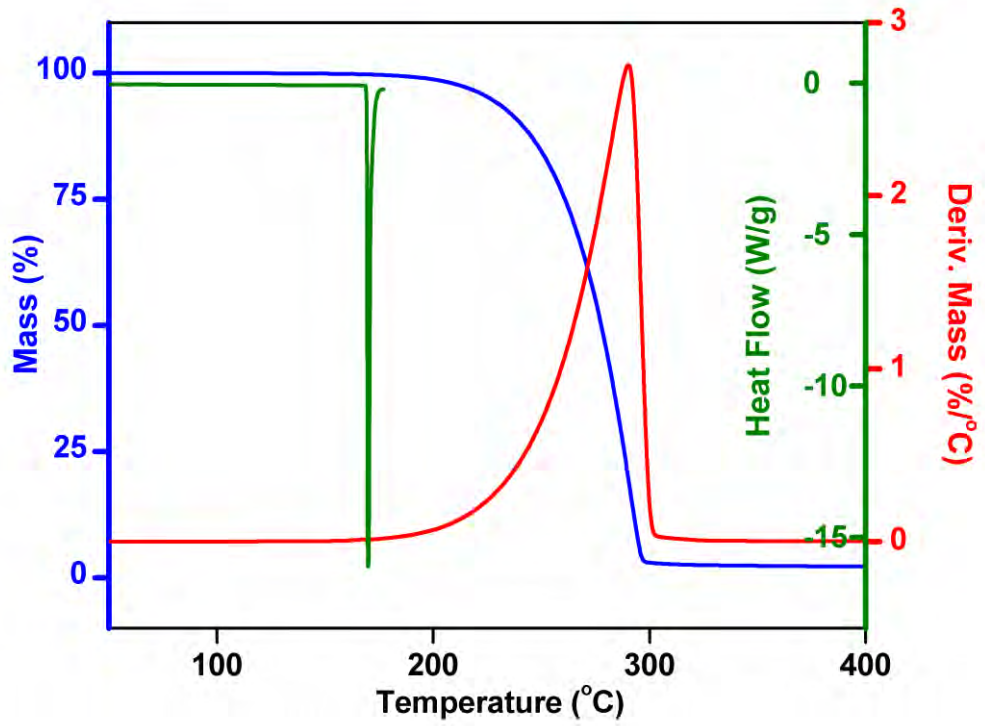

Figure 6.2 TGA and DSC outputs for PA. TG (blue), dTG (red) and DSC heat flow (green). TGA heating rate = 2°C/min. DSC heating rate = 1°C/min.

6.3.1 TSC spectroscopy

SDC and TSPC experiments (Figure 6.3) identified possible molecular motion in PA at temperatures below the melting point. In SDC the 'natural motion' of molecules in the sample begins at around 50°C and is of greater dipolar displacement at 100 to 110°C. The same experiment conducted using a constant electrical field (TSPC) shows that the mobility of the molecules in PA can be induced at a much lower temperature of 0°C. This phenomenon is the result of the strong, static electrical field 'pulling' molecules from their native equilibrium positions via dipole-electrical field interactions (Shmeis and Krill 2005).

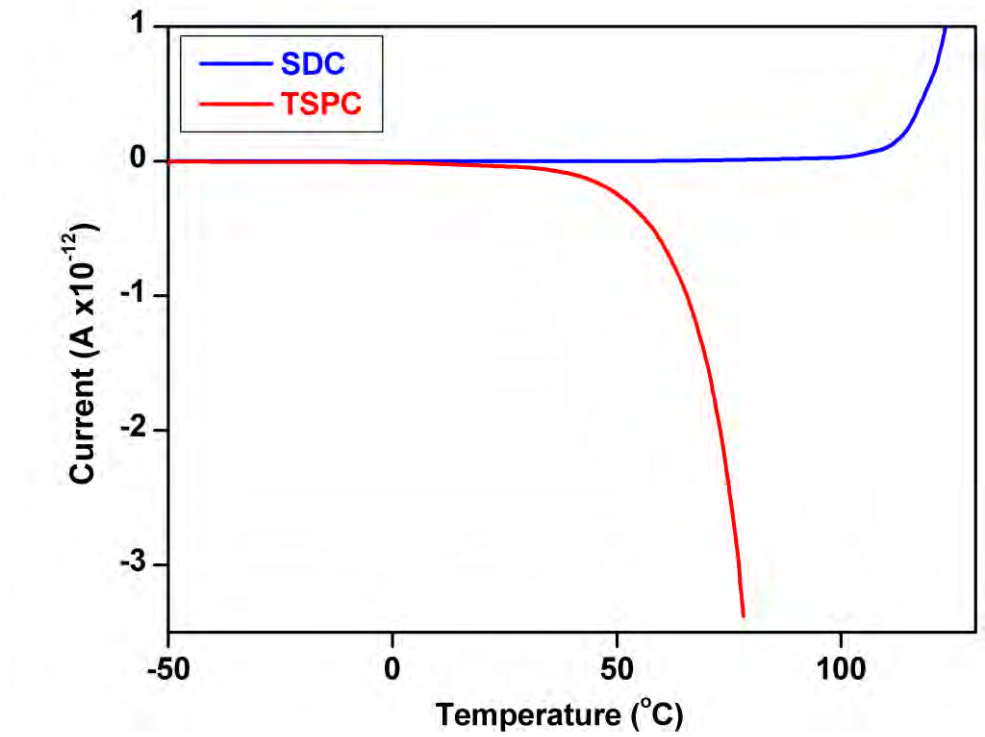

Figure 6.3 SDC and TSPC curves for PA at E_p = 200 V/mm.

TSDC experiments (Figure 6.4) show curves representative of pre-polarisation at differing polarisation temperatures. A trend of increasing peak position (T_m) with T_p values of 50°C = 55.34°C, T_p 75°C = 78.9°C, T_p 100°C = 90.0°C and T_p 125°C = 90.1°C was realised. At higher polarisation temperatures, a greater number of molecules in the sample have enough energy to move within the appropriate time window, and align with the electrical field, than would be available at a lower temperature. This increase can only be sustained until an appropriate polarisation temperature is reached where all molecules (or the vast

majority thereof) are able to align with the field, in a given time frame (Williams 1975; Vanderschueren and Gasiot 1979). In this instance, this point is reached at 100°C and is represented by very similar peak characteristics at T_p = 100 and 125°C.

Additional to the main global peaks, there are two other notable features of these spectra. Firstly, the sharp increase in current after the global peak at + 100°C could be the result of two scenarios. It could be representative of anomalous phenomena, often referred to in dielectric literature as space-charges or Maxell-Wagner-Sillars type current, which originate from discontinuities in the sample or poor sample-electrode contact (Diogo et al. 2007; Antonijevic et al. 2008). Alternatively, it could be the start of another dipolar relaxation process. Without heating to higher temperatures (risking damage to the sensitive instrumentation) and witnessing a return to the baseline it is difficult to distinguish the origin of the post 100°C current. However, it did not hinder analysis of the sample and was therefore not considered an issue. The second additional notable feature of the spectra lies in the 0 to 40°C temperature region. There is clearly a reproducible, distinguishable shallow peak in this region. This is believed to be representative of dipolar relaxation phenomena prior to the more intense peak in the 40 to 100°C temperature region. The origin of the low temperature process and its relationship with the higher temperature process is likely to be elucidated by TW experiments.

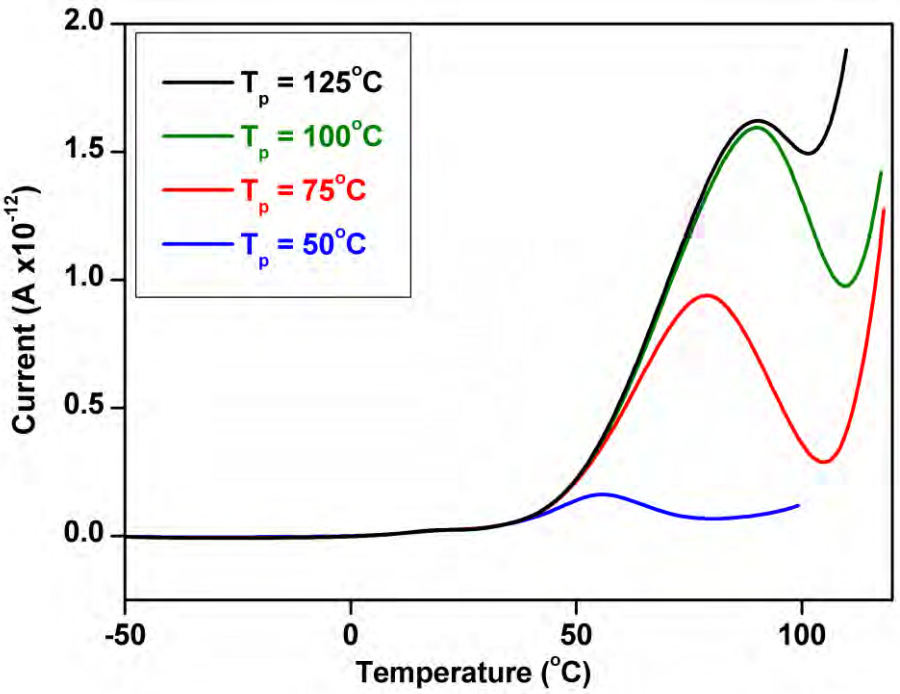

Figure 6.4 TSDC curves for PA at different polarisation temperatures.

6.3.2 Thermal windowing and compensation analysis

Note: *For the sake of clarity throughout this section, curves or points in red refer to relaxation domain A, which is the TW data obtained from T_p values of 25, 30, 35 and 40°C. Curves or points in blue refer to relaxation domain B; a combination of the data from domain A, plus, three additional T_p values of 45, 50 and 55°C.*

Thermal windowing was undertaken over the polarisation temperature range of 25 to 100°C (Figure 6.5) where a series of TW curves occur over a similar temperature range to the global relaxation process observed by standard TSC experiments. As in the case of TSDC experiments the sharp increase in current at 100 to 120°C is also a feature of the TW relaxation profile.

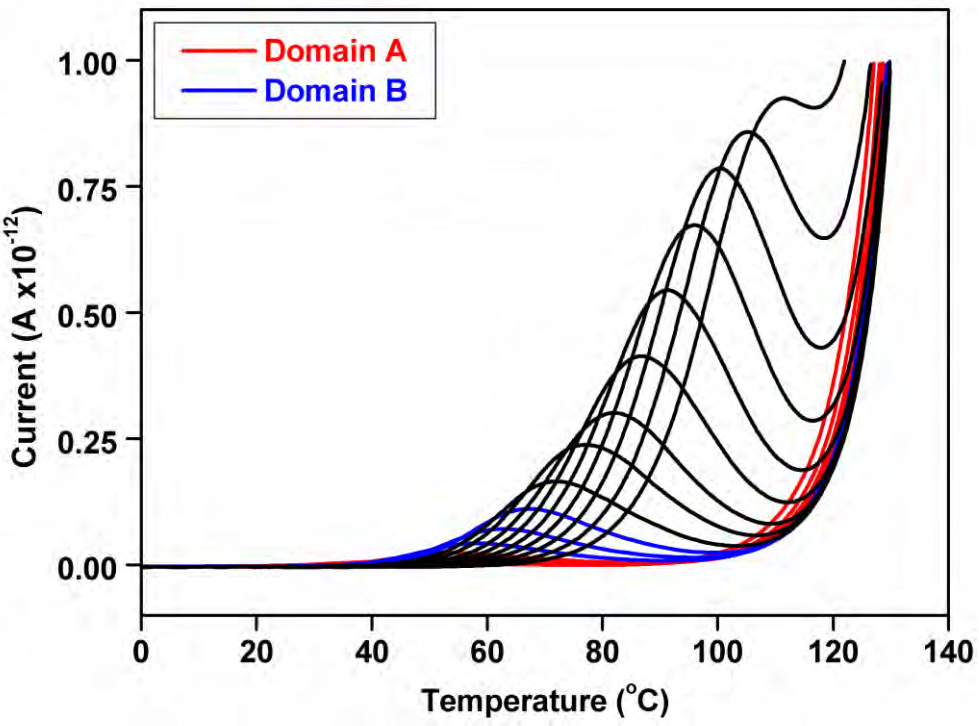

Figure 6.5 TW curves for PA.

Using computational relaxation map analysis (RMA), the TW curves were converted, using the Debye function, to relaxation curves and presented in a 'Bucci plot' style (Figure 6.6). Notably, the relaxation 'curves' are more straight lines, which is to be expected. The more linear the Bucci lines, the more representative the data is considered to be (Williams 1975; Vanderschueren and Gasiot 1979; Correia et al. 2000). Curvature of relaxation lines is believed to represent a system which is not at relaxational equilibrium, as a result of too fast a

heating rate. Interference between the time-scale of the experiment, and the time-scale of depolarisation, is proposed to result in a series of curves with varying slope, resulting in a curve, rather than a straight line (Correia et al. 2000). It can be concluded, in this instance, that the experimental heating rate was of a suitable magnitude in comparison to the time-scale of dipolar relaxation in the system under study.

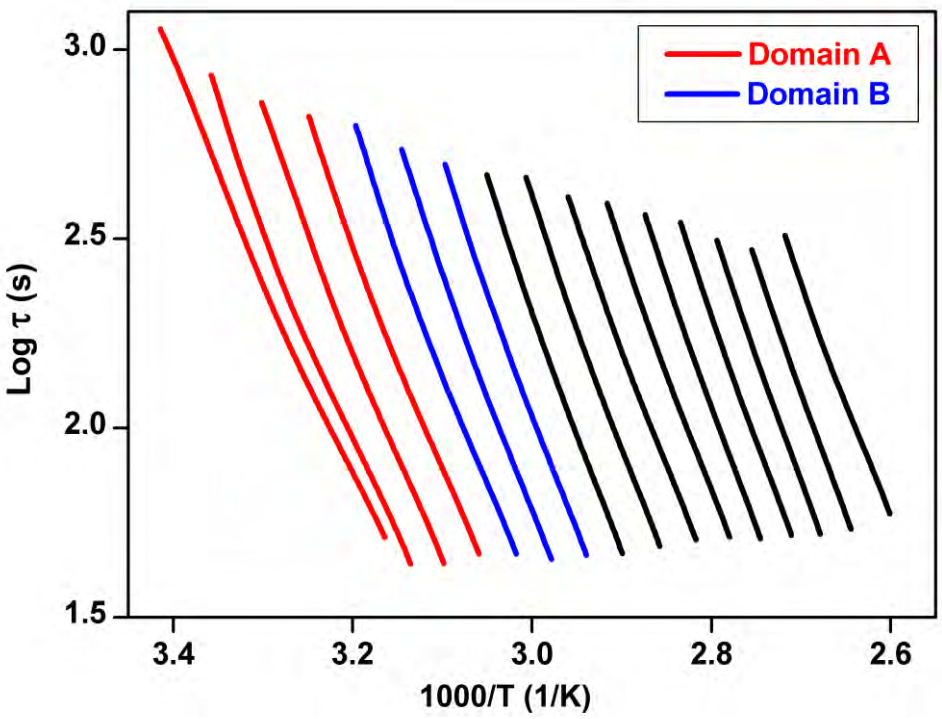

Figure 6.6 Relaxation curves for PA, presented in a 'Bucci plot' style.

Several levels/types of data analysis can be performed on the relaxation curves. A plot of peak position against polarisation temperature (Figure 6.7) helps to explain, and confirm, the dipolar relaxation process. Evidently, there is a linear relationship between T_m and T_p. This behaviour is well known to be indicative of a true dipolar relaxation process (Williams 1975; Vanderschueren and Gasiot 1979) and helps to explain the profile of the TW curves shown in Figure 6.5. Clearly, the position of peak maxima increase in temperature as the experimental polarisation temperature is also increased. On this instance, the height of each peak also increases with polarisation temperature. The reasons for this behaviour has not been explained in the literature, but is well documented.

Compensation analysis was undertaken on the relaxation curves, where each curve is represented by a point on the compensation plot according to its slope and intercept values (Figure 6.7). Linear correlations in compensation points indicate the possibility of compensation behaviour. This is confirmed by a strong compensation correlation coefficient, and feasible values for the compensation temperature, relaxation time and degree of disorder.

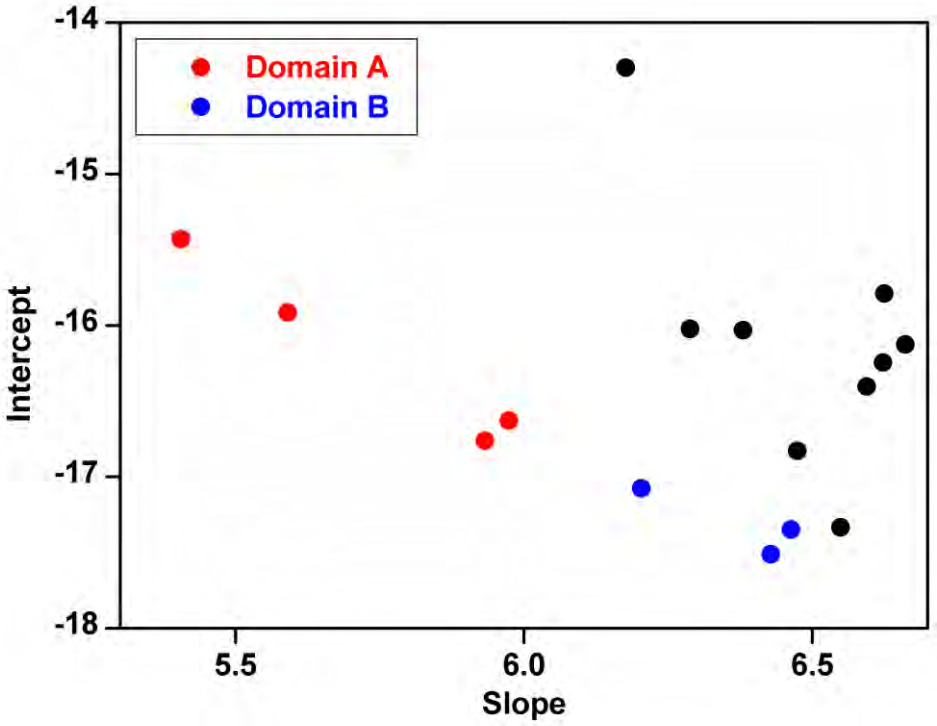

Figure 6.7 Compensation plot for PA.

Usually the existence of two or more linear regions of compensation points would be well defined, and would indicate separate and distinct relaxation domains (as presented for data in previous Chapters of this thesis). However, a rather unique situation is realised in this system. Two compensation domains were realised, but one of the compensation domains (B) is a summation of the other relaxation domain, plus a few extra points. Curves or points in red refer to relaxation domain A, which is the TW data obtained from T_p values of 25, 30, 35 and 40°C. Curves or points in blue refer to relaxation domain B; a combination of the data from domain A, plus, three additional T_p values of 45, 50 and 55°C. In total, compensation domain B represents T_p values of 25, 30, 35, 40, 45, 50 and 55°C.

The reason for such a complicated representation of the relaxation domains becomes clear upon examination of the compensation parameters (Table 6.1). Taking into account the compensation temperatures only at this stage, relaxation domain A has a compensation temperature of 170°C - the melting point of PA (within 1°C). Relaxation domain B has a compensation temperature of 264°C - the onset of mass loss in PA (within 4°C). This shows there is undoubtedly a link between the secondary relaxation and the primary transition. In addition, it highlights the complex relationships involved in the secondary relaxation process; in this system the relaxations of the compensation domains are strongly interlinked, it is difficult to distinguish or isolate them.

Table 6.1 Compensation analysis parameters for PA form 1.

Relaxation domain	**A**	**B**
T_p values (°C)	25, 30, 35, 40	25, 30, 35, 40, 45, 50, 55
T_c (°C)	170	264
τ at T_c (s)	0.0005372	0.000003243
R^2*	0.999	0.999
DOD at T_c	56	65

*R^2 = compensation correlation coefficient.

In reference to the other compensation parameters, the relaxation time of domain B is much faster than domain A. The reasoning behind this assertion can be tentatively linked to the viscosity of the environment surrounding the molecules. At the compensation temperatures the samples will be in the liquid state, therefore fast relaxations would be expected. However, the viscosity of a liquid will decrease with temperature and so a faster relaxation at the higher compensation temperature, in comparison to the lower, may arise from a decreased interaction with neighbouring molecules. An increase in DOD values of 10 units in line with compensation temperatures supports this theory. A lower DOD value at the lower compensation temperature indicates less disorder and more interaction with neighbouring molecules. The opposite is true for a higher DOD value at the higher compensation temperature (Ibar 1991).

As has been discussed in previous Chapters' of this thesis, knowledge of the origin and description of compensation behaviour is incomplete. What has been well documented is the compensation relationship observed between the kinetic functions of the pre-exponential factor and activation energy (Figure 6.8) with the thermodynamic functions of activation

enthalpy and entropy (Figure 6.9). A linear relationship between the functions is thought to be a prerequisite for compensation phenomenon, and in this case is evident for the data points that lie within compensation domains A and B (Moura Ramos et al. 1997; Mano 2005). In the case of dipolar relaxation there is often a linear increase in the change in Gibbs free energy as a function of temperature (Figure 6.10); its relationship with compensation behaviour is unclear.

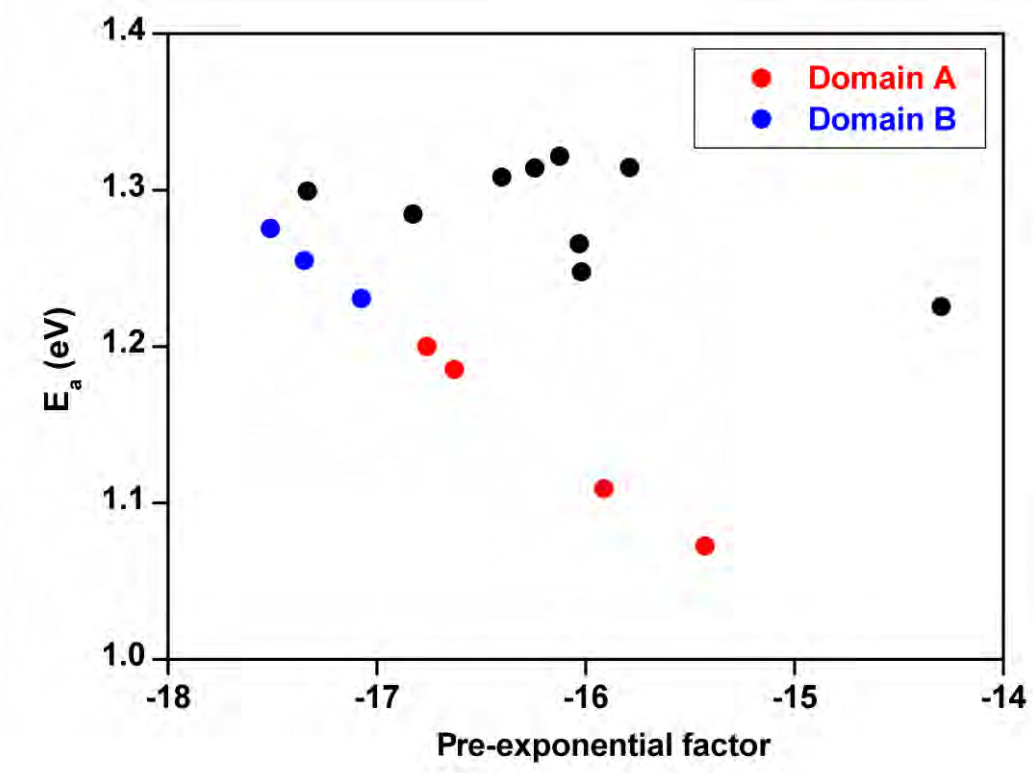

Figure 6.8 Plot of Arrhenius activation energy *vs* pre-exponential factor.

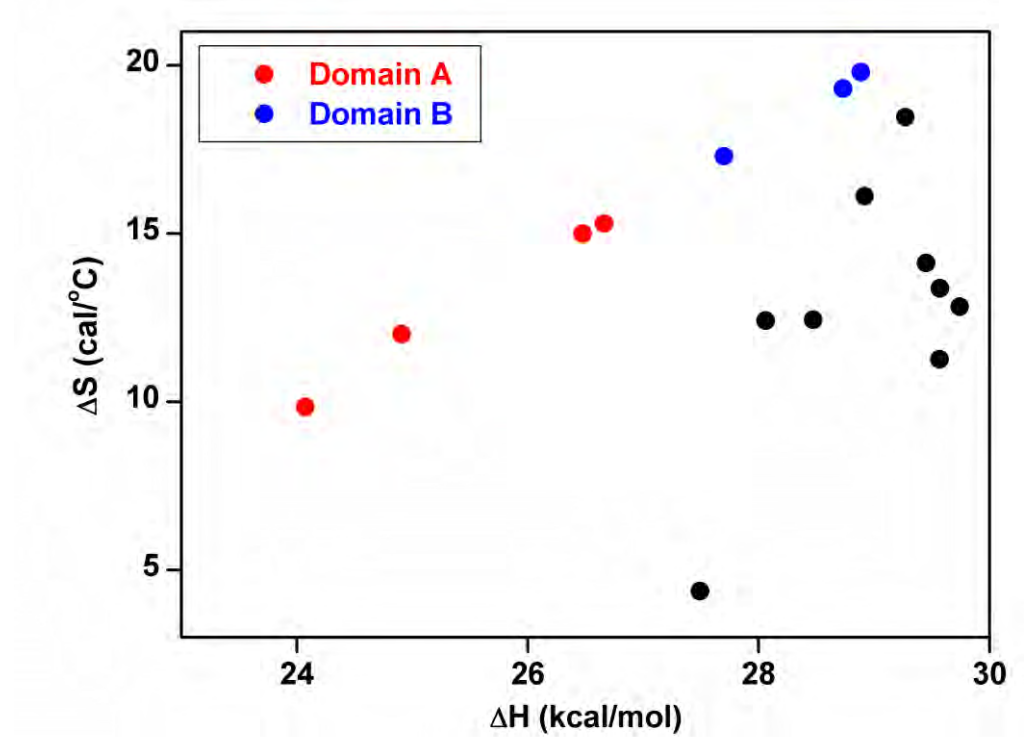

Figure 6.9 Plot of entropy *vs* activation enthalpy.

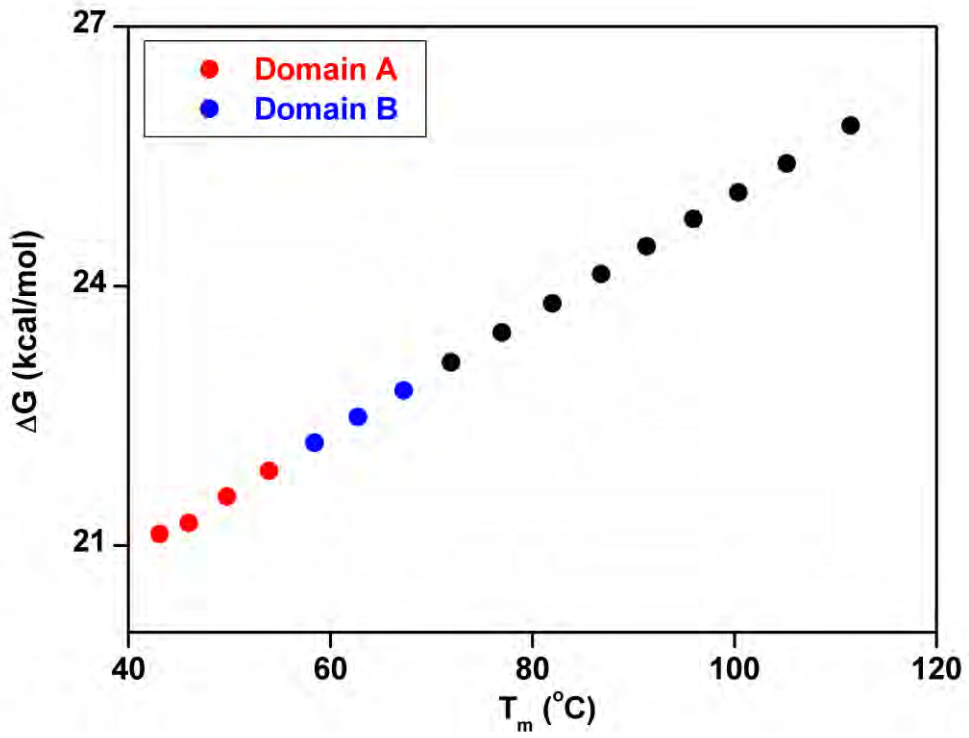

Figure 6.10 Change in Gibbs free energy with peak temperature.

A plot of activation energy *vs* peak temperature (Figure 6.11) highlights a significant increase in activation energy throughout the relaxations of the compensation domains, followed by a decrease in activation energy at 80°C. The significance of the activation energy minima at 80°C is not known for certain, but does appear to be related to a change in cooperativity of the system, as represented in the data in Figure 6.12.

A plot of activation energy *vs* temperature, in comparison to the zero entropy prediction, describes the cooperativity of the system. Activation enthalpies on or close to the zero entropy prediction indicate non-cooperative or low cooperative motions. Those which deviate significantly from the zero entropy prediction indicate cooperative relaxation (Correia et al. 2000). The cooperativity of the system increases as a function of temperature until 70°C, where a decrease in cooperativity is found and attains a minimum at 80°C. At temperatures above 80°C, cooperativity remains fairly constant in comparison to its deviation from the zero entropy line. The significance of the deviation of any of the points from the zero entropy must be taken into account. In this system, a comparison with other literature examples identifies the deviation to be relatively small, and so the cooperativity of the PA system throughout the secondary relaxation region would be considered low-cooperativity (Correia et al. 2000).

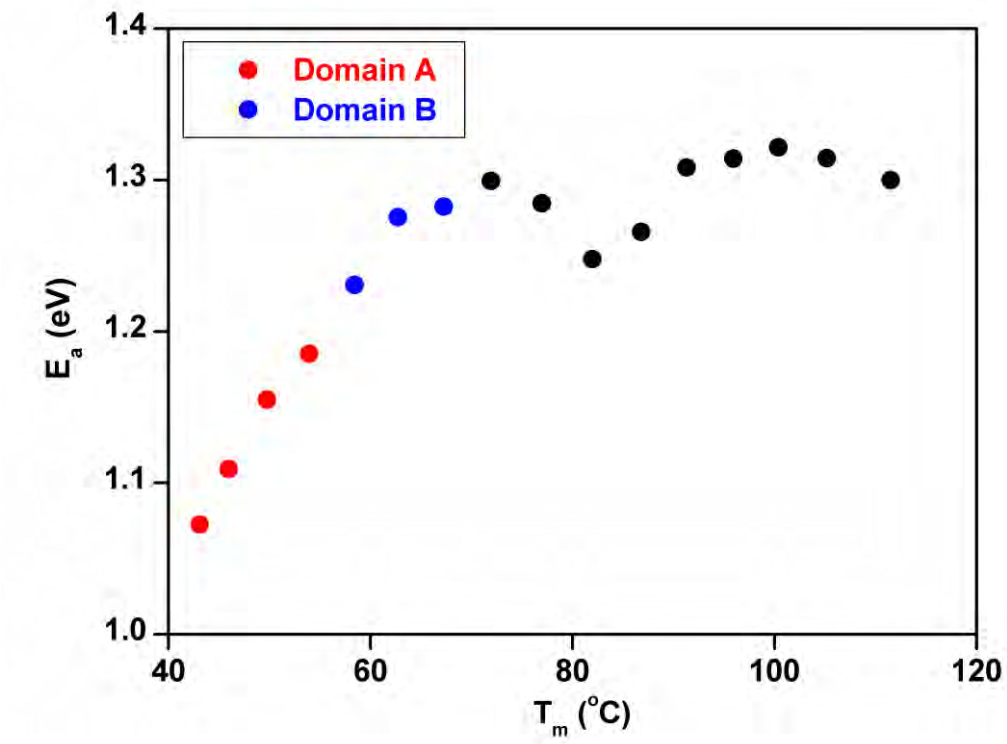

Figure 6.11 Activation energy as a function of peak temperature.

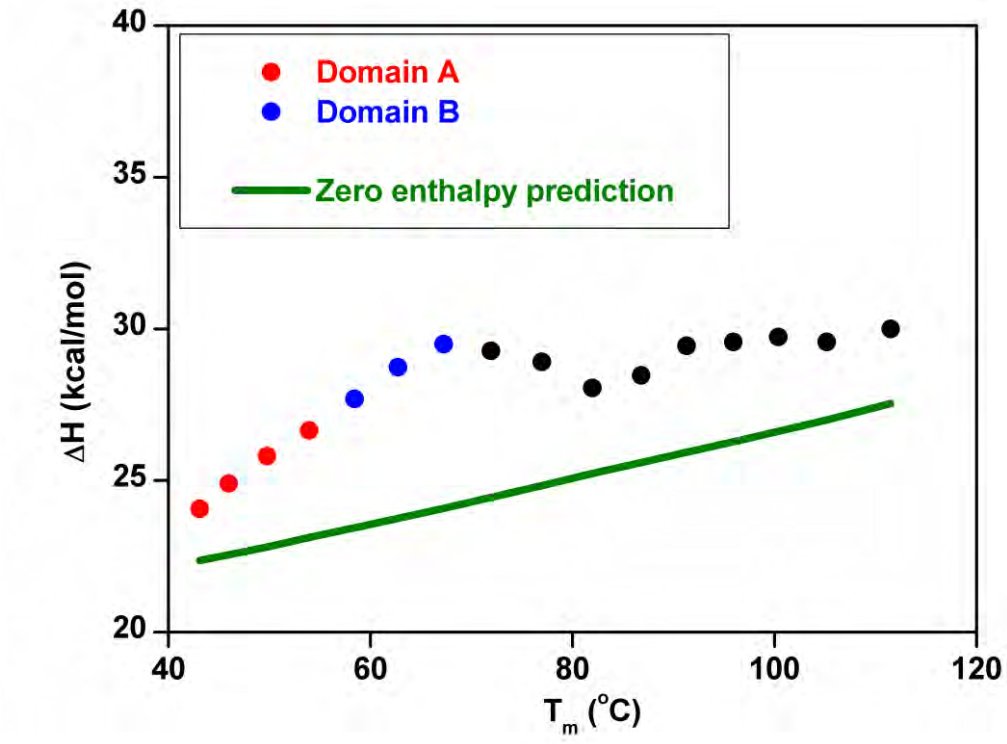

Figure 6.12 Activation enthalpy as a function of peak temperature in comparison to the zero enthalpy prediction.

The fluctuation in activation energy and activation enthalpy at 80°C appears to be a significant event, leading to a change in the cooperativity of the system. This event is not represented in any of the primary experimental outputs (TSC or TW outputs) and highlights the importance of RMA and the additional information that can be gained about the system under study.

6.3 CONCLUSIONS

A secondary relaxation mode has been identified in PA (form I) in the 0 to 120°C temperature region, represented by a global TSDC peak maximum at 90°C. No transition in this temperature region was detected by TGA and DSC. This is believed to be the first reported instance of this relaxation phenomenon detected in PA.

TW data, over the 25 to 100°C temperature region, allows the relaxation to be described as a localised, low-cooperative process. Compensation analysis of the relaxation curves identified compensation behaviour in the 25 to 55°C region. The compensation behaviour was described by the existence of two relaxation domains, A and B. Domain A exhibited a compensation temperature of 170°C - the melting point of PA (within 1°C). Relaxation domain B has a compensation temperature of 264°C - the onset of evaporation in PA (within 4°C). The compensation temperatures provide evidence for a link between the lower temperature secondary process and the higher temperature primary transition. It is, therefore, believed that the secondary relaxation is a precursor molecular motion in preparation for the primary relaxation event.

Taking into account that PA has been extensively studied by the pharmaceutical industry, and has been available as a pharmaceutical product for many years, the discovery of a new transition in such a well characterised material is of significant academic/industrial interest. The exact nature of this secondary relaxation (and secondary relaxations as a whole), at the molecular level, is not completely understood. The principles of the TSC technique, and confirmation of a true dipolar relaxation process, can be used to confirm that the secondary relaxation observed here in PA is ‘real’ and must involve the mobility of molecules in the relaxation temperature region. This highlights the unique and potential applicability of the TSC technique in detecting and thus allowing the characterisation of dipolar relaxation processes in LOMs. If the technique can enhance our knowledge of such a well characterised

material as PA, what could it potentially unearth in other pharmaceutical materials? Perhaps it is time the pharmaceutical industry expanded/adapted by employing new/novel technologies, to aid in the characterisation of new API's and excipients, and to improve their chances of success in marketing new drug products by understanding all possible physical and chemical changes that may occur.

Additionally, the compensation phenomena observed using TSC data affords a unique opportunity to 'predict' transitions that have not yet occurred. In this instance, TSC compensation analysis predicted all higher temperature processes that occur in PA beyond the secondary relaxation. This information could potentially be used to predict stability, define overlapping processes, or model isothermal experiments in situations were forced heating induces transitions that would otherwise not occur (i.e. early degradation or melting).

CHAPTER 7: OVERALL CONCLUSIONS

TSC spectroscopy has been utilised, herein, as an innovative approach to the detection and characterisation of secondary relaxation phenomena in the crystalline solid-state for a number of low-molecular weight organic materials (LOMs). As an innovative technique in this field, TSC experiments have proved challenging to utilise for such applications; nevertheless a considerable output of novel and innovative information (of significant academic and industrial interest) has been collected, analysed and presented in this thesis.

Secondary relaxations have been detected and thoroughly characterised in all samples under study; via the employment of standard TSC methodologies, other (complementary) analytical techniques and complex instrumental and theoretical TSC approaches. The following paragraphs will address the output from each of the four experimental chapters individually, highlighting:

- how the research objectives have been achieved in each instance
- the specific 'on-topic' information achieved through the use of TSC spectroscopy in the context of secondary relaxations
- the 'off-topic' information procured, relating to the materials under study; gained either from fortuitous experimentation or from impromptu (additional) investigation

Chapter three presented the research undertaken on **α-Ala**; specifically it's two stereo-isomeric forms, L- and D-. A previously unreported secondary relaxation in α-Ala in the 40 to 195°C temperature region was discovered by using TSC techniques. Compensation analysis identified two compensation (relaxation) domains. Results suggested that the lower temperature secondary relaxations in α-Ala were precursor motions for the higher temperature primary transition (in this case degradation), and that the secondary relaxation itself is complex, formed of transitional states, each essential for the next process to be initiated. In addition, TSC data was used to clearly-define the ability to differentiate stereo-isomers in the solid-state. Results of all TSC experiments (including SDC, TSDC and TW compensation analysis) highlighted antithesis and/or discrepancy in the TSC spectra for L- and D- forms of Ala; a phenomenon which clearly requires further investigation.

Chapter four presents the investigation of another amino acid, **β-Ala** (the structural isomer of α-Ala). A secondary relaxation process in the 0 to 60°C temperature region (peaking between 45 and 50°C) was identified by TSC experiments; which is comprised of two

distinct relaxation domains, as ascertained by compensation analysis. Interdependence between the secondary relaxations and the primary transitions were evident in β-Ala; a theory which was put to the test via additional isothermal TGA experiments and subsequent kinetic analysis. The primary 'predicted' transition detected by TSC was defined as a zero-order process by TGA analysis, possibly sublimation.

Chapter five focuses on analysis of a **co-crystal system of salicylic acid and benzamide**. This data reported in this Chapter was obtained using synthesis techniques, a varied range of solid-state analytical methodologies, and TSC analysis. In summary, a CC was synthesised successfully using an 'evaporation from solvent' methodology. During analysis of the components it was discovered the same co-crystal could be prepared directly from the heating of a 1:1 molar ratio physical mixture of the components; which arises from a eutectic transition at 110°C. TSC data was used to identify secondary relaxation phenomena in all samples; represented by TSDC peak positions of BA = 20.1°C, SA = 23.4°C, PM = 23.8°C and CC = 28.2°C. Relaxation phenomenon in all samples is concentrated in the -30 to 60°C temperature region; possibly a reason why the components interact to form a CC (overlapping temperature regions of molecular mobility). In the case of the co-crystal and the physical mixture, compensation analysis was used to identify a relationship between secondary relaxation behaviour and primary transitions. As an example, TSC spectroscopy was used to predict the eutectic transition that occurs in the physical mixture, accurate to within one or two degrees Celsius; as well as the melting point of the co-crystal.

Chapter six involved the study of the exceptionally well-characterised drug **paracetamol form I**. Despite the high number of publications pertaining to this drug, this is the first report of TSC analysis, and also the first reported instance of a secondary relaxation (defined to occur in the 0 to 120°C temperature region). Compensation analysis identified two domains of relaxation, each linked to a primary transition. TSC data was used to predict the melting point and the evaporation temperature region for PA form 1, via analysis of the low-temperature secondary relaxations.

In summation, TSC spectroscopy has proven to be effective in the detection and characterisation of secondary relaxations in crystalline LOMs. Its unique ability to directly detect molecular mobility in the solid-state affords many opportunities and advantages to the researcher when dealing with solid-state reactivity. The powerful TW and RMA methodologies offer vast opportunities for the in-depth characterisation of secondary

relaxations. Of notable interest is the compensation analysis tools available; which seemingly allows for the prediction of primary transitions based on experimental investigation in much lower temperature regions. This aspect of the technique has significant implications in all areas of solid-state chemistry; including the prediction of short and long-term stability, or the possible elucidation of 'hidden' thermal events shrouded by overlapping transitions.

Although a niche instrumental technique to this field, TSC has been used to demonstrate (on multiple occasions throughout the research reported herein) that it has substantial potential as an extremely useful analytical technique in the field of LOMs research. With continued assessment of LOMs, and a renewed interest in the fundamental development of the TSC technique and associated theory, TSC spectroscopy could, one day, become a mainstream analytical technique; familiar to researchers investigating solid state phenomena.

CHAPTER 8: FUTURE WORK

As has been mentioned throughout this thesis, TSC spectroscopy can be used as a pioneering technique in the field of LOMs research, and a relative newcomer to the realm of materials characterisation as a whole; beyond niche areas of dielectric and polymer sciences. In light of this, a significant amount of future work is required before the technique can be referred to as a 'mainstream' analytical tool. Therefore, rather than concentrating on the global prospects of the technique (which would be rather lengthy), focus will be placed on the development of the technique to study the specific classes of materials presented here.

The first two experimental chapters dealt with the study of amino acids by TSC techniques. This is, very likely, the first study of its kind. TSC data proved to be particularly useful in detecting secondary relaxations in the α- and β-Ala samples; where, notably, TSC data was used to show that L- and D-Ala could be differentiated. This exciting finding, if proven to be accurate and reproducible, would have a profound impact on our understanding of the solid-state properties of chiral molecules. Obviously, by reproducible, one means between many different samples of L- and D-Ala in the first instance (only duplicate samples were studied here), and then between some different chiral amino acids in the second, and finally between various groups of chiral functionalities. This is a large volume of experimental work to be undertaken.

Another class of materials under study were pharmaceutical type co-crystals; an emerging interest within the industry. Study of these materials has 'gained pace' within the last decade as the potential benefits they offer to the formulator have been realised. However, what is somewhat unclear are the short and long term stabilities of co-crystal materials. As demonstrated in the relevant experimental Chapter, TSC spectroscopy was utilised to gain a wealth of information regarding the stability of the SA-BA co-crystal system. In this instance, the short-term stability was the main focus; although careful monitoring and extrapolation of such stabilities over longer time periods would invariably impart a great deal of information concerning the materials' longer-term stability. This suggested use of the TSC technique would offer some advantages over other complementary thermal techniques; particularly the sensitivity of TSC methods to subtle molecular mobility.

Analysis of drugs such as paracetamol (presented here) is a particularly pertinent area of TSC experimental interest. As well as the use of TSC methodologies to detect subtle molecular

mobility phenomena, TSC could also be used for the characterisation of molecular interactions; such as those between a drug and an excipient. This feature of TSC spectroscopy arises from the ability to experimentally and theoretically deconvolute overlapping relaxations, transitions or signals; often challenging or impossible using many other experimental techniques.

REFERENCES

ANTONIJEVIC, M. D. 2012. Applications of thermally stimulated current spectroscopy in pharmaceutical research. *European Pharmaceutical Review*, 3, 43-46.

ANTONIJEVIC, M. D., CRAIG, D. Q. M. & BARKER, S. A. 2008. The role of space charge formation in the generation of thermally stimulated current (TSC) spectroscopy data for a model amorphous drug system. *International Journal of Pharmaceutics,* 353, 8-14.

BARKER, S, A. & ANTONIJEVIC, M. D. 2011. Thermal Analysis - Dielectric Techniques. *Solid State Characterization of Pharmaceuticals*, John Wiley & Sons, UK.

BARTHES, M., BORDALLO, H. N., DÉNOYER, F., LORENZO, J. E., ZACCARO, J., ROBERT, A. & ZONTONE, F. 2003. Micro-transitions or breathers in L-alanine? *The European Physical Journal B - Condensed Matter and Complex Systems,* 37, 375-382.

BERRY, D. J., SEATON, C. C., CLEGG, W., HARRINGTON, R. W., COLES, S. J., HORTON, P. N., HURSTHOUSE, M. B., STOREY, R., JONES, W., FRISCIC, T. & BLAGDEN, N. 2008. Applying hot-stage microscopy to co-crystal screening: A study of nicotinamide with seven active pharmaceutical ingredients. *Crystal Growth & Design,* 8, 1697-1712.

BHATTACHARYA, S. & SURYANARAYANAN, R. 2009. Local mobility in amorphous pharmaceuticals—characterization and implications on stability. *Journal of Pharmaceutical Sciences,* 98**,** 2935-2953.

BRAGA, C. I., REZENDE, M. C. & COSTA, M. L. 2011. Methodology for DSC calibration in high heating rates. *Journal of Aerospace Technology and Management,* 3**,** 179-192.

BURGER, A. & RAMBERGER, R. 1979. On the polymorphism of pharmaceuticals and other molecular crystals. I. *Microchimica Acta,* 72, 259-271.

BYRN, S. R. & HENCK, J.-O. 2012. Optimizing the physical form – opportunities and limitations. *Drug Discovery Today: Technologies,* 9, 73-78.

BYRN, S. R., XU, W. & NEWMAN, A. W. 2001. Chemical reactivity in solid-state pharmaceuticals: formulation implications. *Advanced Drug Delivery Reviews,* 48, 115-136.

CAROLINE, M. L., SANKAR, R., INDIRANI, R. M. & VASUDEVAN, S. 2009. Growth, optical, thermal and dielectric studies of an amino acid organic nonlinear optical material: l-Alanine. *Materials Chemistry and Physics,* 114, 490-494.

CHAMARTHY, S. P. & PINAL, R. 2008. The nature of crystal disorder in milled pharmaceutical materials. *Colloids and Surfaces A: Physicochemical and Engineering Aspects,* 331, 68-75.

CHIENG, N., RADES, T. & AALTONEN, J. 2011. An overview of recent studies on the analysis of pharmaceutical polymorphs. *Journal of Pharmaceutical and Biomedical Analysis,* 55, 618-644.

COLLINS, G. 2011.Simulation of thermally stimulated polarization current (TSPC) based on the Frohlich two-state model and the complexity of the amorphous phase. *Journal of Thermal Analysis and Calorimetry,* 106,277-284.

CORREIA, N., ALVAREZ, C., MOURA RAMOS, J. & DESCAMPS, M. 2000. Molecular motions in molecular glasses as studies by thermally stimulated depolarisation currents. *Chemical Physics*, 252, 151-163.

CRAIG, R. 2007. Thermal Analysis of Pharmaceuticals. Edited by Duncan Q. M. Craig and Mike Reading. *ChemMedChem,* 3, 1139-1140.

CROWLEY, K. J. & ZOGRAFI, G. 2001. The use of thermal methods for predicting glass-former fragility. *Thermochimica Acta,* 380, 79-93.

CUATRECASAS, P. 2006. Drug discovery in jeopardy. *The Journal of Clinical Investigation,* 116**,** 2837-2842.

DARROCH, J. & MILES, M. P. 2011. A research note on market creation in the pharmaceutical industry. *Journal of Business Research,* 64**,** 723-727.

DIOGO, H. P. & RAMOS, J. J. 2008. Slow molecular mobility in the crystalline and amorphous solid states of glucose as studied by thermally stimulated depolarization currents (TSDC). *Carbohydrate Research,* 343**,** 2797-2803.

DIOGO, H. P., PINTO, S. S. & MOURA RAMOS, J. J. 2007. Slow molecular mobility in the crystalline and amorphous solid states of pentitols: a study by thermally stimulated depolarisation currents and by differential scanning calorimetry. *Carbohydrate Research,* 342**,** 961-969.

ELBAGERMA, M. A., EDWARDS, H. G. M., MUNSHI, T. & SCOWEN, I. J. 2011. Identification of a new cocrystal of citric acid and paracetamol of pharmaceutical relevance. *CrystEngComm,* 13, 1877-1884.

ELBAGERMA, M., EDWARDS, H., MUNSHI, T. & SCOWEN, I. 2010. Identification of a new co-crystal of salicylic acid and benzamide of pharmaceutical relevance. *Analytical and Bioanalytical Chemistry,* 397, 137-146.

ELDER, D. P., HOLM, R. & DIEGO, H. L. D. Use of pharmaceutical salts and cocrystals to address the issue of poor solubility. *International Journal of Pharmaceutics*, 125, 78-84.

FERRANTE. A. & GORSKI, J. 2012. Enthalpy-Entropy Compensation and Cooperativity as Thermodynamic Epiphenomena of Structural Flexibility in Ligand–Receptor Interactions. *Journal of Molecular Biology,* 417, 454-467.

GABBOTT, P. 2008. *Principles and Applications of Thermal Analysis*: Blackwell Publishing.

GAGNIERE, E., MANGIN, D., PUEL, F., RIVOIRE, A., MONNIER, O., GARCIA, E. & KLEIN, J. P. 2009. Formation of co-crystals: Kinetic and thermodynamic aspects. *Journal of Crystal Growth,* 311, 2689-2695.

GALOP, M. & COLLINS, G. L. 2001. Thermally stimulated currents observed in pharmaceutical products. *Thermochimica Acta,* 367-368, 37-41.

GIRON, D. 1995. Thermal analysis and calorimetric methods in the characterisation of polymorphs and solvates. *Thermochimica Acta,* 248, 1-59.

GRANT, D. J. W. & BYRN, S. R. 2004. A timely re-examination of drug polymorphism in pharmaceutical development and regulation. *Advanced Drug Delivery Reviews,* 56, 237-239.

IBAR, J. P. 1991. On the use of the compensation law to describe cooperative relaxation kinetics in thermally stimulated processes: a new view. *Thermochimica Acta*, 192, 91-106.

IKEDA, Y., HIRAYAMA, T. & TERADA, K. 2005. Application of thermally stimulated current measurement to the polymorphic characterization of drug substances. *Thermochimica Acta,* 431, 195-199.

JIMENEZ-RUIZ, M., GONZALEZ, M. A. & BERMEJO, F. J. 1999. Relaxation dynamics in the glassy, supercooled liwuid and orientationally disorderd crystal phases of polymeric molecular materials. *Physical Review B,* 59**,** 9155-9166.

JOHARI, G. P. & GOLDSTEIN, M. 1970. Viscous Liquids and the Glass Transition. II. Secondary Relaxations in Glasses of Rigid Molecules. *The Journal of Chemical Physics,* 53**,** 2372-2388.

KAUFFMAN, J. F., BATYKEFER, L. M. & TUSCHEL, D. D. 2008. Raman detected differential scanning calorimetry of polymorphic transformations in acetaminophen. *Journal of Pharmaceutical and Biomedical Analysis,* 48**,** 1310-1315.

KAUZMANN, W. 1948. The nature of the glassy state and the behaviour of liquids at low temperatures. *Chemical Reviews*, 43, 219-256.

KAWAKAMI, K. 2012. Modification of physicochemical characteristics of active pharmaceutical ingredients and application of supersaturatable dosage forms for improving bioavailability of poorly absorbed drugs. *Advanced Drug Delivery Reviews,* 64**,** 480-495.

KERC, J. & SRCIC, S. 1995. Thermal analysis of glassy pharmaceuticals. *Thermochimica Acta,* 248, 81-95.

KESSEL, M. 2011. The problems with today's pharmaceutical business[mdash]an outsider's view. *Nat Biotech,* 29**,** 27-33.

KHANKARI, R. K. & GRANT, D. J. W. 1995. Pharmaceutical hydrates. *Thermochimica Acta,* 248, 61-79.

KHAWAM, A. & FLANAGAN, D. R. 2006. Basics and applications of solid-state kinetics: A pharmaceutical perspective. *Journal of Pharmaceutical Sciences,* 95**,** 472-498.

KUMAR, S., KUMAR RAI, A., RAI, S. B., RAI, D. K., SINGH, A. N. & SINGH, V. B. 2006. Infrared, Raman and electronic spectra of alanine: A comparison with ab intio calculation. *Journal of Molecular Structure,* 791, 23-29.

LIEN, Y. C. & NAWAR, W. W. 1974. Thermal decomposition of some amino acids. Journal of Food Science, 39, 9114-913.

LIN, S. Y., WANG, S. L. & CHENG, Y. D. 2000. Thermally induced structural changes of acetaminophen in phase transition between the solid and liquid states monitored by combination analysis of FT-IR/DSC microscopic system. *Journal of Physics and Chemistry of Solids,* 61**,** 1889-1893.

MANO, J. F. 2005. Intrinsic compensation phenomenon in thermally stimulated depolarisation studies. *Thermochimica Acta,* 430**,** 135-141.

MELOUN, M. & FERENČÍKOVÁ, Z. 2012. Enthalpy–entropy compensation for some drugs dissociation in aqueous solutions. *Fluid Phase Equilibria*, 328, 31-41.

MORISSETTE, S. L., ALMARSSON, Ö., PETERSON, M. L., REMENAR, J. F., READ, M. J., LEMMO, A. V., ELLIS, S., CIMA, M. J. & GARDNER, C. R. 2004. High-throughput crystallization: polymorphs, salts, co-crystals and solvates of pharmaceutical solids. *Advanced Drug Delivery Reviews,* 56, 275-300.

MOURA RAMOS, J. J., CORREIA, N. T., DIOGO, H. P., ALVAREZ, C. & EZQUERRA, T. A. 2005. Slow relaxations in salicylsalicylic acid studied by dielectric techniques. *Journal of Non-Crystalline Solids*, 351, 3600-3606.

MOURA RAMOS, J. J., DIOGO, H. P. & PINTO, S. S. 2008. Local motions in l-iditol glass: Identifying different types of secondary relaxations. *Thermochimica Acta,* 467**,** 107-112.

MOURA RAMOS, J. J., PINTO, S.S., DIOGO, H. P. 2007. The slow molecular mobility in amorphous trehalose. *ChemPhysChem*, 8, 2391-2396.

NEAGU, E. R. & NEAGU, R. 2003. Comments on the compenstaion effect observed in thermally stimulated depolarization current analysis. *Thermochimica Acta,* 395, 193-189.

NEAGU, E. R., DIAS, C. J., LANÇA, M. C., IGREJA, R., INACIO, P. & MARAT-MENDES, J. N. 2011. The use of the final thermally stimulated discharge current technique to study the molecular movements around glass transition. *Journal of Non-Crystalline Solids,* 357**,** 385-390.

OLAFSON, P. G. & BRYAN, A. M. 1970. Evaluation of thermal decomposition temperatures of amino acids by differential enthalpic analysis. *Michrochimica Acta*, 58, 871-878.

PANAGOPOULOU, A., KYRITSIS, A., SERRA, S., RIBELLES, J. L. G., SHINYASHIKI, N. & PISSIS, P. 2011. Glass transition and dynamics in BSA-water mixtures over a wide range of composition studied by thermal and dielectric techniques. *Biochimica and Biophysica Acta-Proteins and Proteomics,* 1814**,** 1984-1996.

PINTO, S. S., DIOGO, H. P., NUNES, T. G. & MOURA RAMOS, J. J. 2010. Molecular mobility studies on the amorphous state of disaccharides. I--thermally stimulated currents and differential scanning calorimetry. *Carbohydrate Research,* 345**,** 1802-1807.

QIAO, N., LI, M., SCHLINDWEIN, W., MALEK, N., DAVIES, A. & TRAPPITT, G. 2011. Pharmaceutical cocrystals: An overview. *International Journal of Pharmaceutics,*

419**,** 1-11.

REMIZOV, A. B. & SKOCHILOV, R. A. 2012. Compensation and cooperative effects in H-bond thermodynamics of hydroperoxides. *Journal of Molecular Structure*, 1018, 35-38.

RODANTE, F. 1992. Thermodynamics and kinetics of decomposition processes for standard [alpha]-amino acids and some of their dipeptides in the solid state. *Thermochimica Acta,* 200, 47-61.

ROHANI, S. 2010. Applications of the crystallization process in the pharmaceutical industry. *Frontiers of Chemical Engineering in China,* 4, 2-9.

SAFFELL, J. R., MATTHIESEN, A., MCINTYRE, R. & IBAR, J. P. 1991. Comparing thermal stimulated current (TSC) with other thermal analytical methods to characterize the amorphous phase of polymers. *Thermochimica Acta,* 192, 243-264.

SAUER, B. B., AVAKIAN, P., STARKWEATHER, H. W. & HSIAO, B. S. 1990. Thermally Stimulated Current and Dielectric Studies of Poly(aryl ether ketone ketone). *Macromolecules,* 23**,** 5119-5126.

SCHARTMAN, R. R. 2009. On the thermodynamics of cocrystal formation. *International Journal of Pharmaceutics,* 365, 77-80.

SCHICK, C. 2009. Differential scanning calorimetry (DSC) of semicrystalline polymers. *Analytical and Bioanalytical Chemistry,* 395**,** 1589-1611.

SHMEIS, R. A. & KRILL, S. L. 2005. Weak solid-solid transitions in pharmaceutical crystalline solids detected via thermally stimulated current. *Thermochimica Acta,* 427, 61-68.

SIGURD, B. 2010. Future manufacturing approaches in the chemical and pharmaceutical industry. *Chemical Engineering and Processing: Process Intensification,* 49**,** 993-995.

SIMMONS, J. G. 1965. Potential barrier attenuation due to electric field penetration of the electrodes. *Physics Letters,* 16, 233-234.

SIMMONS, J. G. 1971. Theory of metallic contacts on high resistivity solids—I. Shallow traps. *Journal of Physics and Chemistry of Solids,* 32, 1987-1999.

SINGHAL, D. & CURATOLO, W. 2004. Drug polymorphism and dosage form design: a practical perspective. *Advanced Drug Delivery Reviews,* 56, 335-347.

SMITH, G. D. & BEDROV, D. 2007. Relationship between the α- and β-relaxation processes in amorphous polymers: Insight from atomistic molecular dynamics simulations of 1,4-polybutadiene melts and blends. *Journal of Polymer Science Part B: Polymer Physics,* 45**,** 627-643.

STARIKOV, E.B., NORDÉN, B. 2012. Entropy–enthalpy compensation as a fundamental concept and analysis tool for systematical experimental data. *Chemical Physics Letters,* 38, 118-120.

SURIYA KUMAR, K., RAGHAVALU, T., MATHIVANAN, V., KOVENDHAN, M., SIVAKUMAR, B., RAMESH KUMAR, G., GOKUL RAJ, S. & MOHAN, R. 2008.

Structural, optical, spectral and thermal studies of nonlinear optical pure and deuterated l-alanine single crystals. *Journal of Crystal Growth,* 310, 1182-1186.

THAKURIA, R., DELORI, A., JONES, W., LIPERT, M. P., ROY, L. & RODRÍGUEZ-HORNEDO, N. Pharmaceutical cocrystals and poorly soluble drugs. *International Journal of Pharmaceutics*, 453, 101-125.

THIELEN, A., NIEZETTE, J., VANDERSCHUEREN, J., FEYDER, G., LE, Q. T. & CAUDANO, R. 1997. Thermally stimulated current study of space-charge formation and contact effects in metal-polyethylene terephthalate films-metal systems. III. Influence of heat treatments. *Journal of Physics and Chemistry of Solids,* 58, 607-622.

VANDERSCHUEREN, J. & GASIOT, J. 1979. *Thermally stimulated relaxation in solids. Field induced thermally stimulated currents.*, Berlin Springer.

VIPPAGUNTA, S. R., BRITTAIN, H. G. & GRANT, D. J. W. 2001. Crystalline solids. *Advanced Drug Delivery Reviews,* 48, 3-26.

VISHWESHWAR, P., MCMAHON, J. A., BIS, J. A. & ZAWOROTKO, M. J. 2006. Pharmaceutical co-crystal. *Journal of Pharmaceutical Sciences,* 95, 499-516.

VYAZOVKIN, S. & DRANCA, I. 2006. Probing Beta Relaxation in Pharmaceutically Relevant Glasses by Using DSC. *Pharmaceutical Research,* 23**,** 422-428.

VYAZOVKIN, S., BURNHAM, A. K., CRIADO, J. M., PÉREZ-MAQUEDA, L. A., POPESCU, C. & SBIRRAZZUOLI, N. 2011. ICTAC Kinetics Committee recommendations for performing kinetic computations on thermal analysis data. *Thermochimica Acta,* 520**,** 1-19.

WUNDERLICH, B. 1999. A classification of molecules, phases, and transitions as recognized by thermal analysis. *Thermochimica Acta,* 340-341, 37-52.

YONG, C. 2007. A material science perspective of pharmaceutical solids. *International Journal of Pharmaceutics,* 339, 3-18.

YU, L. 2001. Amorphous pharmaceutical solids: preparation, characterization and stabilization. *Advanced Drug Delivery Reviews,* 48, 27-42.

ZHANG, G. G. Z., LAW, D., SCHMITT, E. A. & QIU, Y. 2004. Phase transformation considerations during process development and manufacture of solid dosage forms. *Advanced Drug Delivery Reviews,* 56**,** 371-390.

ZIMMERMANN, B. & BARANOVIC, G. 2011. Thermal analysis of paracetamol polymorphs by FT-IR spectroscopies. *Journal of Pharmaceutical and Biomedical Analysis,* 54**,** 295-302.

APPENDIX

Compensation phenomena observed in TSC

This appendix serves to provide supplementary information on the determination of the compensation point and the nature of compensation behaviour witnessed in TW data; for the interested reader, as a starting point, before consulting the specialist literature mentioned in the main text.

Compensation analysis is applied to TW data, where the elementary relaxation spectra (obtained directly from TW experiments) are assumed to have a single relaxation time; where the temperature dependence of τ can be described by the Arrhenius equation:

$$\tau = \tau_0 \exp\left(\frac{E_a}{kT}\right)$$

Where τ_0 is the pre-exponential factor and E_a the apparent activation energy. If compensation behaviour is observed, there is a concomitant increase in τ_0 and E_a so that the Arrhenius lines converge to a single point, of co-ordinates τ_c and T_c, the relaxation time and temperature at the compensation point; defined by:

$$\tau_0 = \tau_c \exp\left(-\frac{E_a}{kT_c}\right)$$

Substitution of the above equation into the Arrhenius equation yields:

$$\tau_0 = \tau_c exp\left[\frac{E_a}{k}\left(\frac{1}{T} - \frac{1}{T_c}\right)\right]$$

the compensation equation; often written as:

$$\tau = \tau_0 exp\left[\frac{T_c}{T} ln\left(\frac{\tau_c}{\tau_0}\right)\right]$$

Therefore, the compensation phenomenon is essentially a linear relationship between the logarithm of the pre-exponential factor of the Arrhenius equation and the apparent activation energy.

Alternatively, the compensation behaviour can be evident from a thermodynamic view point using a modified Eyring equation:

$$\tau = \frac{h}{kT} exp\left(-\frac{\Delta S}{k}\right) exp\left(\frac{\Delta H}{kT}\right)$$

where a linear relationship between activation enthalpy (ΔH) and activation entropy (ΔS) can be observed.

The nature of compensation phenomena and the nature of the compensation point have been debated for many years in most disciplines of science. Compensation behaviour is routinely witnessed in biology/biochemistry and has perplexed physicists and chemists alike.

One side of the argument portrays compensation behaviour as being an artefact, with the linear relationship between enthalpy/entropy and/or pre-exponential factor/activation energy resulting in a statistical compensation pattern; derived solely from experimental error.

The alternative argument does not -essentially- offer evidence against such a statistical/error based foundation. Instead, those who believe in compensation behaviour refuse to accept such a situation as the sole reasoning for compensation behaviour; i.e., understanding that it is a possibility, but does not hold true in most instances. The dominant argument for the existence of compensation behaviour and the compensation point is the (growing) body of evidence that relates experimentally derived compensation points to *real* physical processes; such as the many examples presented in this thesis.

It should be noted that compensation analysis should only be attempted on experimental data where the 'Bucci lines' are linear (or close to). This stems from the assumptions regarding linearity that are made in the Arrhenius equation (i.e. a Debye like process with a single relaxation time) and during the determination of the compensation point (i.e. a linear relationship between enthalpy/entropy or pre-exponential factor/activation energy). No such study has been undertaken to assess the impact of non-linearity in compensation equations; therefore there are no rules/advisories as to 'how linear' data must be. Although it can be assumed that any error in determining compensation point parameters is ultimately the result of non-linear dependencies.

Further information about compensation behaviour observed in TSC, as well as opinions for or against its existence can be found in the following references: Correia et al. 2000; Mano 2005; Moura-Ramos et al. 2007.